

An Equivalent Structural Stress-Based Frequency Domain Fatigue
Assessment Approach for Welded Structures Under Random Loading

by

Uchenna Kalu

A thesis submitted to the Faculty of Graduate Studies of
the University of Manitoba
in partial fulfillment of the requirements of the degree of

MASTER OF SCIENCE

Department of Mechanical Engineering
University of Manitoba
Winnipeg

Copyright © Uchenna Kalu, 2023

Abstract

Welded structures under random loading are susceptible to fatigue-induced failure, posing significant economic and safety risks. However, accurately predicting these structures' fatigue damage and life remains challenging due to the limitations associated with the traditional weld stress extrapolation methods, such as nominal, hotspot, and notch stress methods. These methods struggle with precisely defining and characterizing the stresses at the weld toe and root, as they vary depending on factors like weld stress concentration effects, joint geometry, and loading modes. Consequently, there is a need for a fatigue analysis approach that employs a more robust and reliable stress evaluation method, leading to significantly improved accuracy in predicting the fatigue damage and life of welded structures under random fatigue loading conditions.

This research introduces an Equilibrium Equivalent Structural Stress (EESS)-based frequency domain fatigue analysis approach for welded structures subjected to random loading. The proposed method utilizes the EESS formulations, which are based on the decomposition and characterization of weld toe stresses with a single stress parameter, together with incorporating structural dynamic properties' effects on the stresses acting on the weld joints and the corresponding accumulated fatigue damage of the structure.

Numerical demonstration and validation of the proposed method have been performed using a welded Rectangular Hollow Section (RHS) T-joint structure subjected to a stationary random fatigue load. The proposed method's fatigue damage and life results are compared with fatigue test data and the equivalent hotspot stress extrapolation-based technique. The EESS-based frequency domain fatigue analysis method accurately predicts fatigue crack initiation locations, consistent

with literature findings. It also demonstrates a 26% improvement in fatigue life prediction compared to the hotspot method. Furthermore, the proposed method achieved a maximum computational efficiency gain of 58% compared to the alternative hotspot stress-based fatigue analysis method.

Acknowledgment

I want to express my deepest gratitude to my supervisor, Dr. Xihui Liang, for his exceptional guidance and unwavering support throughout this project. His expertise, patience, and belief in my abilities have shaped this research and kept me motivated even during challenging times. His insightful suggestions and valuable comments have improved my research work and enriched my understanding of engineering and research. I am truly grateful for his mentorship, which has played a pivotal role in my further development as an engineer and researcher.

I would also like to thank the members of my examining committee, Dr. Nan Wu and Dr. Chuang Deng, for their time, expertise, and valuable input during the evaluation of my thesis. Their constructive comments and suggestions have helped me refine my work and make it more robust.

I am deeply indebted to my family for their unwavering support throughout this program. Their love, understanding, and encouragement have been my pillars of strength. I want to express my heartfelt gratitude to my wife and daughter for their sacrifices and for standing by me, even from miles away. Their constant support and belief in me have inspired me, and I am truly fortunate to have them in my life.

I am humbled and grateful for the collective support and guidance I have received, which has enabled me to complete this research successfully. Each individual mentioned here has played an important role in this achievement, and I am indebted to them.

Dedication

To my daughter, Stephanie Uchechi Kalu

Table of Contents

Abstract	i
Acknowledgment	iii
Dedication	iv
Table of Contents	v
List of Tables	viii
List of Figures	ix
Abbreviations	xii
Nomenclature	xiii
1 Introduction	1
1.1 Welded Structures Fatigue Evaluation Approaches Based on Loading Type	2
1.2 Stresses at the Welded Joints	4
1.3 Motivation	6
1.4 Objectives	7
1.5 Thesis Structure	8
2 Literature Review	10
2.1 Random Loadings in Fatigue Assessment of Welded Structures	10
2.2 Fatigue Analysis of Welded Structures in the Frequency Domain	13
2.2.1 Stress Response Evaluation and Extrapolation	14
2.2.2 Stress Response Cycle Counting and PDF	22
2.2.3 Fatigue Damage and Life Prediction Using the S-N Curve	25
2.3 EESS Fatigue Evaluation Method for Welded Structures	29
2.3.1 Equilibrium Equivalent Structural Stress (EESS)	30

2.3.2	Master S-N Curve	33
2.4	Summary of the Literature Review	36
3	Proposed Fatigue Damage and Life Evaluation Method.....	38
3.1	Structural Dynamics of Randomly Loaded Structures.....	39
3.2	Development of the Weld's Dynamic EESS Evaluation Equation.....	41
3.2.1	Modal EESS.....	41
3.2.2	EESS Mode-based Frequency Response Function (FRF)	52
3.2.3	EESS Stress Response PSD and Cycle Counting	58
3.3	Fatigue Damage and Life Estimation Using the Master S-N Curve	61
3.4	Summary of the Proposed Method.....	63
4	Numerical Demonstration and Validation of the Proposed Method for Welded RHS Structures	65
4.1	Parameters and Preliminary Analysis of the Structure.....	65
4.1.1	Geometry and Material Properties of the Structure	66
4.1.2	Finite Element Model of the Structure.....	69
4.1.3	Preliminary Analysis for Reliability Validation of the FE Model.....	73
4.2	EESS-Based Frequency Domain Fatigue Analysis.....	75
4.2.1	Calculating the Modal EESS of the Structure.....	76
4.2.2	Calculating the EESS FRF of the Structure	77
4.2.3	Calculating the EESS PSD Response of the Structure	78
4.2.4	Estimating the Fatigue Damage and Life.....	79

4.3	Results and Discussions	81
4.3.1	Preliminary Analysis Results and Discussions	82
4.3.2	Frequency Domain Fatigue Analysis Results and Discussion.....	84
4.4	Validation of the Fatigue Damage and Life Results	96
4.5	Summary	101
5	Conclusions and Recommendations.....	103
5.1	Conclusions	103
5.2	Recommendations	105
	References	108

List of Tables

Table 2-1: Master S-N curve parameters [43].....	34
Table 4-1: Structure and weld profile dimensions and thickness [19].....	67
Table 4-2: Structure's material properties [19].....	68
Table 4-3: First ten natural frequencies of the structure with the corresponding modes, participation factors and effective mass proportion	86
Table 4-4: EESS and hotspot frequency domain methods predicted fatigue life comparison	100
Table 4-5: Simulation memory, runtime, and output database requirements for EESS and hotspot frequency domain methods	100

List of Figures

Figure 1-1: Time and frequency domain fatigue analysis approaches [5].....	3
Figure 2-1: Typical stationary random loadings time histories and PSDs of structures [5]	11
Figure 2-2: Stress response PSD calculation from Input loading PSD and FRF	14
Figure 2-3: Fillet weld stress state: (a) Throat area and leg size (b) stress components in a weld (Adapted from [1]).....	15
Figure 2-4: Stress extrapolation approaches at the welded joint location	18
Figure 2-5: Notch stress state and definition at the welded joint location [37]	21
Figure 2-6: Stress spectral moments determination from stress PSD.....	23
Figure 2-7: Typical S-N curve for welded steel structures under different weld stress categories	26
Figure 2-8: EESS method: weld through-thickness stress decomposition	30
Figure 2-9: Structural stress definition and calculation procedures from FE model mesh elements	31
Figure 3-1: Displacement response of a structural system based on the MSUP method	43
Figure 3-2: FE mesh element nodal forces and moments in the global and local CS	45
Figure 3-3: Element modal line forces and moments calculation from corresponding nodes global modal forces and moments nodal forces and moments	49
Figure 3-4: Modal structural stress computation from individual structural stress mode shapes.	50
Figure 3-5: Modal coordinates of the structural system corresponding to three modal responses	55
Figure 3-6: EESS FRF Computational approach from Modal EESS and Modal Coordinates.....	57
Figure 3-7: Flowchart of the frequency domain fatigue analysis method based on the EESS.....	62
Figure 4-1: Geometrical details of the RHS T-joint welded structure (dimensions are in mm) ...	67

Figure 4-2: Finite element model and boundary condition of the structure	70
Figure 4-3: (a) Modeled weld toe paths (b) defined weld connection to the beam components ..	72
Figure 4-4: Finite element model with 1T mesh size, loading and boundary conditions	74
Figure 4-5: Input base acceleration PSD Load in the time domain and frequency domain form.	79
Figure 4-6: Mean and Standard Deviations Master S-N curves	80
Figure 4-7: EESS along weld toe path for <i>1T</i> , <i>2T</i> and <i>3T</i> mesh sizes	82
Figure 4-8: Calculated fatigue life along the weld path due to constant amplitude cyclic loading	83
Figure 4-9: Mode shapes contour and corresponding natural frequencies of the first ten modes of the structure	85
Figure 4-10: Evaluated modal EESS for the first ten modal responses of the structure along the weld toe paths	88
Figure 4-11: Evaluated frequency response coordinates for the first ten modal responses of the structure.....	89
Figure 4-12: Calculated EESS FRF for the twenty-six nodes on the structure's weld toe paths .	90
Figure 4-13: Maximum EESS FRF at node six on the weld toe paths	91
Figure 4-14: Maximum EESS response at node six: critical response at modes 2 and 10	92
Figure 4-15: PDF of EESS amplitudes for the maximum EESS PSD	93
Figure 4-16: PDF of fatigue damage intensity	94
Figure 4-17: Predicted fatigue damage intensity along the weld toe path	95
Figure 4-18: Predicted fatigue life along the weld toe path	96
Figure 4-19: Predicted crack initiation comparison with experiment and hotspot results	98

Figure 4-20: Extrapolated maximum principal hotspot stress convergence with mesh size

variation 99

Abbreviations

CS	Coordinate System
EES	Equilibrium Equivalent Structural Stress
EQVM	Equivalent Von Mises Stress
FEA	Finite Element Analysis
FRF	Frequency Response Function
IIW	International Institute of Welding
MDOF	Multiple Degrees of Freedom
MSUP	Mode Superposition
PDF	Probability Density Function
PSD	Power Spectral Density
RHS	Rectangular Hollow Section
SDOF	Single Degree of Freedom
S-N	Stress-Life

Nomenclature

C	Damping
D	Fatigue Damage
f	Frequency
$G(f)$	Input Load PSD
$G^\sigma(f)$	Stress PSD
$G_{eq(ns)}^\sigma(f)$	Equivalent Nominal Stress PSD
$G_{eq(hs)}^\sigma(f)$	Equivalent Hotspot Stress PSD
$G^{\Delta S_s}(f)$	Equilibrium Equivalent Structural Stress PSD
$H^\sigma(f)$	Frequency Response Function
$H^{\Delta S_s}(f)$	EESS Frequency Response Function
K	Stiffness
L_F	Fatigue Life
M	Inertia
m_n	Spectral Moments

$m_n(\Delta S_s)$	EESS-based Spectral Moments
N	Number of Cycles to Failure
$p(S)$	PDF of Stress Amplitudes
$p(\Delta S_s)$	PDF of EESS Amplitudes
S	Cyclic Stress Amplitude
$S^{\Delta S_s}$	EESS Amplitude
μX	Random Loading Mean
$X(t)$	Random Loading
σ_s	Normal Structural Stress
τ_s	Perpendicular Shear Structural Stress
τ_z	Parallel Shear Structural Stress
ΔS_s	Equilibrium Equivalent Structural Stress
$\sigma^2 X$	Random Loading Variance
$\phi_i(x)$	i^{th} Displacement Mode Shape
$\phi_i^{\tau_{\Delta s}}$	i^{th} Modal Structural Stress
$\phi_i^{\Delta S_s}$	i^{th} Modal Equilibrium Equivalent Structural Stress

η_i

i^{th} Modal Coordinate

1 Introduction

Welding is the most popular and preferable technique for connecting parts of steel structures in various industries. Welded connections are preferred over bolted and riveted connections in steel structures due to their unique characteristics of low cost, aesthetics, high strength-to-weight ratio, geometrical flexibility, and, most importantly, high resistance to fatigue loadings. However, the complex nature of the welding process, usually associated with induced defects (e.g., slag inclusion, porosity, lack of fusion), residual stresses, microstructural distortion around the heat-affected zone, and notch-based stress concentrations, implies that the fatigue resistance at the welded connection region is always inferior in comparison to the other unwelded areas of the structure [1]. Hence, the increased propensity of a structure to failure at stress levels well below its material yield strength.

Different from easily detectable static loading failures, which are mainly due to material plastic deformation, fatigue failures, which account for more than 80% of the total failures experienced by welded structures, usually occur with undetectable crack initiation and, more often, lead to severe economic, and in some cases, fatal consequences [2]. Therefore, it justifies the continuously increasing stringent requirements for guaranteed integrity, robustness, and a high degree of accuracy in the engineering design of welded structures and systems against fatigue loads. Determination of the time to failure, otherwise also referred to as fatigue life of welded structures, can be accomplished through physical means such as in experiments and accelerated life cycle tests or numerical finite element analysis (FEA) approach at both the design and operational stages.

The use of the FEA approach for fatigue damage and life evaluation of welded structures is attributed to the ease of modifications at the design stage, cost, and time-saving benefits on prototype components and structure accelerated fatigue life testing [3]. Stress-based, strain-based or linear fracture mechanics analysis approaches can be used in FEA to evaluate the fatigue life of welded structures at the different damage failure stages. While the stress and strain-based approaches are used for life estimation before damage crack initiation, the linear fracture mechanics approach depends on an initial crack to predict the remaining life of the structure based on the crack propagation rate and size. The stress-based approach, also known as high cycle fatigue and characterized by stress within the elastic region of the material, requires the load exposure history, stress at the welded joint locations, and a damage prediction model that compares the evaluated cyclic stresses S to the material's number of cycles to failure properties (life) N [4]. The stress-life (S - N) cycle curves of welded structures are obtained from experimental data that are based on a series of constant amplitude cyclic load tests for different welded joint geometry categories and loading modes.

1.1 Welded Structures Fatigue Evaluation Approaches Based on Loading Type

The fatigue loadings of welded structures, categorized according to their distinctive characteristics, mainly consist of constant amplitude cyclic, variable amplitude cyclic, and random loadings [5], [6]. While the stress and fatigue response behaviours of constant and variable amplitude cyclic loadings are described using deterministic equations suitable for block cyclic loading conditions, the stress and fatigue responses due to random loadings are evaluated using stochastic approaches and equations. To evaluate the fatigue damage and life of welded structures exposed to random loadings, the time domain, frequency domain or time-frequency domain fatigue analysis approaches can be used.

In the time domain fatigue analysis approach, the cumulative fatigue damage intensity and failure time are determined by considering the time-based stress response due to each excitation of the time-based random loading using the rainflow cycle counting technique, as shown in Figure 1-1. Although this approach elaborates a structure's response and behaviour for stationary and non-stationary random loads [7], it is computationally demanding, especially for large and complex structures with long-duration load history and considerable numbers of nodes to discretize.

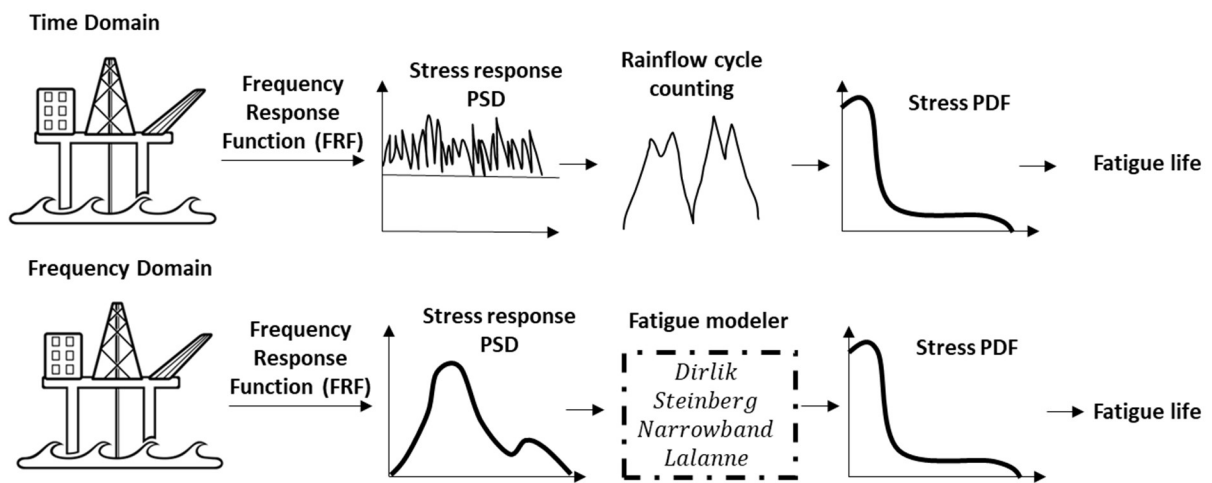


Figure 1-1: Time and frequency domain fatigue analysis approaches [5]

Conversely, in the frequency domain approach, a structure's loads and stress responses are considered in the Power Spectral Density (PSD) form. The PSD of the loading and the stress response, characterized by amplitude and frequency variables, exposes the energy content of the process over the random loading frequency range [6]. Fatigue damage of a structure is then calculated by accumulating the damage caused by each stress spectral component using any stochastic fatigue models. Unlike the time domain approach, the frequency domain approach does not require a structure's lifetime random loading condition history, making it more computationally efficient. The fatigue life of welded structures in automotive, aerospace, and offshore industries

exposed to Gaussian and stationary road random loadings having frequency spectrums close to their natural frequencies are preferably and accurately evaluated using the frequency domain fatigue analysis approach. This is because the frequency domain approach considers statistical techniques to represent the probabilistic nature of the random loading process and includes the frequency response function (FRF) parameter to describe the severe effects of the dynamic properties response in the calculated PSD stress and cumulative damage. Although not as uniquely and extensively developed as the time and frequency domain fatigue analysis approaches, the time-frequency domain fatigue analysis approach combines the time and frequency domain techniques to evaluate the damage and life of welded components and structures exposed to non-stationary random loading conditions such as automotive engine, helicopter rotors and wind turbine blades vibrations [6]. This approach involves the characterization of the non-stationary random loading and structural response in the time-frequency domain, thereby enabling the identification of the most damaging frequency component in the load history and stress response spectrum. The fatigue damage of a structure is evaluated for each frequency component using similar approaches considered in the frequency domain fatigue analysis approach.

1.2 Stresses at the Welded Joints

As already stated, to determine the fatigue life of welded structures, the complete stress state within and around the welded joints is required; thus, they must be extrapolated. Traditional methods for evaluating weld toe stress include nominal, hotspot, and notch weld stress evaluation methods [8]–[10]. Studies and research in works of literature on fatigue analysis of welded structures in the frequency domain [6], [11], [12] are based on the use of any of these traditional methods for evaluating the weld toe stress PSD.

The weld toe stresses calculated using the nominal stress extrapolation method are based only on direct load effects and are extracted from locations outside the weld toe region [8]. Therefore, the calculated stresses do not include local stress concentrations due to defined weld toe notches and joint geometry raiser effects, which are already included in S-N curves. Thus, this method is only suitable for structures with simple joint geometry and no combined load modes.

The hotspot stress extrapolation method is an improvement on the nominal stress extrapolation method and is the most widely used method. It provides a more accurate stress value by including stress raiser effects due to welded joint geometry and notches not categorically defined by relevant standards [10]. However, it excludes the nonlinear peak stress caused by weld toe notches. This method is suitable for simple and complex structures but is limited by the dependence of the calculated stress concentrations on unique welded joint geometry and loading modes. This dependence requires the selection of many different S-N curve plots from experimental test data for structures with multiple welded joints and loading modes.

The notch stress extrapolation method includes all stress raiser effects due to geometrical discontinuities, weld toe and root notches, excluding the peak stress effect due to welded joint geometry already accounted for in the experimental S-N curve test data [9], [13]. Local sub-modelling and extreme mesh refinement are required in using this method in FE fatigue analysis. Hence, applying this method in large and complex structures becomes practically impossible.

The traditional methods for evaluating weld stress have their advantages, but they also pose challenges in accurately characterizing weld toe stress concentration variations with welded joint geometry, loading modes, and the selection of appropriate S-N curves. Consequently, these challenges can lead to varying accuracy in the predicted fatigue damage crack location and life.

This issue is particularly significant in FE fatigue analysis, where mesh properties highly influence the local weld toe stress concentrations.

An alternative method called the Equilibrium Equivalent Structural Stress (EESS) [14]–[17] has been developed to overcome some of the challenges and limitations associated with the use of traditional weld stress evaluation methods. This approach characterizes the weld toe stress concentrations using an equivalent stress-based parameter that consolidates a large amount of S-N test data into a single, narrow scatter band. In addition, a unique master S-N curve [18], [19] for welded structures is also developed using this method. Using the master S-N curve and the calculated EESS - which is insensitive to the mesh properties of FE models, the accuracy of the evaluated weld stress, predicted fatigue damage crack location and life of welded structures prior to damage crack initiation are significantly improved.

1.3 Motivation

The Equilibrium Equivalent Structural Stress (EESS) method has been widely recognized and utilized in various welding-related industries and research. This method has primarily been used for analyzing the fatigue behaviour and life of welded structures under constant amplitude cyclic uniaxial [20]–[23] and multiaxial [24], [25] loads. Researchers have also modified the procedure for spot welded structures [26]–[28] and evaluated welded structures exposed to variable amplitude or random loading conditions [29], [30] using time domain fatigue analysis based on the path-dependent maximum range approach.

However, there is currently no established method for applying the EESS method to welded structures whose fatigue behaviour and life are predicted using the frequency domain fatigue

analysis approach. Therefore, there is a need to develop a frequency domain fatigue analysis procedure that integrates the EESS stress and damage evaluation equations and methods.

This research proposes modifications to the EESS formulations. These modifications will extend the application of the EESS method's weld stress concentration characterization, mesh insensitivity, and master S-N curve properties to welded structures exposed to random fatigue. The proposed modification involves evaluating the stress probability density function (PDF) and fatigue damage due to calculated EESS power spectral density (PSD) responses. The EESS PSD responses are based on stationary random loading input conditions and structural dynamic frequency response functions. In addition, a new frequency domain approach will also be developed, incorporating the proposed EESS PSD response and master S-N curve parameters for fatigue analysis of welded structures. This approach will improve the accuracy of the predicted damage crack location and life of welded structures and improve computational efficiency by eliminating the need for extreme mesh refinement in the FE model.

1.4 Objectives

As already explained, the EESS equations and procedures cannot be directly used for those welded structures where the random loading and corresponding responses are evaluated directly in the PSD form. It, thus, becomes imperative to modify the static EESS stress and fatigue damage evaluation equations using the mode superposition technique to adapt it to the specificity of the frequency domain fatigue analysis procedural approach. Specific steps are required to achieve the research's overall goals. Therefore, the objectives of this research are to:

1. Develop equations for evaluating welded structures' EESS-based frequency response function and PSD response due to random loading.

2. Propose a frequency domain fatigue analysis computational procedure incorporating the EESS-based FRF, stress PSD equations, and the master S-N curve to predict the fatigue damage crack location and life of welded structures prior to damage crack initiation.
3. Numerically verify the proposed frequency domain fatigue analysis method using a rectangular hollow section (RHS) welded T-structural frame exposed to road surface profile-induced ergodic stationary random loadings.
4. Compare the accuracy of the computed fatigue stress, damage crack location, and life results of the developed methodology with those of the established hotspot method and experimental fatigue damage data to determine its significance, utility, and potential variability to existing fatigue evaluation methods.

1.5 Thesis Structure

The structure of the thesis is as follows:

Chapter 1 discusses the background and theories related to fatigue loadings, failures, and life evaluation approaches of welded structures. The motivations for proposing alternative techniques for evaluating the stress at the weld toe are also enumerated. Finally, the objectives of the research and thesis structure are presented.

Chapter 2 provides a comprehensive review of the existing literature on fatigue assessment of randomly loaded welded structures. The traditional stress evaluation methods, PSD stress cycle counting models, fatigue damage and life estimation in the frequency domain fatigue analysis approach are more elaborately discussed. In addition, the challenges and shortcomings associated with these methods, particularly the stress evaluation methods, are discussed.

Chapter 3 presents the development of the analytical equations and computational procedures that comprise the framework of the proposed frequency domain fatigue analysis method for predicting the fatigue damage and life of welded structures prior to damage crack initiation under random loading. The data, assumptions, theoretical equations, and models for developing the proposed equations and methodology are discussed. It also extends the development of the main equations and procedures to determine EESS-based equations to evaluate welded structures' modal stress response and frequency response function.

Chapter 4 numerically implements the proposed EESS equations and EESS-based frequency domain fatigue analysis procedure for a welded rectangular hollow section (RHS) structure exposed to stationary random loadings using a combination of MATLAB and ANSYS software. In addition, the chapter discusses the implications of the fatigue stress, damage, and life results in detail and validates the proposed methodology results with experimental fatigue damage data in the literature and hotspot method results for further interpretations.

Chapter 5 summarizes the research and results and briefly discusses inferences from the results. The chapter also provides future recommendations related to the research study.

2 Literature Review

This chapter provides a comprehensive review of the existing approaches and literature on fatigue assessment of randomly loaded welded structures. Specifically, the fundamental theories of the traditional stress evaluation methods, stress PSD cycle counting models, fatigue damage and life estimation considerations in the frequency domain fatigue analysis approach are briefly discussed to provide some background to the concepts proposed in Chapter 3. In addition, the challenges and shortcomings associated with using the traditional stress evaluation methods leading to the problem addressed in this research are discussed.

2.1 Random Loadings in Fatigue Assessment of Welded Structures

As explained in Section 1.1, assessing the fatigue behaviour and life of structures requires a comprehensive knowledge of the cyclic loading history category to which they are subjected; random loading has been identified as one of the characterized loading categories leading to structural fatigue.

Random loadings exhibit time-varying amplitude, frequency, and phase characteristics [12], which cannot be directly predicted using the deterministic fatigue equations. These loadings can be classified into two categories: stationary random loads and non-stationary random loads. In the case of non-stationary random loading, although the statistical properties can be deterministically approximated over a short windowed period (e.g., seconds, hours, or days), they are not constant throughout the entire duration of the load history [31]. Therefore, the fatigue assessment of structures exposed to these loadings primarily uses the time or time-frequency domain fatigue analysis approaches. On the other hand, stationary random loadings have statistical properties such

as average values, ensemble, auto-correlation function, and probability distribution, which are constant and deterministic throughout the lifetime exposure duration. Furthermore, the stationarity property of the loading and the corresponding stress response enables their characterization using the PSD, which is essential for evaluating the fatigue of structures using the frequency domain fatigue analysis approach.

Stationary random loadings can also be ergodic and represented by the Gaussian distribution process. In this process, the random loading variables follow a normal distribution characterized by its mean μ_X and variance σ^2_X [12] properties. The ergodicity of these loads arises from the equality of the statistical average and time average values. Stationary random loadings can be further classified according to their energy content (PSD) characteristics and distribution across the loading frequency range [32]. This classification, which includes the narrow band, wide band, sine sweep, and white noise processes, as depicted in Figure 2-1, is crucial in determining a structure's appropriate stress response cycle counting and fatigue damage estimation strategies.

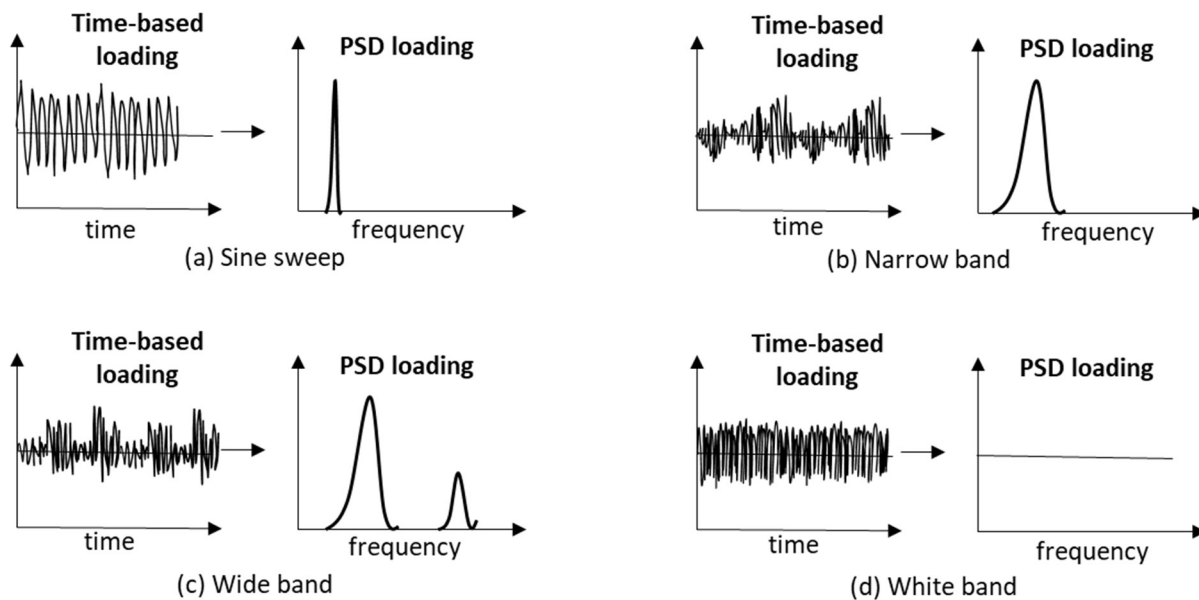


Figure 2-1: Typical stationary random loadings time histories and PSDs of structures [5]

For fatigue analysis in the frequency domain, the time-based stationary random loadings history is transformed into the PSD form ($unit^2/Hz$) mainly using the Fast Fourier Transform (FFT). The loading in PSD form reduces the randomness in a structure's response without sacrificing the inherent random properties effects of the loading [31]. It is important to note that the phase information of the loading is disregarded in this process. In this research, Equation (2.1) [32] represents the specific implementation of the Fast Fourier Transform used to convert the time-domain random loading to the frequency domain PSD loading.

$$G(f) = \frac{1}{2\pi} \int_{-\infty}^{\infty} R_X(t) e^{-i\omega t} dt \quad (2.1)$$

Where f denotes the frequency of the load in Hz and $R_X(t)$, the auto-correlation function of the random loading in the time domain defines the similarity measure between time-shifted loading samples as given by Equation (2.2) [31].

$$R_X(t) = \frac{1}{2T} \int_{-\infty}^{\infty} X(t) X(t + T) dt \quad (2.2)$$

In practical scenarios, many random loadings encountered in real life, such as wind, ocean waves, and vibration loads, typically have energy content values across a broad frequency range [31], [33]. Usually, the time histories of this loading class can be effectively approximated using the wide band PSD loading in the frequency domain, as depicted in Figure 2-1 (c). In the scope of this research, the fatigue analysis of a welded structure is conducted in the frequency domain using a wide band stationary random loading characterized by ergodic and Gaussian properties [34]. The subsequent section explains the main procedures and equations for analyzing welded structures' fatigue response and damage using the frequency domain approach.

2.2 Fatigue Analysis of Welded Structures in the Frequency Domain

The frequency domain fatigue analysis considers a structure's stationary random loadings and the resulting stress response in their condensed PSD form. A structure's fatigue damage is subsequently assessed by accumulating the damage caused by each spectral stress component across the loading frequency range using stochastic fatigue models.

When used during the design stage [12], the frequency domain fatigue analysis approach enables the identification and mitigation against extremely critical resonant loading frequencies that can lead to severe fatigue damage. In the frequency domain fatigue analysis, a structure's response is considered without including the effects of any material and geometric nonlinearities. Hence, a structure's dynamic behaviour and response to random loadings can be mainly defined and governed by its Frequency Response Function (FRF).

The FRF of a structure can be determined through frequency response analysis in FEA-based fatigue analysis or physical tests for the whole structure or only at specific locations of interest [35]. The frequency response analysis involves applying a unit input load and examining the resulting displacement, acceleration or stress response across different directions and frequency spectrums. Notably, the FRF is not dependent on a structure's input loading magnitude but solely determined by its structural stiffness K , damping C , and inertia M properties. Hence, the FRF is a deterministic parameter that relates the input loading PSD to the output stress PSD at specific locations of a physical or FEA model representation of a structure, as illustrated in Figure 2-2.

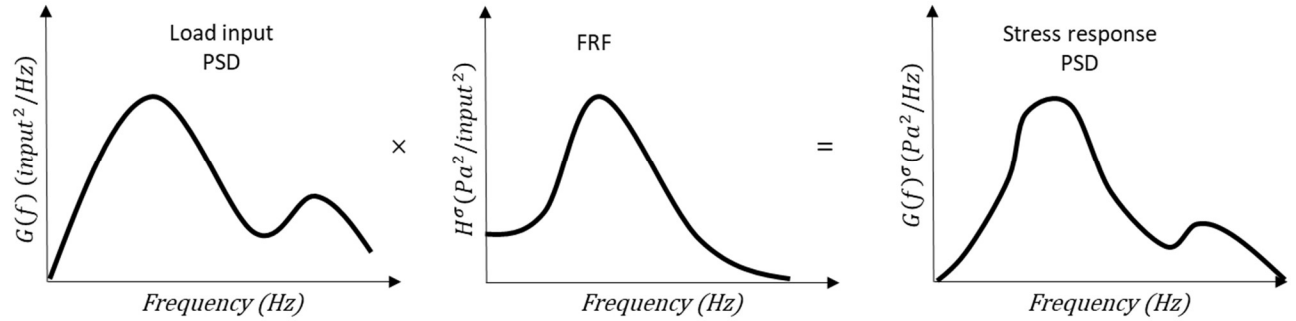


Figure 2-2: Stress response PSD calculation from Input loading PSD and FRF

By analyzing the FRF, valuable insights can be gained into a structure's behaviour and ability to withstand fatigue loading.

2.2.1 Stress Response Evaluation and Extrapolation

Fatigue damage in the form of crack initiation and propagation typically occurs at stress raiser locations, such as the weld toes and geometrical notches present in a structure [8]. In random fatigue analysis, a structure's welded joints' nonlinear stress response state exhibits inherent random variations over time due to the random nature of the applied loads. Like the loading, the stress responses of a structure are represented in the PSD form.

The nonlinear peak stress PSD at the welded joint locations can involve uniaxial normal stresses σ_{\perp} (tension or compression) acting along orthogonal directions or shear stress components – τ_{\perp} and τ_{\parallel} acting on the weld throat planes, represented by a 3×3 stress tensor in three-dimensional structures [12], [36], as shown in Figure 2-3. These welds' stress state significantly influences and dominates the welded joints' fatigue crack damage. Uniaxial stresses can be directly calculated by multiplying the FRF response variables matrix with the input loading PSD matrix. The individual stress PSD components are determined once the FRF of a structure is calculated for a known random loading condition, utilizing Equation (2.3) [12].

$$[G^\sigma(f)] = [H^\sigma(f)]^* \cdot [G(f)] \cdot [H^\sigma(f)]^T \quad (2.3)$$

Where, $[G(f)]$ denotes the random load input matrix for all the load application directions and $[H^\sigma(f)]^*$ and $[H^\sigma(f)]^T$ are the complex conjugate and transpose of a structure's FRF, respectively.

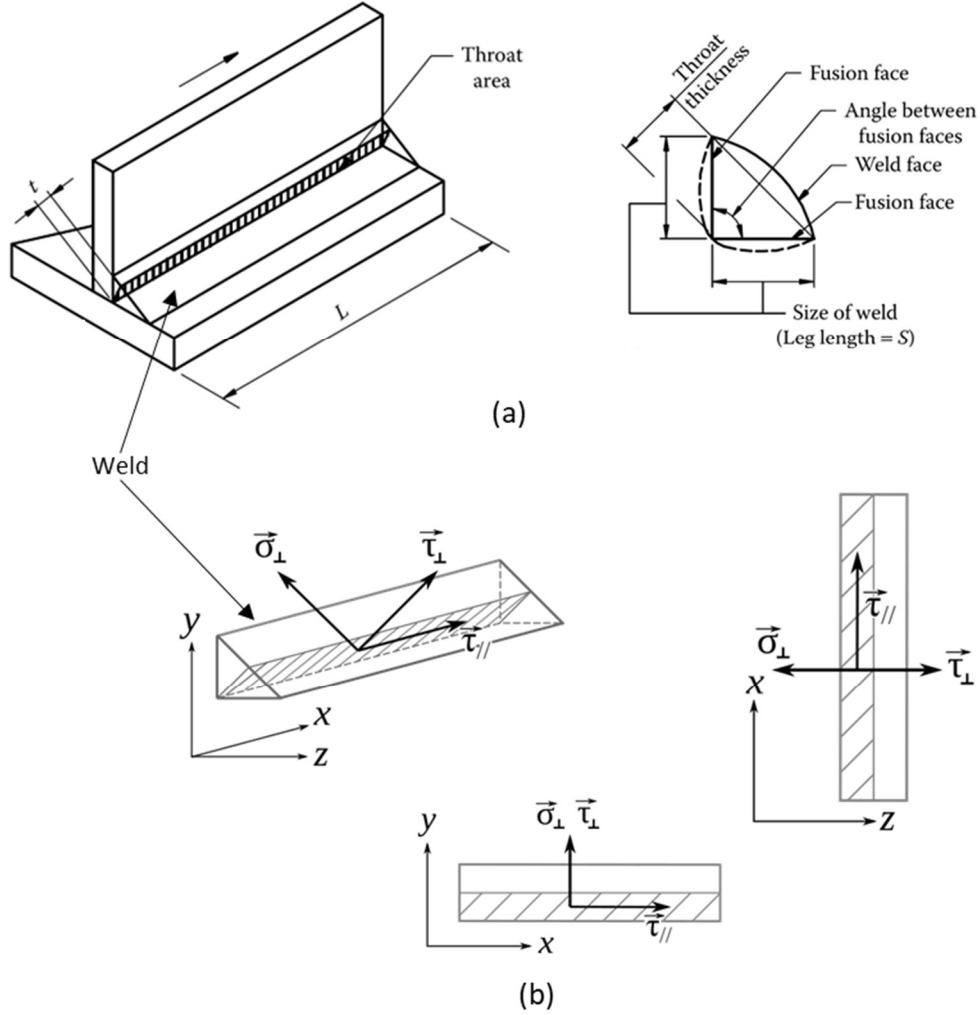


Figure 2-3: Fillet weld stress state: (a) Throat area and leg size (b) stress components in a weld

(Adapted from [1])

However, based on the nature of the welding processes and random loadings, the stress PSD at the welded joints of structures is complex and multiaxial. The Equivalent Von-Mises (EQVM) equation proposed and developed by Pitoiset, Equations (2.4) - (2.6), [36] is considered the most

reliable and suitable method for calculating the random multiaxial principal or equivalent Von-Mises stress PSD at the weld joints in frequency domain fatigue analysis. It is based on the characterization of the multiaxial stress PSD $G_{eq}^\sigma(f)$ by an equivalent uniaxial stress PSD.

The EQVM method is implemented in commercial FEA software for fatigue analysis. First, the normal and shear stress PSD components are calculated and extracted from FEA mesh models. Then, using the EQVM equation, the complex multiaxial stress responses at the welded joints can be effectively represented and assessed in the frequency domain fatigue analysis.

$$[G_{eq}^\sigma(f)] = \begin{bmatrix} G_{xx}^\sigma(f) & \dots & G_{xz}^\sigma(f) \\ \vdots & G_{yy}^\sigma(f) & \vdots \\ G_{zx}^\sigma(f) & \dots & G_{zz}^\sigma(f) \end{bmatrix} \quad (2.4)$$

$$[G_{eq}^\sigma(f)] = \text{trace}(QG^\sigma(f)) = G_{xx}^\sigma(f) + G_{yy}^\sigma(f) - \text{Re}(G_{xy}^\sigma(f)) + 3G_{xy}^\sigma(f) \quad (2.5)$$

Where:

$$Q = \begin{bmatrix} 1 & -0.5 & -0.5 & 0 & 0 & 0 \\ -0.5 & 1 & -0.5 & 0 & 0 & 0 \\ -0.5 & -0.5 & 1 & 0 & 0 & 0 \\ 0 & 0 & 0 & 3 & 0 & 0 \\ 0 & 0 & 0 & 0 & 3 & 0 \\ 0 & 0 & 0 & 0 & 0 & 3 \end{bmatrix} \quad (2.6)$$

The planar stress constant matrix state is denoted by Q, $G_{xx}^\sigma(f)$, $G_{yy}^\sigma(f)$ and $G_{zz}^\sigma(f)$ are the normal PSD stress tensor components and $G_{xy}^\sigma(f)$, $G_{xz}^\sigma(f)$, $G_{yz}^\sigma(f)$, $G_{zx}^\sigma(f)$, $G_{zy}^\sigma(f)$ and $G_{yz}^\sigma(f)$ are the shear PSD stress tensor components.

In this research, the EQVM method is employed in Chapter 4 to perform a structure's hotspot stress PSD verification analysis. However, this method is not applicable for determining the

equivalent Effective Equivalent Stress Spectrum (EESS) PSD at the weld joints. A more detailed explanation is provided in Section 2.3 of this document.

Unlike in unwelded components or structures where the calculated stress PSD responses can be directly used in fatigue equations and models for estimating fatigue life, welded components and structures require a method to characterize and extrapolate the stress PSD response at the weld toe and root. Therefore, it is crucial to carefully consider selecting an appropriate method for evaluating and extracting these nonlinear and complex stresses, as the calculated weld stress values significantly impact the predicted fatigue damage and life of welded structures. In the frequency domain fatigue analysis of welded structures, traditional methods such as nominal stress extrapolation method, hotspot stress extrapolation method, and notch stress extrapolation method [8]–[10] describe and evaluate the stress PSD response within and around the welds.

2.2.1.1 Nominal Stress Extrapolation Method

The nominal stress extrapolation method is the most basic and straightforward approach for extrapolating the stresses within and around the welds of welded steel structures. It is primarily suitable for structures with simple welded joint geometry and loads, where shear deformation effects are minimal or nonexistent at the plane of the welded joints [8]. In this method, the extrapolated weld toe nominal stress PSD $G_{eq(ns)}^{\sigma}(f)$ is calculated and extracted from the cross-sections of a structure away from the weld toe region. The nominal stress PSD can be extrapolated directly from mesh elements or nodes in FE fatigue analysis, as illustrated in Figure 2-4. Alternatively, classical structural mechanics principles, such as axial tension, compression and bending theories and equations, can be employed in analytical calculations to determine the nominal stress PSD.

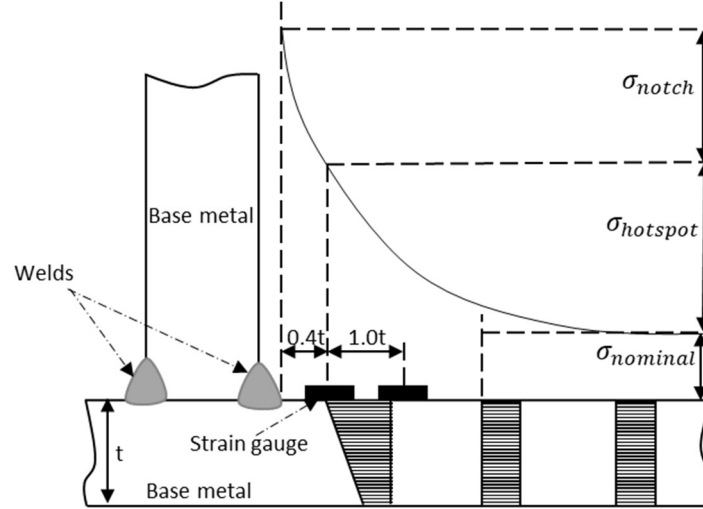


Figure 2-4: Stress extrapolation approaches at the welded joint location

However, the application of the nominal stress extrapolation method is limited by the lack of consideration of the stress concentration effects caused by welds and geometrical cross-section notches in the extrapolated stresses used for comparing against S-N curves to determine the fatigue life of welded structures. Furthermore, while fatigue classes for different weld joint categories, details, thicknesses, and loading modes are defined in guidelines and codes [10], [17], [37], the nominal stress extrapolation method cannot be applied to most large and complex structures with numerous welded joints due to lack of actual S-N curve for some weld details.

2.2.1.2 Hotspot Stress Extrapolation Method

The weld stress calculated in the hotspot stress extrapolation method includes the stress concentration effects caused by both the weld joint details and the geometric cross-section notches and discontinuities disregarded in the nominal stress extrapolation method [10]. In this method, the hotspot stress PSD $G_{eq(hs)}^{\sigma}(f)$ at the welded joints is extrapolated linearly or quadratically in FEA or physical test from the surface of the welded structural component's cross-section [37]. In FEA, a refined mesh is required to extrapolate the hotspot stress mesh nodes and elements

accurately. The quality of the FE model mesh significantly affects the magnitude and distribution of the stresses around the modelled weld region, as these stresses are in areas of the structure with high strain gradients. Consequently, the fatigue damage and life results obtained using this approach are highly influenced by meshing characteristics and the expertise of the engineer or researcher.

Several fatigue design guidelines and codes for welded structures define the weld's stress recommended reference point distances and extrapolation techniques, typically $0.4t$ and $1.0t$ away from the weld toe, as shown in Figure 2-4, where 't' represents the thickness of the adjoining structural members. Some variations in the predicted fatigue damage and life of welded structures arise from these different considerations in calculating the weld's hotspot stress. The recommendations of the International Institute of Welding (IIW) [37] are widely recognized as the most comprehensive and applicable guidelines among the traditional stress extrapolation methods. Equations (2.7) for linear elements and (2.8) for higher-order elements provided in the IIW recommendations are commonly used to extrapolate the hotspot stress $G_{eq(hs)}^\sigma(f)$ from reference points at welded joints in fatigue evaluations. These equations are considered for the extrapolation of the weld's hotspot stress response PSD that is compared to the results of the proposed methodology developed in this research in Chapter 3 of this document.

$$G_{eq(hs)}^\sigma(f) = 1.67 \times G_{0.4t}^\sigma(f) - 0.67G_{1.0t}^\sigma(f) \quad (2.7)$$

$$G_{eq(hs)}^\sigma(f) = 1.5 \times G_{0.5t}^\sigma(f) - 0.5G_{1.5t}^\sigma(f) \quad (2.8)$$

Where, $G_{0.4t}^\sigma(f)$, $G_{1.0t}^\sigma(f)$, $G_{0.5t}^\sigma(f)$, and $G_{1.5t}^\sigma(f)$ represents stresses at the indicated reference points from the weld toe, and t denotes the adjoining structural members' minimum thickness.

The hotspot stress extrapolation method provides an improved and more accurate estimation of the weld's stress state compared to the nominal extrapolation stress method. It is widely used and suitable for simple and large structures with complex fatigue loading conditions and multiple welded joints involving plates, angles, channels, and beam sections. However, it is essential to note that this method does not consider the local weld toe notch stress raiser effects and stress distribution across the thickness of the structural components.

Camilla et al. [11] utilized the hotspot stress criterion to extrapolate the multiaxial random stress field of an agricultural arm sprayer's welded tubular T-joints structure under multiaxial random loading. The fatigue damage and life of the structure were determined using Dirlik's cycle counting and damage estimation equations without including tubular member thickness variation influence on the weld's nonlinear peak stress. The welding process-induced residual stress effect on the extrapolated weld's hotspot stress of welded orthotropic steel decks was investigated by Wang et al. [35]. They observed a linear and exponential increase in weld stress with load magnitude and frequency, highlighting the significant contribution of residual stress to crack initiation at the weld toe. Adam and Michal [38] proposed two frequency domain methods that consider the impact of mean stress on the calculated weld stress and subsequent fatigue life estimation of welded steel plate structures. The correction methodology is based on transforming the hotspot mean stress PSD using time domain mean stress compensation models.

2.2.1.3 Notch Stress Extrapolation Method

The notch stress extrapolation method was developed to improve the nominal stress extrapolation and hotspot stress extrapolation methods, aiming to address their limitations. By considering the macro-geometrical features, weld details, and stress concentration effects from notches in the

weldment, the extrapolated notch stress PSD $G_{eq(nots)}^\sigma(f)$ provides a more comprehensive representation of the stress state at the weld toe and root [9]. These considered parameters improve the accuracy in calculating fatigue stress and predicting the fatigue life of welded structures, based on the appropriate S-N curve selection.

In the notch stress method, the Neuber rule [13] is applied to model the weld toe notch details using a fictitious radius of 1mm when the plate thickness exceeds 5mm. This rule is utilized in FEA to account for the localized stress concentration effects. A well-grinded and peened weld toe is employed in physical fatigue tests to facilitate the placement of strain gauges, as depicted in Figure 2-5. Due to the need for detailed modelling of the local weld toe and the requirement for extreme mesh refinement in fatigue FEA, the notch stress extrapolation method application is typically limited to local sub-models that represent critical fatigue failure locations in welded structures. Similar to the nominal and hotspot stress methods, the notch stress σ_{nots} is extrapolated from the surface of the welded structural component's cross-section in fatigue FEA and tests without considering the through-thickness stress distribution.

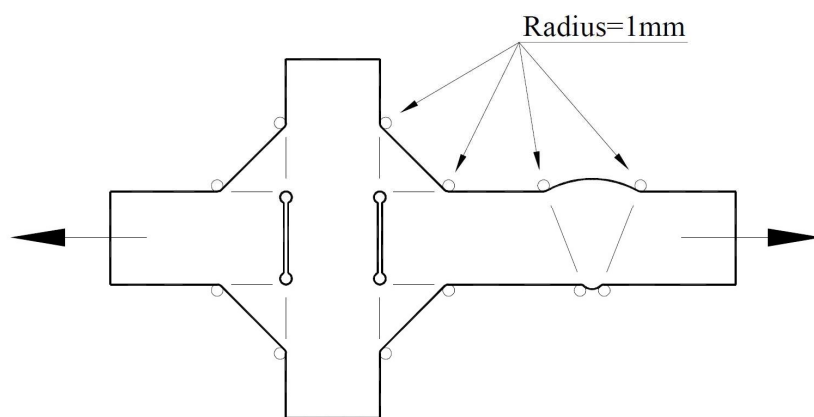


Figure 2-5: Notch stress state and definition at the welded joint location [37]

2.2.2 Stress Response Cycle Counting and PDF

The Probability Density Function (PDF) $p(S)$ of the cyclic stress range amplitudes are required to determine the fatigue damage and life of the welded structure. The PDF describes the likelihood of different stress ranges occurring within the frequency spectrum and is mainly characterized by the stress spectral moments m_n [31].

The spectral moments are calculated from the nominal $G_{eq(ns)}^\sigma(f)$, hotspot $G_{eq(hs)}^\sigma(f)$ or notch $G_{eq(nots)}^\sigma(f)$ stress response PSD extrapolated from the welded joint location depending on the specific stress consideration for design. The spectral moments calculation from the single-sided hotspot stress PSD, $G_{eq(hs)}^\sigma(f)$ as shown in Figure 2-6 is given by Equation (2.9), [32].

$$m_n = \int_0^{+\infty} f^n G_{eq(hs)}^\sigma(f) df \quad (2.9)$$

Where, $G_{eq(hs)}^\sigma(f)$ (Pa^2/Hz) represents the single-sided hotspot stress PSD at a frequency value of $f^n(Hz)$ and df denotes the frequency increment.

To calculate the stress PDF and subsequent fatigue damage of a structure, only the first four spectral moments m_0, m_2, m_3 and m_4 are required [32].

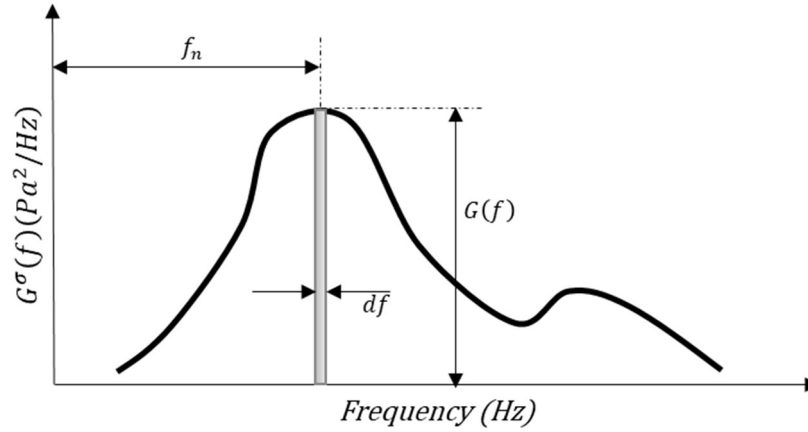


Figure 2-6: Stress spectral moments determination from stress PSD

The PDF of stress amplitudes is determined using cycle counting techniques and damage models in the frequency domain fatigue analysis. Fatigue damage models, such as Dirlik, Lalanne, Narrow band, and Steinberg [32], are commonly used to calculate the PDF based on the calculated spectral moments, depending on the characteristics of the random loading as described in Section 2.1.

Initially proposed by Bendat in 1964 [39], the Narrow band model predicts the stress amplitude PDF within a specific stress range of interest and is suitable for random loadings and stress responses within limited frequency ranges. The Steinberg damage model is closely related to the Narrow band model and assumes that the PDF of stress peaks is the same as the PDF of the entire stress distribution. Therefore, it calculates the stress PDF for stress cycle ranges within $1 \times \text{RMS}$, $2 \times \text{RMS}$, and $3 \times \text{RMS}$, assuming that the number of cycles falls within those selected ranges 68.27%, 95.96%, and 99.73% of the time, respectively.

While the Bendat Narrow band and Steinberg models provide conservative results for broad band processes, Lalanne and Dirlik's models are suitable for estimating stress probabilities across a wider frequency spectrum. These models are beneficial for structures exposed to broad band

frequency random loading. The Lallane model extends the Steinberg model by modifying it to accommodate longer-time history random loadings. Dirlik's formulation, developed by Dirlik, is the most accurate and widely used fatigue damage model for broad band frequency spectrum loading. This research considers Dirlik's empirical cycle counting Equations (2.10) – (2.18) [39] for estimation of the stress cycle counting $p(S)$ and fatigue damage D .

$$p(S) = \frac{\frac{D_1}{Q} \cdot e^{\frac{-Z}{Q}} + \frac{D_2 \cdot Z}{R^2} \cdot e^{\frac{-Z^2}{2 \cdot R^2}} + D_3 \cdot Z \cdot e^{\frac{-Z^2}{2}}}{2 \cdot \sqrt{m_0}} \quad (2.10)$$

Where,

$$D_1 = \frac{2 \cdot (x_m - \gamma^2)}{1 + \gamma^2} \quad (2.11)$$

$$D_2 = \frac{1 - \gamma - D_1 + D_1^2}{1 - R} \quad (2.12)$$

$$D_3 = 1 - D_1 - D_2 \quad (2.13)$$

$$Q = \frac{1.25 \cdot (\gamma - D_3 - D_2 \cdot R)}{D_1} \quad (2.14)$$

$$Z = \frac{S}{2 \cdot \sqrt{m_0}} \quad (2.15)$$

$$R = \frac{\gamma - x_m - D_1^2}{1 - \gamma - D_1 + D_1^2} \quad (2.16)$$

$$\gamma = \frac{m_2}{\sqrt{m_0 \cdot m_4}} \quad (2.17)$$

$$x_m = \frac{m_1}{m_0} \sqrt{\frac{m_2}{m_4}} \quad (2.18)$$

The 0th, 2nd and 4th moment areas under the PSD curve, denoted by m_0, m_2 , and m_4 are determined from Equation (2.9), S represents the stress amplitudes, and γ denotes the irregularity factor with variability from 0 to 1 for wide and narrow band processes, respectively.

2.2.3 Fatigue Damage and Life Prediction Using the S-N Curve

The fatigue damage and life prediction of welded structures prior to damage crack initiation are predicted by comparing the evaluated stress range S to the number of cycles to failure N that is obtained from the material's welded joint S-N curve – derived from experimental fatigue test data. These tests involve subjecting the structure to constant amplitude cyclic axial, bending, or combined fatigue loads at various stress ranges.

2.2.3.1 Stress-Life (S-N) Curve

The S-N curve properties of welded structures for a given material property vary depending on factors such as weld joint geometry, loading modes, and thickness, primarily due to the peak stress concentration at the welds [4]. Consequently, a wide range of available S-N curves in design standards and codes cater to the design of complex welded structures with multiple welded joints.

A typical S-N curve for a single welded joint exhibits a linear inverse slope until it reaches a point where its orientation becomes horizontal, as illustrated in Figure 2-7. Welded structures that endure until the start point of the horizontal line, known as the "fatigue endurance limit," can withstand stress ranges below the horizontal line indefinitely. This fatigue endurance limit is often characterized by a fatigue life of at least 10^7 cycles.

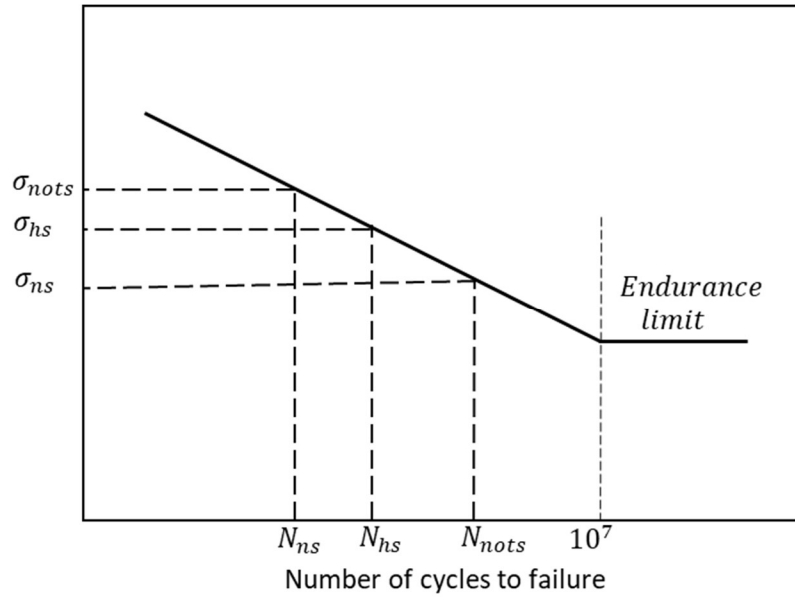


Figure 2-7: Typical S-N curve for welded steel structures under different weld stress categories

In many cases, obtaining detailed S-N curve data for all the welded joints in large and complex structures is impractical, and physical tests may not be feasible. As a result, engineers and researchers often rely on approximations based on their experience, which can lead to varying levels of accuracy in predicting fatigue damage and life. The EESS method, discussed in section 2.3, offers an alternative approach to address this limitation.

Resources such as the IIW standard [37] and works of literature provide S-N curves for different welded joint geometries and loading modes. These curves are based on the nominal, hotspot, or effective notch stresses and are derived from constant amplitude cyclic fatigue load tests on welded structures of varying yield strengths. Section 4.3 of this document considers the S-N curve details from IIW for the comparative hotspot stress extrapolation method analysis.

2.2.3.2 Fatigue Damage and Life Prediction

Since the 1920s and 1930s, various fatigue damage and life prediction models have been developed to estimate fatigue damage in welded and non-welded structures prior to damage crack initiation. These models include linear, nonlinear, two-stage linearization, life curve modification, continuum damage mechanics, and energy-based theories [40], [41].

In a comprehensive review of the existing fatigue damage theories, Fatemi and Yang [40] noted that the Palmgren-Miner's rule, initially developed by Miner in 1945 and later adopted by Palmgren, is the most commonly used and accurate linear accumulated damage estimation model in the industry, standards [2], and research. According to this model, the number of stress cycles n_i , experienced by a structure is compared to an appropriate allowable number of cycles to failure, N_i , obtained from S-N curve test data specific to the welded structure to determine the fatigue life of a structure.

For each stress cycle, the damage is calculated, assuming a linear structural response. The overall fatigue damage of a structure for the load exposure duration is then estimated by accumulating the individual stress range cycle damages without a specific ordering of the cycles using Equation (2.19) [41]. Palmgren-Miner's rule provides a framework for comparing the accumulated damage to a threshold safety factor value and assessing the fatigue life of a structure using Equations (2.20) and (2.21) based on this comparison.

$$D = \sum_{i=1}^k \frac{n_i}{N_i} \quad (2.19)$$

$$L_F = \frac{1}{D} \quad (2.20)$$

$$L_F \leq FDF \times L_T \quad (2.21)$$

Where D denotes the accumulated fatigue damage, n_i represents the load number of cycles at the stress range S_i , N_i is a structure's allowable number of cycles to failure at the stress range S_i , and k is the considered number of stress intervals. L_T and $FDF \leq \frac{1}{D}$ are the design life and fatigue design factors of the welded structure, respectively.

In frequency domain fatigue analysis, Miner's rule is adapted to estimate the damage of a structure per exposed loading frequency. This adaptation considers the stress spectral amplitudes S and stress probability density function $p(S)$ based on the cycle counting damage models described in Section 2.2.2 for random loading processes. Dirlik's damage model, based on the calculated stress probability density function from Equations (2.22) and (2.23) [32], is used to estimate the fatigue damage of a structure. A fatigue damage factor equal to or greater than 1.0 indicates failure and crack initiation at a structure's location for which the damage is calculated. The number of cycles versus stress range for the damage estimation is determined from the stress probability density function, which describes and represents a structure's response to the random loading.

$$D = \frac{E(P)T}{C} \int_0^\infty p(S) \cdot S^m ds \quad (2.22)$$

$$N(S) = E(P) \cdot p(S) \quad (2.23)$$

Where, $N(S)$ denotes the expected number of stress cycles range, T represents the total load exposure time for the damage, $E(P)$ is the expected number of peaks crossing per second from the stress response PSD output, S is the stress amplitude, ds is the incremental stress and m , and C are

the Basquin's exponent and intercept on the S-N curve, respectively, based on the material's property.

2.3 EESS Fatigue Evaluation Method for Welded Structures

The literature review conducted so far has discussed the main principles and equations of frequency domain fatigue analysis for welded structures subjected to random loadings. In addition, it has established the interrelationships and interdependencies between the stress PDFs, damage models, and life prediction models with the extrapolated component or EQVM stress PSDs.

However, the traditional methods for defining and evaluating the component or EQVM stress PSDs, as discussed in Section 2.2.1, and the criteria for selecting standard S-N curves for complex welded structures, as described in Section 2.2.3.1, have inherent challenges and limitations leading to varying accuracy in predicting damage crack location, and fatigue life of welded structures prior to damage crack initiation.

While surface stresses can adequately approximate the stresses in the welds of thin plates or beam structures, the through-thickness stress is essential for butt-welded connections and structural components with thicknesses equal to or greater than 20mm. Additionally, achieving the required mesh refinement for hotspot and notch methods, particularly in large and complex welded structures, becomes challenging and significantly increases FE model preparation time and computational requirements.

Based on the abovementioned issues, the Equilibrium Equivalent Structural Stress (EESS) method and its associated master S-N curve are proposed as an alternative for stress extrapolation and subsequent damage evaluation in this research. However, before addressing the shortcomings of

this method and its inapplicability in the previously described frequency domain fatigue analysis procedures, it is essential to review the principles and current applications of the EESS method in the following sub-sections.

2.3.1 Equilibrium Equivalent Structural Stress (EES)

The EESS fatigue assessment method for welded structures, developed by Dong in 2001 [16], offers an alternative to traditional fatigue assessment methods. The method involves computing the structural stress by decomposing the peak stresses at the weld toe – which are influenced by the weld thicknesses, loading modes and joint geometries, into balanced primary membrane stress σ_m bending stress σ_b and self-equilibrating nonlinear stress σ_{nl} as shown in Figure 2-8. The EESS parameter characterizes these peak stress concentrations, thus enabling mesh insensitive FE analysis and improved stress and fatigue life results accuracy. Initially developed for constant amplitude cyclic loadings, it has been primarily advanced for FE model shell elements rather than solid elements.

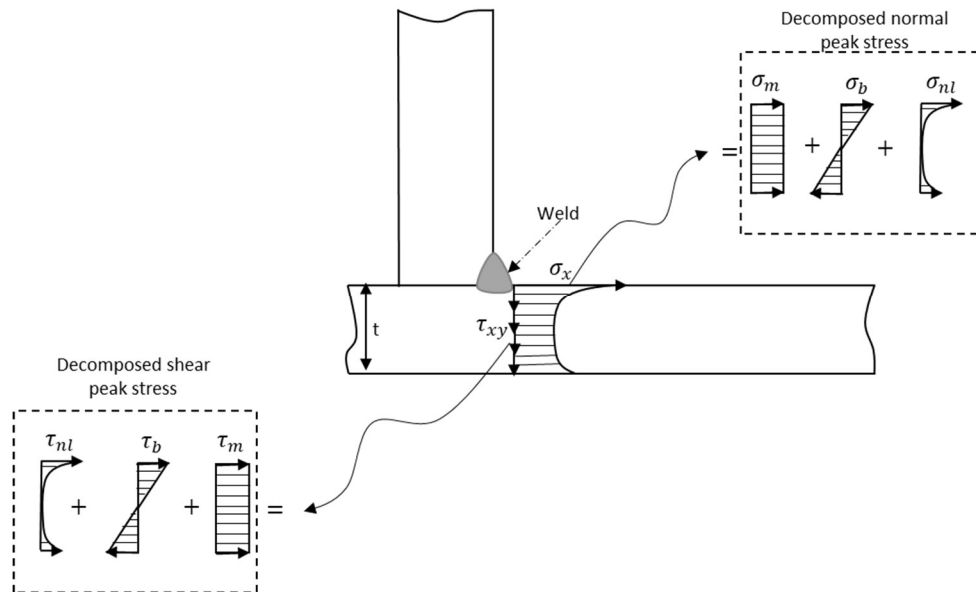


Figure 2-8: EESS method: weld through-thickness stress decomposition

The EESS method in FEA strictly requires modelling the welds using oblique plate shell or solid elements following the guidance stipulated in IIW [42]. The weld plane's normal structural stress σ_s , parallel shear structural stress τ_z , and perpendicular shear structural stress τ_s are calculated from the mesh nodes as shown in Figure 2-8 using Equations (2.24) - (2.26) [16], [18]. The stresses are based on the decomposed primary membrane and bending stresses. Comparison of structural stress results from both FE shell and solid model element types show close relations [14], [17], [19].

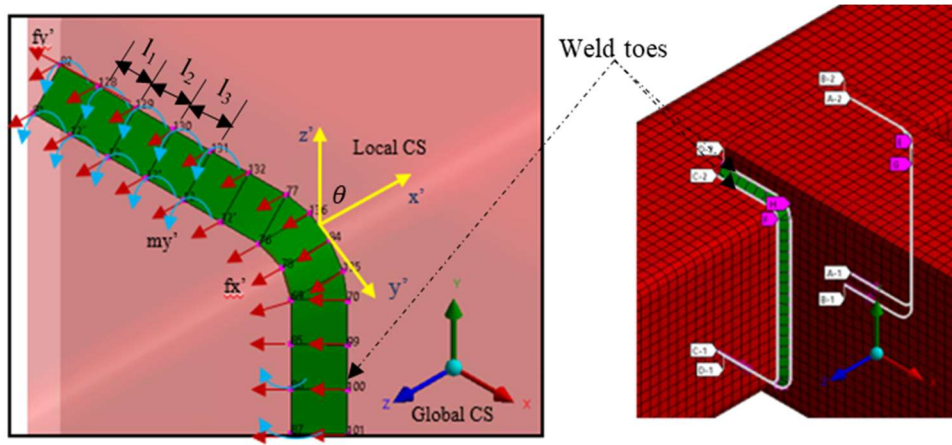


Figure 2-9: Structural stress definition and calculation procedures from FE model mesh elements

$$\sigma_s = \sigma_m + \sigma_b = \frac{f'_x}{t} + \frac{6m'_y}{t^2} \quad (2.24)$$

$$\tau_s = \tau_m + \tau_b = \frac{f'_y}{t} + \frac{6m'_x}{t^2} \quad (2.25)$$

$$\tau_z = \frac{f'_z}{t} \quad (2.26)$$

Where, t represents the weld thickness, σ_m and σ_b are the normal membrane and bending stresses extrapolated from the welded joints. The corresponding shear membrane and bending stresses are given by τ_m and τ_b respectively, and f'_x, f'_y and f'_z are the line forces along the weld mesh

element's local x-axis, y-axis and z-axis coordinate system, respectively, considering each adjacent node's contribution. The line moment values are denoted by m'_x, m'_y and m'_z .

The weld mesh elements' local line forces and moments are calculated from the mesh nodal forces and moments extracted directly from FE analysis in the global coordinate system. A matrix system of mesh elements lengths, global mesh nodal forces and moments of a structure is proposed by Dong [16] to transform the global coordinate node forces and moments into the local line force forces and moments along the local axis of the weld toe path.

$$\begin{bmatrix} F_1 \\ F_2 \\ F_3 \\ \vdots \\ \vdots \\ F_n \end{bmatrix} = \begin{bmatrix} \frac{l_1 + l_{n-1}}{3} & \frac{l_1}{6} & 0 & 0 & \dots & 0 \\ \frac{l_1}{6} & \frac{(l_1 + l_2)}{3} & \frac{l_2}{6} & 0 & \dots & 0 \\ 0 & \frac{l_2}{6} & \frac{(l_2 + l_3)}{3} & \frac{l_3}{6} & \dots & 0 \\ 0 & 0 & \ddots & \ddots & \ddots & 0 \\ \vdots & \vdots & \ddots & \ddots & \frac{l_{n-2}}{6} & \frac{(l_{n-2} + l_{n-1})}{3} \\ 0 & \dots & \dots & 0 & \frac{l_{n-1}}{6} & \frac{l_1 + l_{n-1}}{3} \end{bmatrix} \times \begin{bmatrix} f_1 \\ f_2 \\ f_3 \\ \vdots \\ \vdots \\ f_n \end{bmatrix} \quad (2.27)$$

Where $F_1 \dots F_n$ are the global nodal forces for nodes 1 to n, $f_1 \dots f_n$ are the elements line forces for nodes 1 to n and $l_1 \dots l_n$ are the mesh elements' lengths. The same calculation is repeated to produce the corresponding line moments.

The Equilibrium Equivalent Structural Stress (EESS) considers not only the weld toe stress concentrations but also the variation in structural component thickness and loading modes. It is calculated from the normal and shear structural stresses obtained from Equations Equations (2.24) - (2.26), using Equations (2.28) – (2.31) [19].

$$\Delta S_s = \frac{\sigma_s}{t^{*\frac{2-m}{2m}} \cdot I(r)^{1/m}} \quad (2.28)$$

Where,

$$I(r)^{1/m} = 0.0011r^6 + 0.0767r^5 - 0.0988r^4 + 0.0946r^3 + 0.0221r^2 + 0.014r + 1.223 \quad (2.29)$$

$$r = \frac{|\sigma_b|}{|\sigma_m| + |\sigma_b|} \quad (2.30)$$

$$t^* = \frac{t}{t_{ref}} \quad (2.31)$$

The local correction factor is represented by $I(r)$. While m denotes the hypothetical crack depth – with a value of 3mm and t^{ref} taken as 1mm is the reference plate thickness.

2.3.2 Master S-N Curve

The master S-N curve developed by Dong et al. [18], [22] is a single narrow band S-N curve derived from consolidating many experimental S-N curve data for various categories of structures. To develop the master S-N curve, more than 350 welded components fatigue test results published in literature dating back to 1940 and covering component thicknesses ranging from 2mm to 100mm, yield strengths between 180MPa and 600MPa, varying section profiles and weld joint details, and loading modes are considered. The fatigue life of a welded structure is subsequently evaluated by using the EESS parameter described by Equations (2.28) – (2.31) in conjunction with the master S-N curve's allowable number of cycles to failure N .

The fatigue damage and life evaluated using the master S-N curve eliminate the subjectivity often associated with using typical S-N curves for welded joints found in standards and literature,

resulting in improved accuracy in predicting fatigue life. The equations used for calculation are based on the mean curve characteristics with statistical parameter variation as given by Equation (2.32) [18].

$$N = \left(\frac{\Delta S_s}{C} \right)^{\frac{1}{h}} \quad (2.32)$$

Where C and h are constant statistical parameters derived by curve fitting using regression analysis from large experimental test data on the S-N curve with values as provided in Table 2-1.

Table 2-1: Master S-N curve parameters [43]

Statistical basis	C	h
Mean	19,930	- 0.3195
+2 σ	28,627	
-2 σ	18, 876	
+3 σ	34,308	
-3 σ	11,578	

The efficacy and robustness of the EESS method in predicting the fatigue life of welded structures was first demonstrated internationally by Dong and Kyuba [19] in the 2005 SAE fatigue design and evaluation competition. In this competition, participants utilized various fatigue assessment methods to predict the fatigue life of a welded rectangular hollow section structure subjected to constant amplitude cyclic loading. Among all the methods used, the EESS method provided accurate predictions of the anticipated damage crack initiation location and mean fatigue life of a structure. Subsequently, the EESS method has been extensively applied in assessing constant amplitude cyclic loading for various types of welded steel structures, including seam-welded plates, cylindrical structures, beams, and hollow sections. These applications have been studied

under both uniaxial and multiaxial stress conditions, as documented in works of literature [20], [21], [23]–[25]. Researchers have investigated the calculation of the EESS in FEA solid model simulations by extracting nodal forces and moments from FE models of welded rib-to-deck connections of orthotropic steel decks [23] and full-scale welded thin-walled tubular structures [43].

Spot welds in thin sheet steel plates used in aircraft and automotive structures are primarily subjected to shear forces, which are influenced by their characteristics, size and geometry. As a result, the analysis of spot weld structures differs from that of seam-welded structures. Dong and Kang [26] introduced a numerical procedure based on the tensile-shear and coach-peel principles to apply the EESS method for stress analysis and fatigue life prediction of individual spot-welded structures. Subsequently, this method was further enhanced in [27] and [44] to accommodate complex loading conditions in multiple spot-welded structures.

Zhang et al. [29] extended the application of the EESS method to randomly loaded structures in the time domain by evaluating the fatigue life of a seam-welded support roller of a tracked vehicle exposed to road surface-induced spectral loads. The FEA predicted results were compared to those obtained from tensile cyclic fatigue tests conducted on plate steel samples. Similar EESS stress evaluation approaches were also adopted by Zhao et al. [45] and Chen et al. [46] to predict the fatigue damage and life of steel building structures exposed to wind loading and truck mixer sub-frame, respectively. Also, Tan et al. in [47] proposed a fatigue reliability prediction model for welded drive axle housing based on the EESS method. A median damage-random threshold rule, which reduces the computational cumbersomeness attributed to the randomness of fatigue life and failure prediction of welded under variable amplitude loading, was established and experimentally verified.

These studies utilized the time domain fatigue analysis technique to evaluate the EESS stress response for a single unit loading. The linear structure response assumption was made, and the EESS stress responses due to the entire load spectrum were calculated by scaling the structures' unit load response. The structures' dynamic characteristics were not considered, as these analyses were based on a quasi-static approach, allowing for the direct use of the EESS equations.

2.4 Summary of the Literature Review

The literature review discussed the fundamental principles and considerations of frequency domain fatigue analysis for welded structures exposed to random loadings in Sections 2.1 and 2.2. In addition, it highlighted the limitations of traditional weld stress extrapolation methods, justifying the need for alternative approaches leading to introducing the EESS fatigue assessment methods in Section 2.3 as a potential alternative for this research.

The equations and procedures of the EESS method presented in Section 2.3 were initially developed for constant amplitude cyclic loading applications and are not directly applicable to frequency domain fatigue analysis. To calculate the dynamic stress spectral response $G^{\sigma}(f)$ at the weld locations, it is necessary to consider the dynamic response characteristics, such as the Frequency Response Function (FRF) of a structure and the loading PSD, as explained in Section 2.2.1. Similarly, the master S-N curve fatigue life prediction equation presented in Section 2.2.2 cannot be directly used for fatigue life prediction in the frequency domain, which requires stochastic models and equations for stress Probability Density Function (PDF), damage, and life evaluation as established in Sections 2.2.2 and Section 2.2.3.

Modifications are proposed to the EESS equations and frequency domain fatigue analysis procedures in this research to explore the benefits of mesh insensitivity offered by the EESS

method and the uniqueness of the master S-N curve equations in frequency domain fatigue analysis. These modifications will allow the integration of the σ_s and ΔS_s and master S-N curve parameters h and c into a new frequency domain fatigue analysis procedure developed in this research. The proposed approach aims to improve the accuracy of predicted damage crack locations location D and life L_F prior to damage crack initiation in randomly loaded welded structures using the frequency domain fatigue analysis approach. Additionally, the computational efficiency of the process is expected to be significantly enhanced by reducing the need for extensive mesh refinement in the finite element model while preserving the fidelity of the stress results.

3 Proposed Fatigue Damage and Life Evaluation Method

The limitations associated with the frequency domain fatigue analysis procedures for welded structures regarding the definition and evaluation of the stresses at the weld joints are discussed in Section 2.2.1. This chapter presents the development of the analytical equations and computational procedures that comprise the framework of the proposed frequency domain fatigue analysis method for predicting the fatigue damage and life of welded structures prior to damage crack initiation under random loading. The proposed method is based on integrating the developed dynamic EESS-based weld stress response analytical equations and the associated related stress FRF, stress PDF, and master S-N curve derivatives.

The analytical equations are derived from the well-established quasi-static EESS equations discussed in Section 2.3. These equations are adapted to account for the dynamic characteristics of welded structures using the Mode Superposition (MSUP) method.

Therefore, the proposed method encompasses a multifaceted approach that considers the equations, theories, and principles of the EESS constant cyclic amplitude loading fatigue analysis method for welded structures, frequency domain fatigue analysis equations and models for randomly loaded structures, and dynamic response characteristics and equations for dynamically excited structures.

Before establishing the proposed method, some fundamental theories and equations in structural dynamics are introduced in Section 3.1 to provide background to the governing assumptions and theoretical equations considered in developing the proposed dynamic EESS equations and

corresponding EESS-based frequency domain fatigue analysis computational procedures, which are explained in subsequent sections of this chapter.

3.1 Structural Dynamics of Randomly Loaded Structures

Welded structures, such as those found in vehicles, aerospace systems, and offshore structures, exhibit dynamic behaviour when subjected to loading frequencies close to their natural frequencies [31]. This phenomenon, typically known as random vibration, necessitates analyzing and describing these structures as dynamic systems [33]. In such cases, the conventional quasi-static analysis equations and techniques, which only consider the structural stiffness property of these structures, cannot accurately and adequately interpret their displacement, strain, stress behaviour and response.

To adequately capture the dynamic response of Multiple Degree-Of-Freedom (MDOF) linear structures, considering their dynamic characteristics, including stiffness, damping, and inertia, the equation of motion in the physical coordinates, as represented by Equation (3.1) [48], is employed. This equation comprehensively describes the structural response, accounting for the interplay between stiffness, damping, and inertia effects.

$$\mathbf{M}\ddot{\mathbf{u}}(t) + j\mathbf{C}\dot{\mathbf{u}}(t) + \mathbf{K}\mathbf{u}(t) = \mathbf{f}(t) \quad (3.1)$$

Where $\mathbf{f}(t)$ represents the applied excitation load vector acting on the structure, \mathbf{M} denotes the inertia matrix, \mathbf{C} represents the viscous damping matrix, and \mathbf{K} is the structural stiffness matrix. $\ddot{\mathbf{u}}(t)$, $\dot{\mathbf{u}}(t)$, and $\mathbf{u}(t)$ are the acceleration, velocity, and displacement vector variables, respectively.

In the frequency domain fatigue analysis, the FRF, which is required to evaluate the stress response PSD of a randomly excited linear structure, can be calculated using Equations (3.2) and (3.3) [31]. Equation (3.2) is a direct solution of Equation (3.1) based on considering the relationship between a harmonic structural displacement response $u(t)$ amplitude and a harmonically varying excitation load $f(t)$ the amplitude, with angular frequency ω swept across a frequency spectrum of interest.

$$\mathbf{H}(\omega) = \frac{\mathbf{F}(\omega)}{\mathbf{U}(\omega)} = \frac{\mathbf{F}(\omega)}{[-\omega^2 \mathbf{M} + j\omega \mathbf{C} + \mathbf{K}]} \quad (3.2)$$

Where,

$$U(\omega) = \frac{u(t)}{\cos(\omega t)} \quad (3.3)$$

$$F(\omega) = \frac{f(t)}{\cos(\omega t)} \quad (3.4)$$

And for a unit harmonic excitation and response,

$$\mathbf{H}(\omega) = \frac{1}{[-\omega^2 \mathbf{M} + j\omega \mathbf{C} + \mathbf{K}]} \quad (3.5)$$

The FRF of the structure is represented by $\mathbf{H}(\omega)$, $U(\omega)$ denotes the structural displacement response amplitude, and $F(\omega)$ represents the harmonic load amplitude.

Equations (3.2) and (3.3) establish the fundamental relationship that the FRF of a structure is solely determined by its structural stiffness K , viscous damping C , and inertia M , as well as its natural frequency ω properties. The FRF represents a deterministic function that captures the dynamic response characteristics of the structure. It can be obtained through physical tests using shaker tables or steady-state frequency response analysis in FEA, which combines theoretical and

experimental approaches [49]. The frequency response analysis is also a prerequisite for evaluating and verifying a structure's response to various dynamic loading, including resonance, fatigue and other forced dynamic loads.

3.2 Development of the Weld's Dynamic EESS Evaluation Equation

Considering the structural dynamic principles explained in the preceding section, it is imperative to acknowledge the influence of a welded structure's inherent dynamic characteristics, such as natural frequencies, modes, and damping, when interpreting its stress response and accumulated damage under the action of dynamic random loads. Following this principle, the dynamic EESS must be calculated for each dynamic response, incorporating the dynamic properties specific to the structure.

The theories and equations discussed in Section 3.1 are adopted as the basis for developing the dynamic EESS PSD response evaluation analytical equation. The equations are derived sequentially in the subsequent subsections, commencing with the required modal EESS stress and EESS FRF response equation.

3.2.1 Modal EESS

In structural dynamics, modal analysis is a crucial preliminary analysis before conducting detailed dynamic analysis, such as frequency response, transient, and random vibration analysis [50]. By performing modal analysis under no-load conditions, important information about a structure's mode shapes and natural frequencies dynamic characteristics are exposed. This exposure provides insights into the inherent dynamic response behaviour of the structure and helps identify its

dominant vibration modes. One widely used solution method for evaluating the response of a structure under dynamic loading conditions is the Mode Superposition (MSUP) Method.

3.2.1.1 Modal Superposition (MSUP) Method

The MSUP method leverages the mode shapes and natural frequencies' dynamic properties to define and characterize a structural system's overall dynamic behaviour and response to dynamic loading conditions [31]. This method enables the determination of the overall dynamic response, such as displacement, strain, and stress, of an MDOF system by linearly combining the individual response mode shapes represented by the solution of each SDOF modal solution factored by their modal coordinates.

According to the MSUP theory, the displacement vector of a randomly excited linear structure can be computed in the physical coordinate system by relating the individual displacement mode shapes to the modal coordinate using Equation (3.6) [49], [50] taking into consideration the contribution of each mode to the overall displacement of the structure as shown in Figure 3-1.

$$U(x, t) = \sum_{i=1}^n \phi_i(x) \eta_i(t) \quad (3.6)$$

Where $U(x, t)$ is the displacement response of the structure at location x and time t . $\phi(x)_i$ represents the i^{th} displacement mode shape at location x along the structure, η_i denotes the time-based modal coordinate defining the contribution of each mode shape i to the overall displacement, and n is the maximum number of modes considered in the analysis.

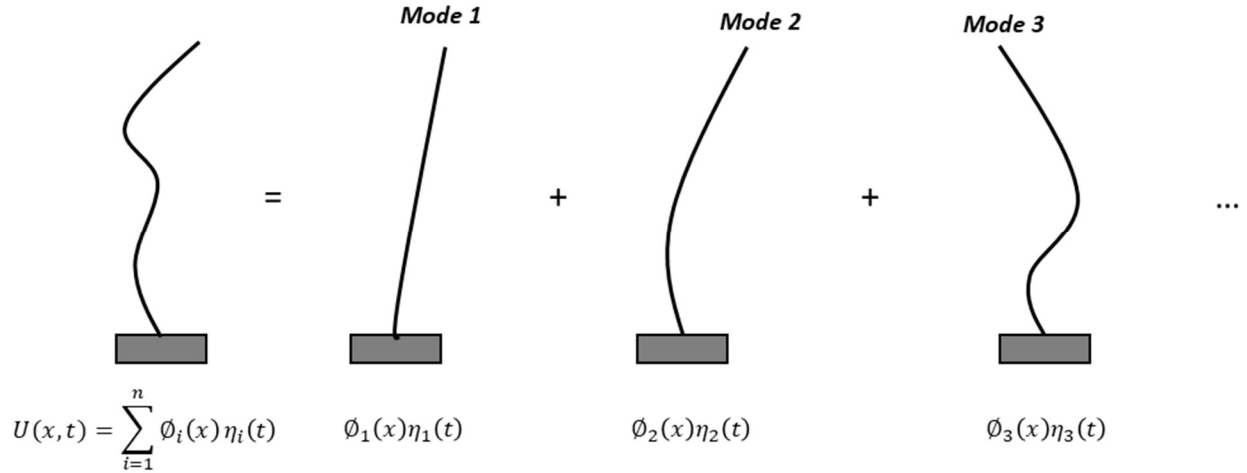


Figure 3-1: Displacement response of a structural system based on the MSUP method

Each degree of freedom of the structure exhibits distinct time-dependent mode shapes, and each mode shape corresponds to a unique natural frequency. Modal analysis, typically performed using FEA packages, can determine these mode shapes and natural frequencies. Furthermore, the modal coordinates that define each mode shape's contribution to the overall dynamic response are obtained through specific frequency response analysis techniques. The selection of an appropriate number of mode shapes crucially depends on several criteria aimed at fully defining and characterizing the dynamic response of the structure. These criteria include the mass participation factor, modal coefficients and the percentages of effective mass distribution [49]. Evaluating these parameters is essential to accurately represent the system's dynamic behaviour in theoretical and experimental verification studies.

3.2.1.2 Modal EESS Evaluation

The weld joints' modal stresses of welded structures from an FE modal analysis solution can be computed using a modal EESS analytical equation. The equation for evaluating the modal EESS

is derived by considering the EESS method equations and principles established in Section 2.3 combined with the MSUP displacement response expression, Equation (3.6).

The considerations in developing the modal EESS equation are the same as those associated with using the MSUP method and modal analysis in structural dynamics. These considerations include [50], [51]:

1. Linear structural response behaviour: Nonlinear material behaviours are ignored
2. Negligible active damping of a structural system: The natural frequencies and mode shapes of a structure become complex for a damped system
3. Constant structural material stiffness throughout the analysis
4. No imposed displacements with time-varying characteristics

For the static structural stress expression given by Equations (2.24) - (2.26), consider Equation (3.7) proposed by Dong et al. [16] and also utilized in [52], that is used to extract the balanced force and moment vectors from the mesh elements nodes of the discretized finite element model of the welded structure in a linear static FEA analysis, as shown in Figure 3-2.

$$[F_e] = [K][U] \quad (3.7)$$

Where,

$$[F_e] = [F_{e(x)}, F_{e(y)}, F_{e(z)}, M_{(x)}, M_{(y)}, M_{(z)}] \quad (3.8)$$

$$[K] = [N \times N] \quad (3.9)$$

$$[U] = [u_x, u_y, u_z, \theta_x, \theta_y, \theta_z] \quad (3.10)$$

The balanced internal global force and moment vectors acting on all the nodes along the weld paths of a welded joint in the fixed global coordinate system are denoted by $[F]$, $[K]$ is the structure's

stiffness related by the mesh element global stiffness matrix with dimensions $N \times N$ and $[U]$ represents the FE weld's node translation u_x, u_y, u_z and rotational $\theta_x, \theta_y, \theta_z$ displacement vector matrix with dimensions $N \times 1$. The displacement vector is dependent on the number of DOFs of the nodes. N is the number of degrees of freedom of the structure.

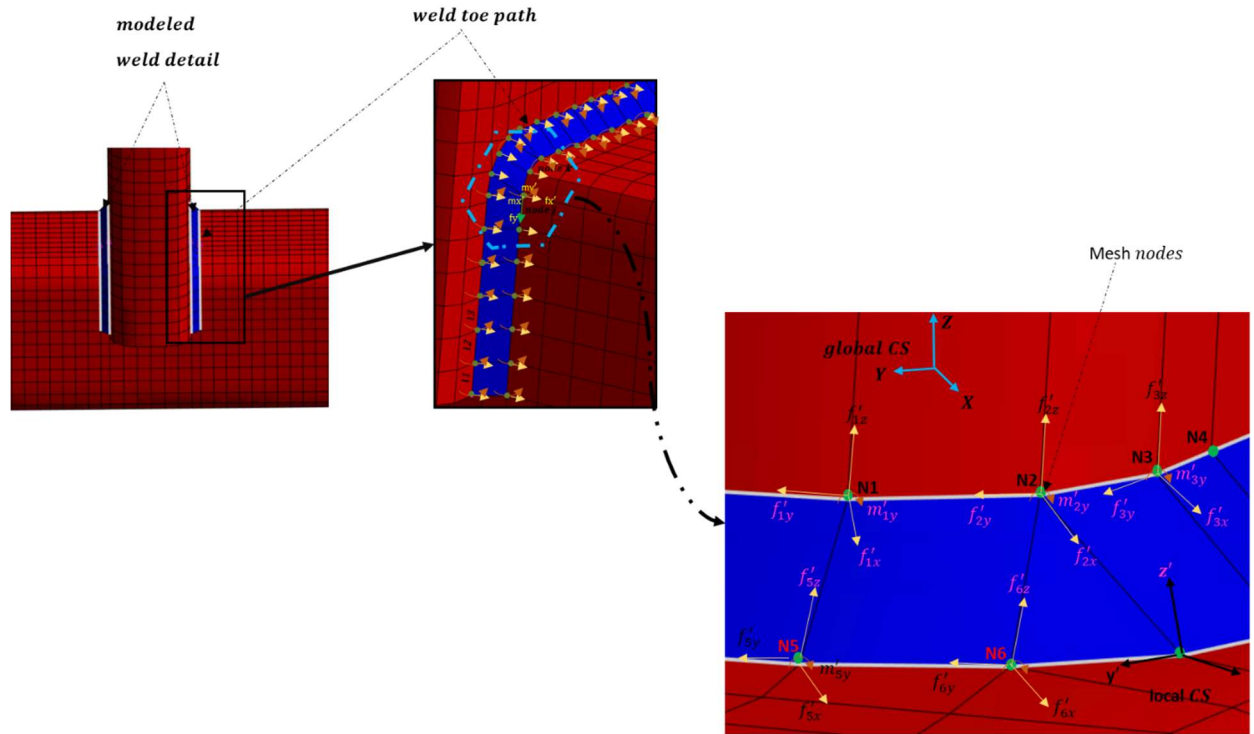


Figure 3-2: FE mesh element nodal forces and moments in the global and local CS

In a dynamic welded structure, the time history of the balanced global forces and moments acting on the nodes of the weld's mesh elements is required for all the modal responses of the structure. To calculate the balanced modal global force and moment vector acting on the mesh elements nodes in the global Coordinate System (CS) of the weld's discretized FE model, Equation (3.6) considered for the evaluation of the displacement vector of a mesh node is substituted into the

nodal force vector expression given by Equation (3.7). The resulting equation for the nodes' modal global forces and moments evaluation is given by Equation (3.11).

$$[F_e] = [K][U] = [K] \sum_{i=1}^n \phi_i(x) \eta_i(t) = \left([K] \sum_{i=1}^n \phi_i(x) \right) \left(\sum_{i=1}^n \eta_i(t) \right) \quad (3.11)$$

Where,

$$\phi_i^{Fe} = [K]\phi_i(x) \quad (3.12)$$

The total modal global force and moment vector acting on any given FE element mesh node along the weld toe paths of the structure is considered as $[F_e]$, $\phi_i^{Fe}(\phi_i^{fe(x)}, \phi_i^{fe(y)}, \phi_i^{fe(z)}, \phi_i^{me(x)}, \phi_i^{me(y)}, \phi_i^{me(z)})$ represents the modal global force and moment vector corresponding to the structure's i^{th} modal response, n denotes the number of modes considered in evaluating the modal forces and moments, and η_i is the i^{th} modal coordinate.

Equation (3.11) calculates the total modal force and moment vector responses in the global CS acting on the mesh element nodes of a welded joint's FE model based on the superposition of all the modal forces and moments corresponding to the various modal responses of the structure. Each modal force's and moment vector's contribution is determined by the modal coordinates magnitude specific to that mode. The balanced nodes' modal global nodal forces and moments can be directly extracted from a welded structure's FE frequency response analysis solution.

The corresponding modal mesh elements line forces and moments along the weld paths of the structure can be determined from the global nodal forces and moments, Equation (3.7), following

the force and moment vector transformation principles and equations Equations (3.13) - (3.15) proposed by Dong et al. [16].

$$[f'] = [F][L] \quad (3.13)$$

Where,

$$[F] = [F_e][T] \quad (3.14)$$

$$[T] = \begin{bmatrix} \cos\theta_{x'X} & \sin\theta_{y'Y} & 0 \\ \sin\theta_{x'X} & \cos\theta_{y'Y} & 0 \\ 0 & 0 & \cos\theta_{z'Z} \end{bmatrix} \quad (3.15)$$

Where $[f']$ denotes the local line forces and moments acting on the weld's mesh elements, $[F]$ is the balanced internal force and moment vectors acting on all the nodes along the weld paths in the element's local coordinate, $[L]$ represents the matrix of mesh elements lengths representing a modelled weld detail based on the consideration of a continuous weld toe line along the mesh nodes [22], [24] ensuring that there are no abrupt stress intensities increase at the weld ends leading to a violation of the EESS principles for weld's stress insensitivity to FE model mesh properties. $[T]$ is the transformation matrix of sines and cosines angles between the structure's global coordinate system and mesh elements' local coordinate system.

The global modal forces and moments acting on the weld's mesh element nodes are transformed to the corresponding element line components by substituting Equation (3.11) into (3.14) to initially give the modal forces and moments in the mesh elements' local coordinate system depicted

in Figure 3-3. The resulting solution is then combined with Equation (3.13) to give Equation (3.16), which calculates the modal mesh elements' line forces and moments along the weld joint paths.

$$[f'] = [T][L][K] \sum_{i=1}^n \phi_i \eta_i \quad (3.16)$$

Where,

$$\phi_i^{f'} = [T][L][K]\phi_i \quad (3.17)$$

The modal line force and moment vector corresponding to the i^{th} modal response of the structure is represented by $\phi_i^{f'} (\phi_i^{f'_x}, \phi_i^{f'_y}, \phi_i^{f'_z}, \phi_i^{m'_x}, \phi_i^{m'_y}, \phi_i^{m'_z})$.

Equation (3.16) calculates the modal line forces and moments on the weld's mesh elements for an FE frequency response analysis solution.

Modal global force and moment

Transformation based on element angles

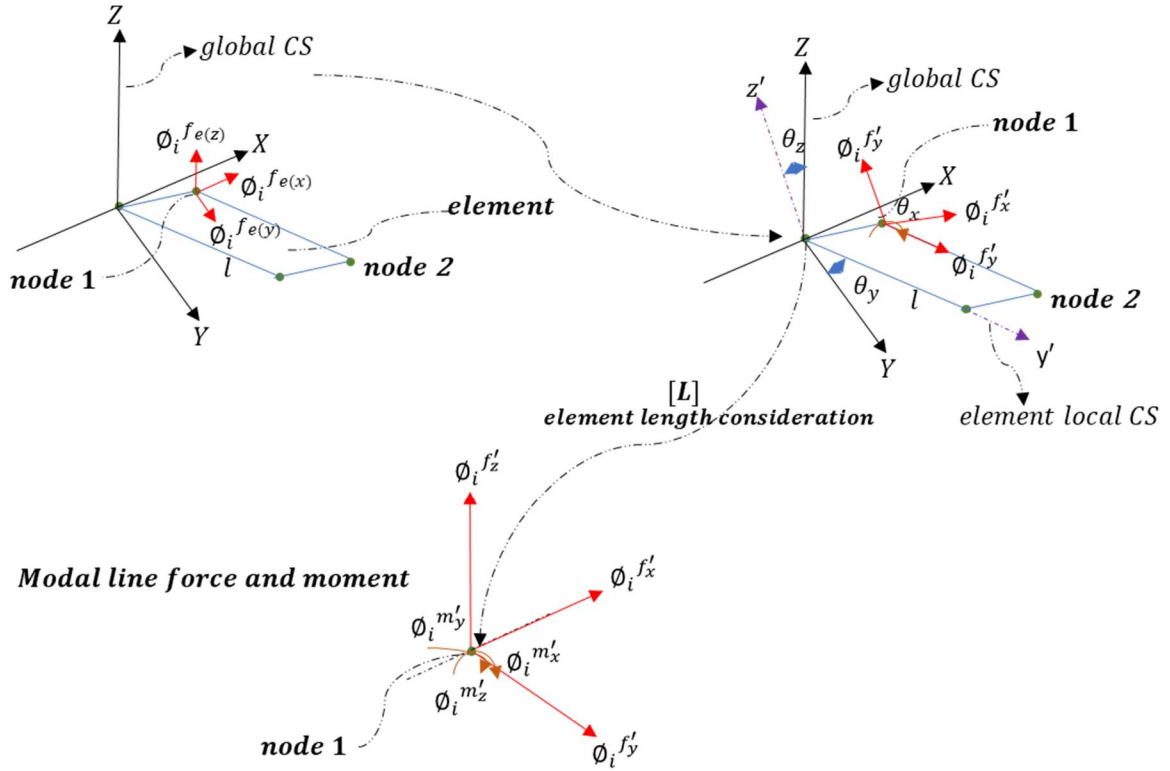


Figure 3-3: Element modal line forces and moments calculation from corresponding nodes global modal forces and moments nodal forces and moments

Once the modal mesh elements' line forces and moments have been determined, the next step is to calculate the modal structural stresses along the weld toe paths of the welded structure. The dynamic modal normal and shear structural stresses can be calculated for any given mesh element node within the FE-modelled weld detail using Equations (3.18) - (3.20). These equations are derived from the combination of the static structural stress equations, Equation (2.24) - (2.26), with the element's line modal force and moment equation, Equation (3.17).

$$\phi_i^{\sigma_{\Delta s}} = \frac{\phi_i^{f'_x}}{t} + \frac{6\phi_i^{m'_y}}{t^2} = \phi_i^{\sigma_m} + \phi_i^{\sigma_b} \quad (3.18)$$

$$\phi_i^{\tau_{\Delta s}} = \frac{\phi_i^{f_y'}}{t} + \frac{6\phi_i^{m_x'}}{t^2} = \phi_i^{\tau_m} + \phi_i^{\tau_b} \quad (3.19)$$

$$\phi_i^{\tau_{\Delta z}} = \frac{\phi_i^{f_z'}}{t} \quad (3.20)$$

Where, $\phi_i^{\sigma_{\Delta s}}$, $\phi_i^{\tau_{\Delta s}}$ and $\phi_i^{\tau_{\Delta z}}$ are the modal normal, modal perpendicular shear and modal parallel stresses relating to the structure's i^{th} modal response. $\phi_i^{\sigma_m}$ and $\phi_i^{\sigma_b}$ are the modal normal membrane and bending stresses, while $\phi_i^{\tau_m}$ and $\phi_i^{\tau_b}$ are the corresponding modal shear components.

From Equations (3.18) - (3.20), a welded structure's modal structural stresses can be calculated for all the mesh elements nodes along the weld path considering all the mode shapes appropriately defining the structure's response as shown in Figure 3-4 below.

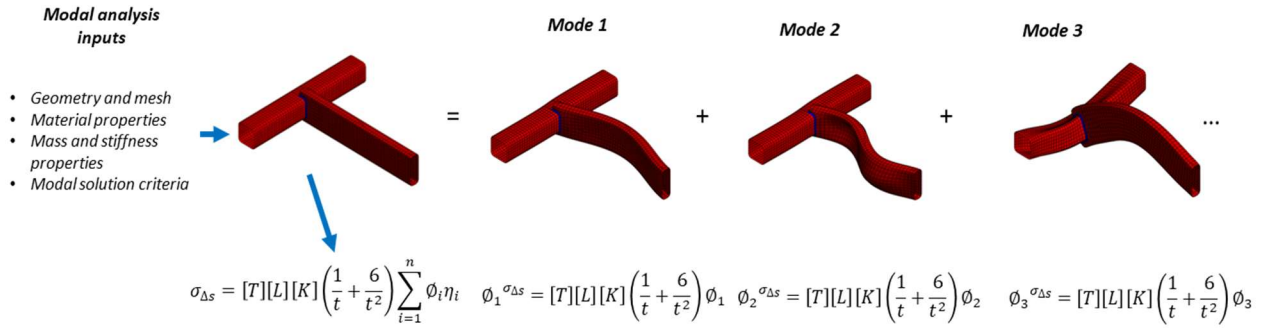


Figure 3-4: Modal structural stress computation from individual structural stress mode shapes

After calculating the modal structural stresses, the next step is determining the modal EESS, which considers the weld toe stress concentrations, structural component thickness, and loading modes. This calculation is based on the static EESS equations, precisely Equation (2.28) - (2.31), in

conjunction with the modal normal and shear structural stresses obtained from Equations (3.18) - (3.20).

By substituting Equations (3.18) - (3.20) into Equations (2.28) - (2.31), the modal EESS equation by Equation (3.21) is derived.

$$\phi_i^{\Delta S_s} = \frac{\sqrt{\phi_i^{\sigma_{\Delta s}^2} + 3(\phi_i^{\tau_{\Delta s}^2} + \phi_i^{\tau_{\Delta z}^2})}}{t^{*\frac{2-m}{2m}} \cdot \phi_i^{I(r)^{1/m}}} \quad (3.21)$$

Where,

$$\begin{aligned} \phi_i^{I(r)^{1/m}} = & 0.0011r^6 + 0.0767r^5 - 0.0988r^4 + 0.0946r^3 + 0.0221r^2 \\ & + 0.014r + 1.223 \end{aligned} \quad (3.22)$$

$$r = \frac{|\phi_i^{\sigma_b}|}{|\phi_i^{\sigma_m}| + |\phi_i^{\sigma_b}|} \quad (3.23)$$

The load correction factor for the i^{th} mode is represented by $\phi_i^{I(r)^{1/m}}$, m and t^* taken as 1mm are the hypothetical crack depth and reference plate thickness, respectively, defined by Equation (2.31).

Equation (3.21) provides a means to calculate the modal EESS, which offers a more accurate representation of the stress distribution, considering the specific characteristics of the weld toe stress concentrations, structural component thickness, and loading modes within the welded structure.

Under proportional loading conditions, with the normal stress components being three times greater than the shear stress components, the initiated and propagated crack at the weld joint is primarily influenced by the normal stress component [53], [54]. In situations where the modal

normal structural stress component outweighs the modal shear structural stress components, Equation (3.21) can be simplified and reduced to Equation (3.24) for calculating the modal EESS at the weld joints without losing fidelity in the calculated stress results.

$$\phi_i^{\Delta S_s} = \frac{\phi_i^{\sigma \Delta s}}{t^{\frac{2-m}{2m}} \cdot \phi_i^{I(r)^{1/m}}} \quad (3.24)$$

3.2.2 EESS Mode-based Frequency Response Function (FRF)

The evaluation of a structure's FRF using Equations (3.2) and (3.5) can be accomplished through two methods in Finite Element Analysis (FEA): the direct frequency response analysis and the mode superposition-based frequency response analysis [54].

The direct frequency response analysis method involves solving the equations of motion directly using computational methods, as outlined in Section 3.1. It provides a comprehensive computational solution for calculating a structure's response to harmonic loading [51]. In contrast, the mode superposition-based frequency response analysis method considers only a structure's relevant and sufficient modes to fully define its response within a specific frequency range of interest.

While the mode superposition-based method offers a more efficient analysis by reducing the computational processing time and memory requirements, particularly for large structures, it may sacrifice some numerical accuracy. On the other hand, the direct method is computationally more intensive but generally yields more accurate results. This research focuses on the mode superposition-based frequency response analysis method to derive the mode superposition-based

EESS FRF at the weld joints of welded structures. Hereafter, the mode superposition-based EESS FRF will be referred to as the "mode-based EESS FRF" in this document.

In FE structural dynamics analysis, a structure's steady-state stress response requires input parameters such as the modal stress output from a modal analysis and the modal coordinates from a frequency response analysis. Therefore, to derive the mode-based EESS FRF for the harmonic response of a welded structure, the modal EESS evaluation equations developed in Section 3.2.1 are considered.

Before delving into the intended mode-based EESS FRF, it is necessary to establish the equations and principles for the modal steady-state stress response from which the mode-based EESS FRF equation is derived. These principles are based on the equations of motion and the FRF established in Section 3.1.

Considering the linear structural system depicted in Figure 3-4, the equations of motion for the MDOF system, as given in Equation (3.2), can be expressed in the modal coordinates by Equation (3.25) [48], [51] based on the MSUP theory and considering an initial displacement mode shape.

$$-\omega^2 \Phi^T \mathbf{M} \Phi \eta(\omega) + j\omega \Phi^T \mathbf{C} \Phi \eta(\omega) + \Phi^T \mathbf{K} \Phi \eta(\omega) = \Phi^T \mathbf{F}(\omega) \quad (3.25)$$

Where,

$$\Phi = [\varphi_1, \varphi_2, \varphi_3, \dots \varphi_n] \quad (3.26)$$

$$\eta = [\eta_1, \eta_2, \eta_3, \dots \eta_n] \quad (3.27)$$

The transpose of the matrix of mode shapes is Φ^T , $M = \Phi^T M \Phi$ represents the modal mass matrix, $C = \Phi^T C \Phi$ denotes the modal viscous damping matrix, $K = \Phi^T K \Phi$ is the modal stiffness matrix, and $\Phi^T F(\omega)$ is the modal force vector.

Equation (3.25) represents the coupled equation of motion solution for MDOF linear structural systems. The uncoupled form of Equation (3.25) consisting of a set of modal Single Degree of Freedom (SDOF) equations in the modal coordinate system is given by Equation (3.28) [36], [51].

$$-\omega^2 m_i \eta_i(\omega) + j\omega c_i \eta_i(\omega) + k_i \eta_i(\omega) = f_i(\omega) \quad (3.28)$$

Where, m_i , c_i , k_i and f_i are the i^{th} modal mass, i^{th} modal viscous modal damping, i^{th} modal structural stiffness and i^{th} modal force vector respectively corresponding to a structure's i^{th} modal response.

From Equation (3.28), the modal coordinates and displacement FRF of a structural system can be calculated using Equation (3.29) [36] and Equation (3.30) [48], [50], [55], respectively.

$$\eta_i(\omega) = \frac{1}{[-\omega^2 m_i + j\omega c_i + k_i]} \quad (3.29)$$

$$H(\omega)^U = \sum_{i=1}^n \frac{\phi_i \phi_i^T}{[-\omega^2 m_i + j\omega c_i + k_i]} \quad (3.30)$$

Equation (3.29) calculates the modal coordinates which describe the modal dynamic response behaviour of the SDOF structural system. These coordinates, representing the amplitudes and phases associated with each mode, can be computed in FE frequency response analysis for all the considered modes of the structure, as shown in Figure 3-5. The computed modal coordinates are

also called “modal coordinates FRF.” Equation (3.30) implies that the displacement FRF of a structure can be expressed as the summation of the product of the individual modal coordinates FRF $\eta_i(\omega)$ given by equation (3.29) and the corresponding individual displacement mode shapes within the selected frequency range of interest [50].

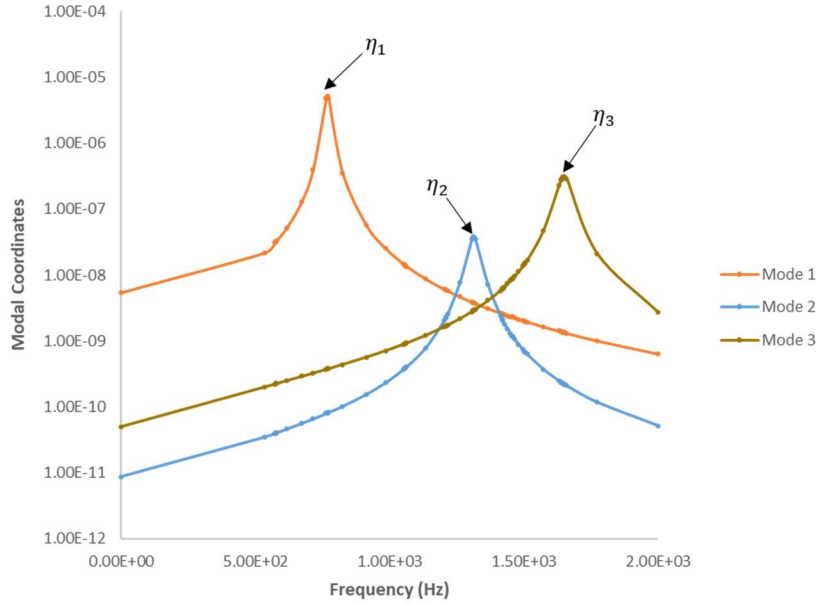


Figure 3-5: Modal coordinates of the structural system corresponding to three modal responses

In the frequency domain, the steady-state stress FRF of a structure can be computed using Equation (3.31), which is derived based on the modal coordinate FRF provided by Equation (3.29). This calculation is performed by considering the relationship between the dynamic displacement response, $U(x, t)$, the strain response, $\varepsilon(x, t)$ and the stress response, $\sigma(x, t)$ at a specific location x within the structure and at a given time t [48], [51].

$$H^\sigma(\omega) = \sum_{i=1}^n \phi_i(x)^\sigma \eta_i(t) = \sum_{i=1}^n \frac{\phi_i(x)^\sigma \phi_i^T}{[-\omega^2 m_i + j\omega c_i + k_i]} \quad (3.31)$$

Where,

$$\phi_i(x)^\sigma = E \cdot \phi_i(x)^\varepsilon \quad (3.32)$$

$$\phi_i(x)^\varepsilon = D \cdot \phi_i(x) \quad (3.33)$$

The total mode-based stress FRF at a location x and time t on the structure which relates the input random PSD loading to the output stress PSD, is denoted by $H^\sigma(\omega)$, $\phi_i(x)^\sigma$ represents the i^{th} stress mode shape at location x , which is typically a hotspot normal or shear stress mode shape for welded structures, with E being the modulus of elasticity. $\phi_i(x)^\varepsilon$ denotes the i^{th} strain mode shape at location x , with D being the differential operator and $\eta_i = \frac{1}{\omega^2 m_i + j\omega c_i + k_i}$ is i^{th} modal coordinate FRF as expressed by Equation (3.29).

Similar to the principle of the displacement FRF of a structure, Equation (3.30) implies that the mode-based stress FRF of a structure can be obtained by summing the product of the individual modal coordinates FRF $\eta_i(\omega)$ given by Equation (3.29) and the corresponding individual stress mode shapes given by Equation (3.34) within the selected frequency range of interest.

Considering the established principles and methodology leading to Equation (3.29) for modal coordinates evaluation and the modal EESS evaluation equation given by Equation (3.24), the mode-based EESS FRF equation can be derived, as depicted in Figure 3-6.

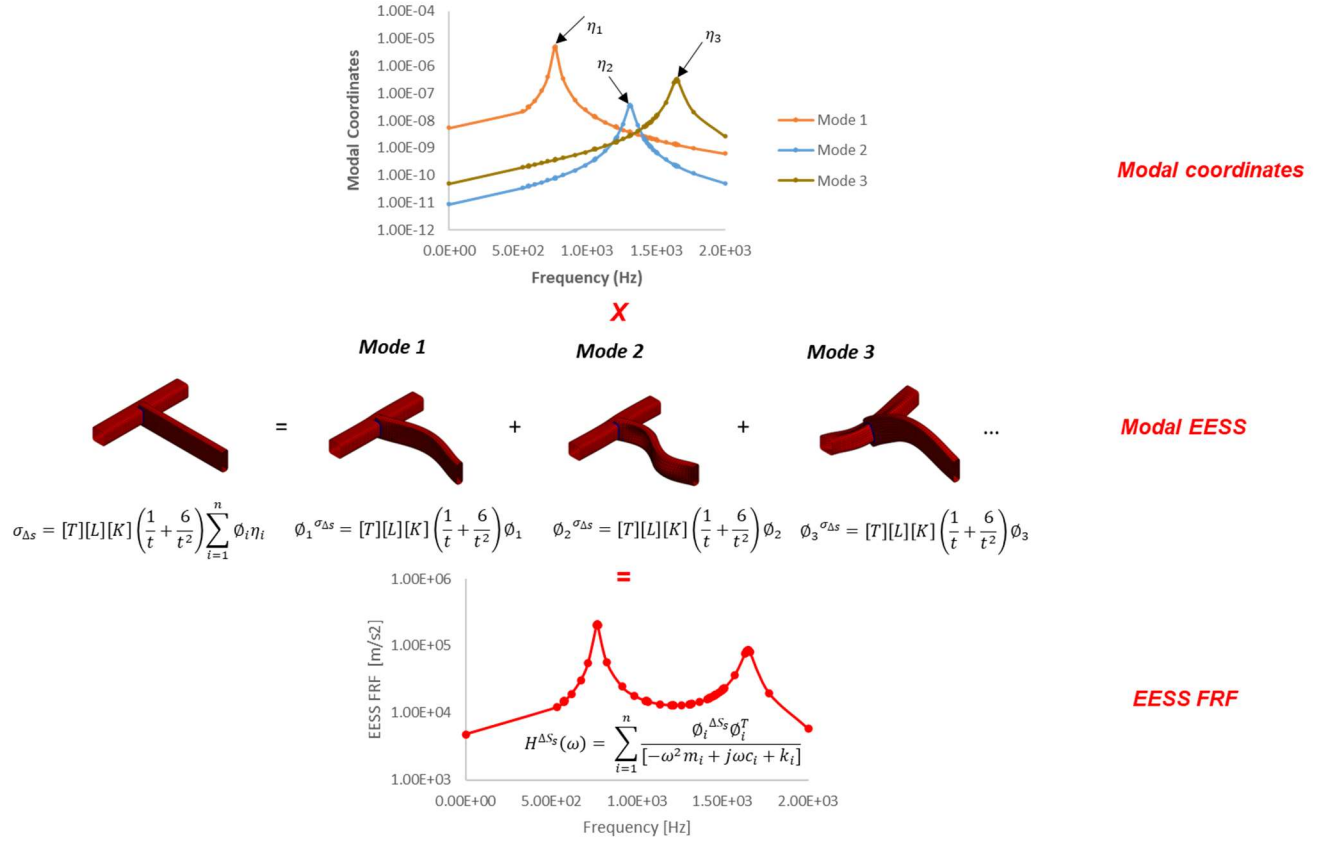


Figure 3-6: EESS FRF Computational approach from Modal EESS and Modal Coordinates

To obtain the mode-based EESS FRF equation, Equation (3.31) is modified by substituting the traditional weld stress parameter, represented by the modal stress $\phi_i(x)^\sigma$, with the modal EESS parameter $\phi_i^{\Delta s_s}$ derived from Equation (3.24).

This substitution accounts for the influence of the EESS in the weld joint area, which is crucial in accurately assessing the stress response of welded structures. The resulting solution is given by Equation (3.35), providing a comprehensive equation to calculate the mode-based EESS FRF.

$$H^{\Delta S_s}(\omega) = \sum_{i=1}^n \frac{\phi_i^{\Delta S_s} \phi_i^T}{[-\omega^2 m_i + j\omega c_i + k_i]} \quad (3.35)$$

Where $H^{\Delta S_s}(\omega)$ is the EESS-based FRF and $\phi_i^{\Delta S_s}$ denotes the modal EESS parameter.

Equation (3.35) enables evaluating the steady stress response of harmonically excited dynamic welded structures at the weld joint locations. This equation incorporates the modal EESS parameter, derived from Equation (3.24), to enhance the accuracy of stress extrapolation by considering the specific joint details characteristics of the welded structure.

3.2.3 EESS Stress Response PSD and Cycle Counting

In the previous section, the mode-based EESS FRF was derived by incorporating the modal EESS and the modal coordinates obtained from a frequency response analysis. As discussed in Section 2.2.1, the stress PSD response of a structure can be computed using Equations (2.3), which is based on the relationship between the input load PSD and the FRF of the structure.

3.2.3.1 EESS Stress Response PSD Evaluation

Following Equations (2.3) and (3.35), the stress PSD response of a randomly loaded welded structure can be computed using the EESS approach rather than traditional stress extrapolation methods. To calculate the EESS PSD response on each mesh element node along the weld joint path depicted in Figure 3-2, Equations (2.3) is modified by replacing the conventional extrapolated stress FRF with the mode-based EESS FRF derived from Equation (3.35). This modification yields Equation (3.36).

$$[G^{\Delta S_s}(f)] = [H^{\Delta S_s}(f)]^* \cdot [G(f)] \cdot [H^{\Delta S_s}(f)]^T \quad (3.36)$$

Where,

$[G^{\Delta S_s}(f)]$ represents the EESS PSD reponse matrix, $[G(f)]$ is the random input load PSD, and $[H^{\Delta S_s}(f)]^*$ and $[H^{\Delta S_s}(f)]^T$ are the complex conjugate and transpose of the structure's EESS FRF.

Based on the multiaxial response stress state criteria for structures under multiaxial loading conditions established in [36], [48], the multiaxial EESS FRF and EESS PSD for $n \times n$ structural system characterized by n DOFs can be calculated using Equations (3.37) and (3.38) respectively.

$$[H^{\Delta S_s}(f)] = \begin{bmatrix} H_{11}^{\Delta S_s}(f) & \dots & H_{1n}^{\Delta S_s}(f) \\ \vdots & \ddots & \vdots \\ H_{n1}^{\Delta S_s}(f) & \dots & H_{nn}^{\Delta S_s}(f) \end{bmatrix} \quad (3.37)$$

$$[G^{\Delta S_s}(f)] = \begin{bmatrix} G_{xx}^{\Delta S_s}(f) & \dots & G_{xz}^{\Delta S_s}(f) \\ \vdots & G_{yy}^{\Delta S_s}(\omega_m) & \vdots \\ G_{zx}^{\Delta S_s}(f) & \dots & G_{zz}^{\Delta S_s}(f) \end{bmatrix} \quad (3.38)$$

Where the multiaxial EESS FRF parameter is denoted by $H^{\Delta S_s}(f)$ and $G^{\Delta S_s}(f)$ represents the multiaxial EESS PSD state at the weld's crack initiation region comprising independent stress PSD components $G_{xx}^{\Delta S_s}(f), G_{xy}^{\Delta S_s}(f) \dots G_{xz}^{\Delta S_s}(f)$.

3.2.3.2 EESS Stress PSD Response Cycle Counting

Dirlik's cycle counting method and formulations, as given in Equations (2.10) - (2.18) [39] and described in Section 2.2.2, are used to determine the PDF of the EESS amplitudes at the weld joints. By substituting the parameter representing the hotspot stress PSD $G_{eq(hs)}^\sigma(f)$ in the expression for spectral moments given by Equation (2.9), with the EESS PSD response $G^{\Delta S_s}(f)$, from Equation (3.36), the spectral moments can be directly calculated from the single-sided EESS PSD using Equation (3.39) below.

$$m_n(\Delta S_s) = \int_0^{+\infty} f^n G^{\Delta S_s}(f) df \quad (3.39)$$

Where, $m_n(\Delta S_s)$ is the calculated EESS-based spectral moments, $G^{\Delta S_s}(f)$ (Pa^2/Hz) is the single-sided EESS PSD at a frequency of $f^n(Hz)$ and df is the frequency increment.

Equation (3.39) calculates the first four 0th, 2nd and 4th spectral moments required to compute the parameters of Dirlik's empirical cycle counting equation. Substituting the EESS amplitude $S^{\Delta S_s}$ and the estimated parameters based on the spectral moments of Equation (3.39) into Equations (2.10) - (2.18) give the EESS PDF $p(\Delta S_s)$ following Dirlik's formulation [39].

$$p(\Delta S_s) = \frac{\frac{D_1}{Q} \cdot e^{\frac{-Z}{Q}} + \frac{D_2 \cdot Z}{R^2} \cdot e^{\frac{-Z^2}{2 \cdot R^2}} + D_3 \cdot Z \cdot e^{\frac{-Z^2}{2}}}{2 \cdot \sqrt{m_0}} \quad (3.40)$$

Where $D1, D2, D3, R, Q, Z$ and m_0 , the parameters in Dirlik's formulation defined in Equation (2.9) are modified based on the EESS spectral moments of Equation (3.39).

3.3 Fatigue Damage and Life Estimation Using the Master S-N Curve

The procedures and considerations for estimating the fatigue damage and corresponding life of welded structures prior to damage crack initiation in the frequency domain have been presented in Section (2.2). It was established that the fatigue damage at the welded joints could be estimated using Equation (2.22), which inherently considers the hotspot stress amplitudes PDF $p(S)$ given by Equation (2.10) and the allowable number of cycles to failure N parameter obtained from the S-N curve specific to the material grade of the welded joint detail.

Here in this section, the fatigue damage and life estimation prior to damage crack initiation analytical equations for a randomly loaded welded are proposed by modifying the damage estimation equation given by Equation (2.22) [32]. This modification is based on incorporating the mode-based EESS amplitudes PDF expression, Equation (3.41), as well as the master S-N parameters and equations, Equation (2.32) [18], discussed in Section 2.3.2, into the established damage estimation equation.

Therefore, substituting the EESS amplitudes $S^{\Delta S_s}$, EESS amplitudes PDF $p(\Delta S_s)$, and the master S-N curve parameters C and h into Equation (2.32), Equation (3.41) for estimating the induced fatigue damage resulting from the induced EESS PSD is derived.

$$D = \frac{E(P)^{\Delta S_s} T}{C^{1/h}} \int_0^{+\infty} p(\Delta S_s) \cdot (S^{\Delta S_s})^{1/h} ds \quad (3.41)$$

Where C and h are the master S-N curve parameters defined in Table 2-1 [43], $S^{\Delta S_s}$ represents the EESS stress amplitude, $E(P)^{\Delta S_s}$ is the expected number of peaks crossing per second from

the EESS response PSD output, T denotes the total load exposure time for the damage, and ds is the incremental stress.

From Equation (3.41), the damage at the weld joints can be estimated directly at all the mesh nodes within a discretized FE model representing welded structure in FE frequency domain fatigue analysis.

The overview of the proposed frequency domain fatigue analysis computational method for fatigue damage and life evaluation of welded structures prior to damage crack initiation is presented in the flowchart in Figure 3-7.

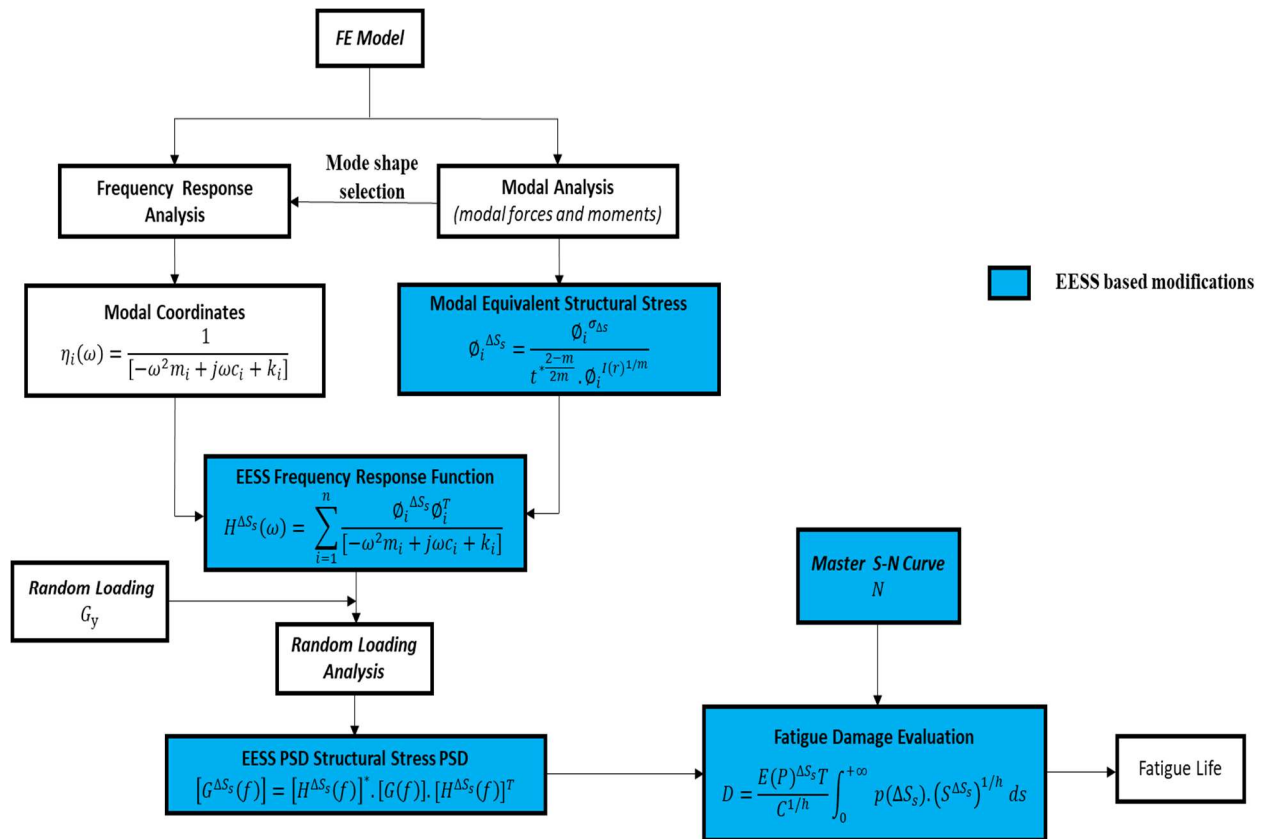


Figure 3-7: Flowchart of the frequency domain fatigue analysis method based on the EESS

The flowchart in Figure 3-7 provides a clear overview of the computational methodology employed in this research, emphasizing the integration of the proposed EESS-based considerations in the frequency domain fatigue analysis approach for randomly loaded welded structures. The main inputs and steps depicted by the blue boxes involve:

- (i) Evaluation of the modal EESS $\phi_i^{\Delta S_s}$ along the weld joints paths of the structure using Equation (3.24), which considers the modal line element forces $\phi_i^{f'_x}$ and moments $\phi_i^{m'_y}$ extracted from the solution of a numerical modal analysis of the structure and the weld throat thicknesses
- (ii) Evaluation of the EESS Frequency Response Function (FRF) $H^{\Delta S_s}(\omega)$ at the same weld locations using Equation (3.35), which considers the modal coordinates extracted from the solution of a numerical frequency response analysis of the structure and the calculated modal EESS $\phi_i^{\Delta S_s}$ from step (i)
- (iii) Calculating the EESS Power Spectral Density (PSD) $G^{\Delta S_s}(f)$ based on the solution from step (ii) and the input load PSD $G(f)$
- (iv) Estimating the fatigue damage D due to EESS PSD at the weld joints using Equation (3.41) and also considering the master S-N curve parameters from Equation (2.32)

The existing methods utilized in completing the computational process are depicted in the white boxes.

3.4 Summary of the Proposed Method

A frequency domain fatigue evaluation method for estimating the fatigue damage D and life L_F of randomly loaded welded structures prior to damage crack initiation has been proposed in this

chapter. The method is based on the integration of the developed analytical modal EESS $\emptyset^{\Delta S_s}$, EESS FRF $H^{\Delta S_s}(\omega)$, EESS PSD $G^{\Delta S_s}(f)$, EESS amplitudes $S^{\Delta S_s}$, PDF $p(\Delta S_s)$ equations, including the master S-N curve parameters C and h into a frequency domain fatigue evaluation framework.

The basis of the analytical equations development are the frequency domain fatigue evaluation models established in Section 2.2, quasi-static EESS fatigue evaluation equations established in Section 2.3, and the MSUP principles and dynamic response characteristics in structural dynamics established in Sections 3.1 and 3.2.1.1, respectively.

The proposed frequency domain fatigue evaluation method combines and integrates the strengths of contemporary fatigue evaluation methods. It leverages the improved accuracy of fatigue damage and life prediction the EESS method provides while considering the frequency domain approach's dynamics characteristics and computational efficiency benefits. As a result, this method enables a computationally efficient evaluation of the stress frequency response, stress PSD response, predicted fatigue damage crack and life estimation prior to damage crack initiation for randomly loaded welded structures, with improved accuracy.

4 Numerical Demonstration and Validation of the Proposed Method for Welded RHS Structures

In this chapter, the viability of the theoretical equations and methodological approach proposed in Chapter 3 for the frequency domain fatigue analysis is numerically demonstrated and validated using a Rectangular Hollow Section (RHS) T-joint welded structure subjected to random loading. RHS T-joint welded structures are widely used in many welded structural systems, including automotive structures such as structural supports and frames [56], considered in this research.

The proposed method is numerically implemented using ANSYS FEA [57] and MATLAB [58] software packages. The fatigue response variables of the structure are assessed at critical locations, particularly the weld joints susceptible to fatigue failure. These locations are considered the most vulnerable points on the structure for the likely occurrence of fatigue damage. The obtained results are thoroughly analyzed and discussed, considering the implications of the findings.

To validate the accuracy of the results obtained using the proposed method, they are compared with fatigue damage test results reported in the literature and results obtained from the traditional hotspot stress extrapolation method. This comparative analysis provides further insights and comprehensively evaluates the performance of the proposed frequency domain fatigue analysis method.

4.1 Parameters and Preliminary Analysis of the Structure

This section describes the geometric and material parameters of the RHS T-joint welded structure utilized for the verification analysis. The structural characteristics, features, and considerations regarding the representation of the structure in the FEA model are also discussed.

The geometrical parameters of the RHS T-joint welded structure, such as the dimensions of the sections and the weld details, are outlined. Additionally, the material properties of the components used in the structure, including their Young's modulus, Poisson's ratio, and yield strength, are specified.

In terms of the FEA model, the details of the structural representation, including information on the meshing strategy, element types, and boundary conditions employed in the model, are provided. Furthermore, the preliminary analysis conducted to ensure the reliability and accuracy of the FEA model is explained. This initial analysis helps validate the structural response obtained from the FE simulations. Also, it ensures that the model adequately captures the behaviour of the actual structure for the subsequent analysis and evaluation of the welded structure's fatigue behaviour and life estimation.

4.1.1 Geometry and Material Properties of the Structure

The geometrical and material properties of the RHS T-joint welded structure considered for the validation analysis in this research are the same as those used and validated by Dong et al. [19] for constant amplitude cyclic fatigue loading conditions in their study.

The RHS T-joint welded structure is a three-dimensional steel structure composed of two RHS beam components and three plates with drilled holes. The dimensions, cross-sectional profiles, welding details of the RHS beams, and the specifications of the plates and drilled holes are consistent with the configuration employed in [19]. The overall arrangement and layout of the structure can be visualized in Figure 4-1. This figure illustrates the positioning and connectivity of the various components, providing a clear representation of the structural configuration.

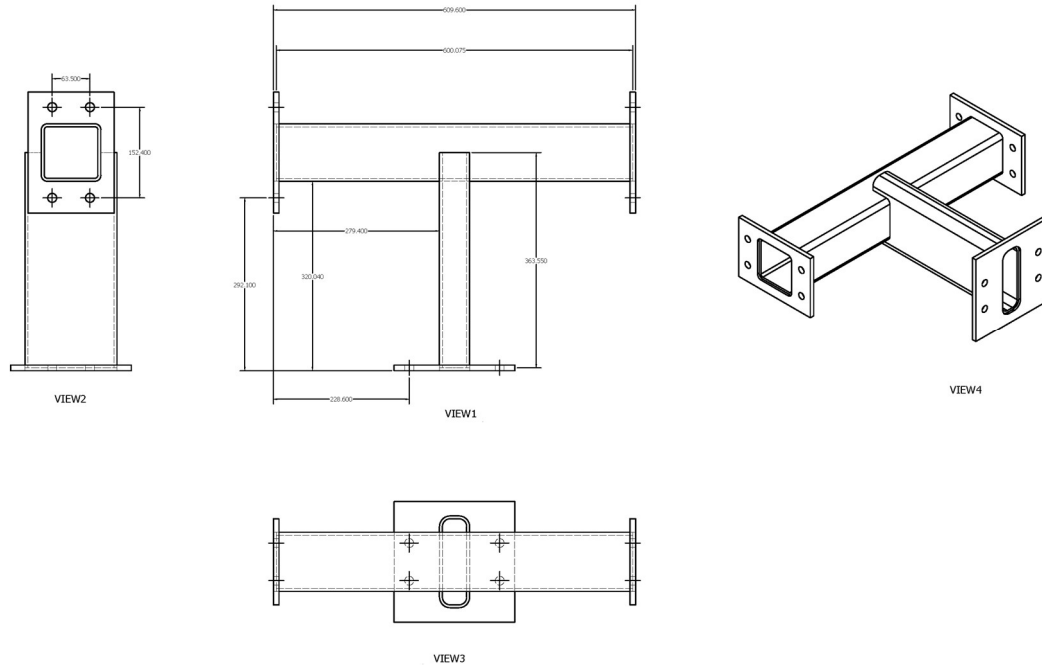


Figure 4-1: Geometrical details of the RHS T-joint welded structure (dimensions are in mm)

The structural components of the beams in the RHS T-joint structure are interconnected using continuous double fillet welds, which are applied on both sides of the structure. These welds provide strength and stability to ensure the assembly's structural integrity. To provide a comprehensive understanding of the geometrical characteristics of the structure, Table 4-1 presents the key parameters and dimensions associated with the RHS T-joint welded structure.

Table 4-1: Structure and weld profile dimensions and thickness [19]

Component	Length (mm)	Cross-Section (mm)	Thickness (mm)
Beam 1	609.6	101.6 × 101.6	7.9
Beam 2	363.6	50.8 × 152.4	7.9
Weld	-	-	7.9

Table 4-1 provides detailed information regarding the structural components' cross-sectional profiles, dimensions, and other relevant geometric properties.

The mechanical properties of the steel, with A13R-RC7 material grade, are in accordance with the considerations in [19] and given in Table 4-2.

Table 4-2: Structure's material properties [19]

Property	Value	Unit
Density	7850	kg/m ³
Module of Elasticity	207000	MPa
Poisson's Ratio	0.3	-
Yield strength, F_y (N/mm ²)	355	MPa
Tensile strength, F_u (N/mm ²)	470	MPa

The verification analysis considers that the weld mechanical properties of the RHS T-joint structure are equivalent to those of the base structural components, as outlined in Table 4-2. This consideration implies that any potential effects from dissimilar weld filler or base metal materials are negligible.

Considering the weld mechanical properties to be the same as those of the base structural components simplifies the analysis process and reduces the complexity associated with accounting for different material properties within the welded joints. This assumption is often made when the weld and base metals have similar compositions and properties.

The decision to consider the weld mechanical properties identical to the base structural components is based on the understanding that the weld joints are intended to provide continuous and reliable load transfer between the connected components. Therefore, assuming comparable mechanical properties helps to simplify the analysis while still capturing the essential behaviour of the welded structure.

By utilizing the same structural components and weld geometrical and material properties as in [19], this research ensures the comparability and consistency of the analysis, thus enabling a direct validation and assessment of the proposed frequency domain fatigue analysis method for the RHS T-joint welded structure under irregular road surface profile induced stationary random loading conditions.

4.1.2 Finite Element Model of the Structure

As indicated in Section 3.3, the proposed method computational process begins by creating a detailed three-dimensional FE model of the welded structure, incorporating the geometric, material, and welding details. ANSYS FEA is used to create the FE model of the structure. The FEA model considers the structural misalignment according to the requirements in [59].

4.1.2.1 Structural Components Modeling and Boundary Conditions

To accurately analyze the weld joints and transfer the loads to the desired locations, this research adequately represents the structural components and weld details using Shell 181 elements, as shown in Figure 4-2.

The Shell 181 element is suitable for analyzing thin to moderately thick structures and is computationally efficient [60]. It allows for considering linear, large rotation, transverse shear deformation linear effects against large bending loads and large nonlinear strain. This element type is commonly used in structural analysis for its ability to capture the essential behaviour of thin-walled structures. The Shell 181 element is a 4-node linear element with six degrees of freedom at each node: translation in the x, y, and z directions and rotation about the x, y, and z axes.

Furthermore, it provides the flexibility to model the structural components and weld details accurately.

In the FEA model, the thickness of the structural components and welds is defined and assigned to the mid-surface of the shell elements. This thickness assignment consideration allows for the proper geometry representation and ensures that the loads are appropriately transferred through the structure.

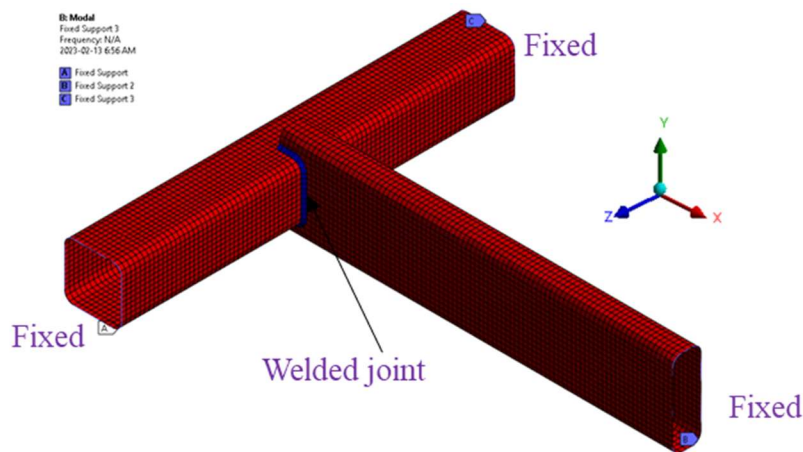


Figure 4-2: Finite element model and boundary condition of the structure

Unless otherwise specified, the boundary conditions used in the analyses presented in this document include complete constraints on translation and rotation in all degrees of freedom at the ends of the structural beam components to simulate the actual physical condition of the structure accurately.

These boundary conditions are chosen to eliminate any boundary effects in the computed results and ensure that the results are a realistic representation of the actual structure. To achieve this, the FEA model incorporates sufficient lengths of the structural components, which helps minimize boundary-related distortions in the computed results. By considering an appropriate size for the

structural components, the analysis captures the essential behaviour of the system. It ensures the results are reliable and represent the actual welded structure conditions.

4.1.2.2 Weld and Contacts Connections Details Modeling

The EESS method requires the accurate modelling of weld details in the finite element analysis to ensure proper load transfer and accurate stress extrapolation at the weld joints, especially when local bending effects significantly influence the results. The recommended modelling techniques for welds outlined by Hobbacher in [59] have been employed to achieve this.

The weld details are represented by a row of inclined plate shell elements at a 45-degree angle to accurately capture the welds' geometry, stiffness, and strength properties at the joint connection locations. These oblique plates' defined thickness and cross-section properties are equivalent to the weld's throat thickness and dimensional characteristics. They are attached to both beam components at the intersecting nodes of the welds and the main structural components, ensuring complete transfer of the applied loads with no inclusion of additional stress concentrations due to nodal or element offsets, as depicted in Figure 4-3.

The weld paths, which represent the actual weld toe and surface regions, are defined in the model and highlighted in Figure 4-3. Four weld paths are considered in the analysis, where stresses and other fatigue variables are computed for the structure. However, the FEA model does not account for the consequences of weld imperfections associated with the welding process. This is because the fatigue S-N curves used in the analysis already include the effects of stress concentrations resulting from weld details and geometry, as well as normal fabrication standards, loading directions, high residual stresses, metallurgical and microstructural conditions, inspection procedures, and post-weld treatment effects [59].

The connections between the structural beam components and the welded joints are defined using CONTA175 and TARGE170 elements in ANSYS, as illustrated in Figure 4-3. These elements provide the necessary contact and interaction behaviour between the components, ensuring accurate load transfer and stress distribution within the welded connections.

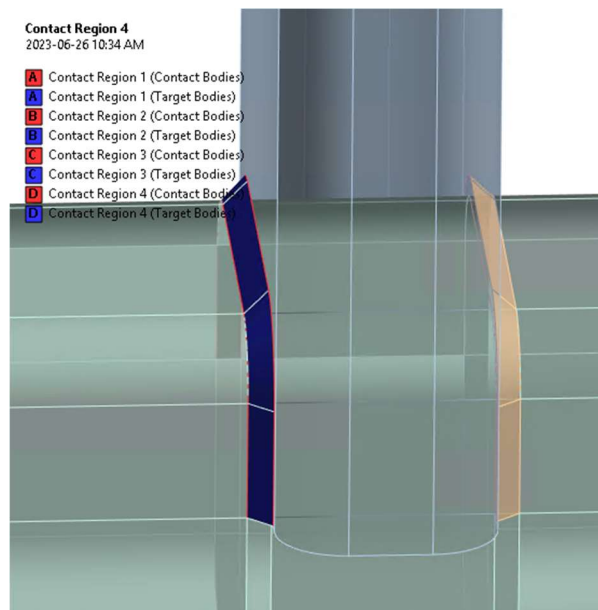
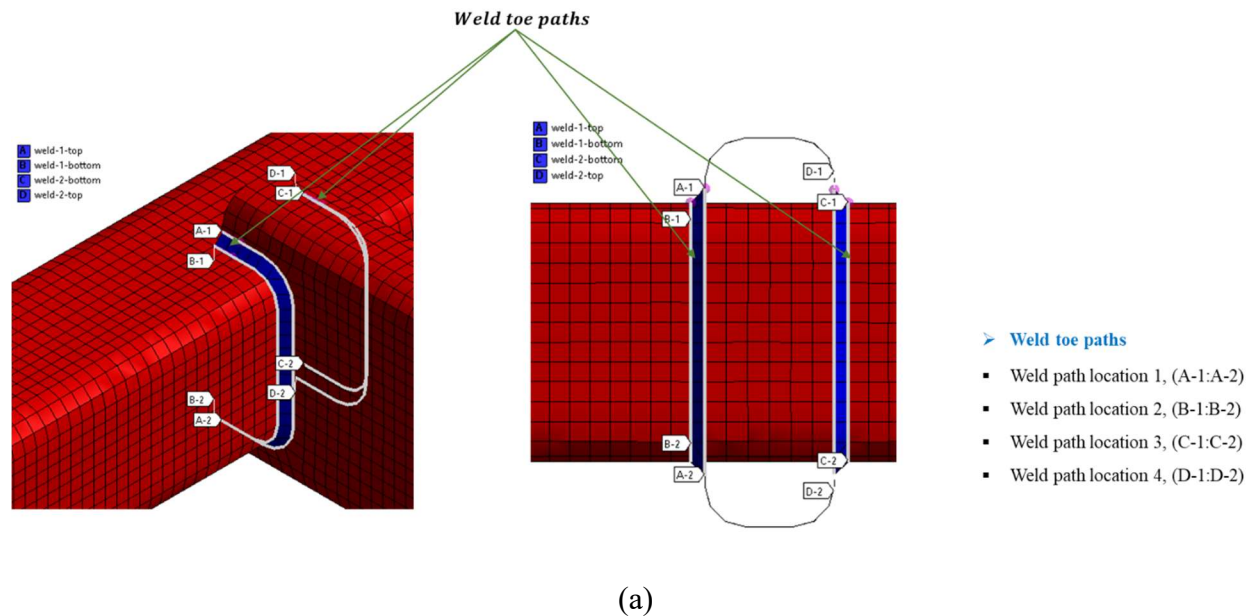


Figure 4-3: (a) Modeled weld toe paths (b) defined weld connection to the beam components

CONTA175 allows for 2-D or 3-D, no penetration and separation contacts, and no sliding between surfaces or nodes of shell, solid or beam elements [60]. Hence, they are suitable for adequately simulating the connection behaviour of the structure at the weld joint locations by connecting nodes at the weld toes to nodes on both structural beam components.

4.1.3 Preliminary Analysis for Reliability Validation of the FE Model

Before using the RHS T-joint welded structure finite element model created in Section 4.1.2 to verify the viability of the developed frequency domain fatigue analysis method, preliminary simulation and computational analysis are initially performed. The initial analysis ensures that the subsequent frequency domain fatigue analysis stress, damage and life results computed using the FE model are a reliable and accurate representation of the actual physical scenario with negligible or significantly reduced modelling and simulation effects induced errors.

The following analyses are performed as part of the FE model reliability verification process:

- (i) Mesh size insensitivity and selection analysis, based on the calculated EESS at the weld joints using the equations and procedures established in Sections 2.3.1 and comparison to the results provided in [19] for the same structure. The mesh insensitivity analysis is performed for varying mesh element sizes of $1T$, $2T$ and $3T$, where T is the minimum weld throat thickness corresponding to $7.9mm$. The mesh sizes are constant throughout the structure. Based on the mesh insensitivity analysis outcomes, the appropriate mesh size and element property type are selected for all subsequent analyses performed in this report.
- (ii) Geometrical characteristics, material, load, and boundary conditions validation analysis is performed to ensure the extracted results from the FE model are reliable.

A Fully reversible ($R = -1$) constant amplitude cyclic load of $17.8kN$ magnitude following the considerations in [19] is utilized for the FE model validation analysis. The load is applied at a remote point on one end of the beam, and using rigid links, a connection between the load application reference node and the structure's end surface is established, as shown in Figure 4-4. The other two ends of the beam are constrained in all translation and rotation directions.

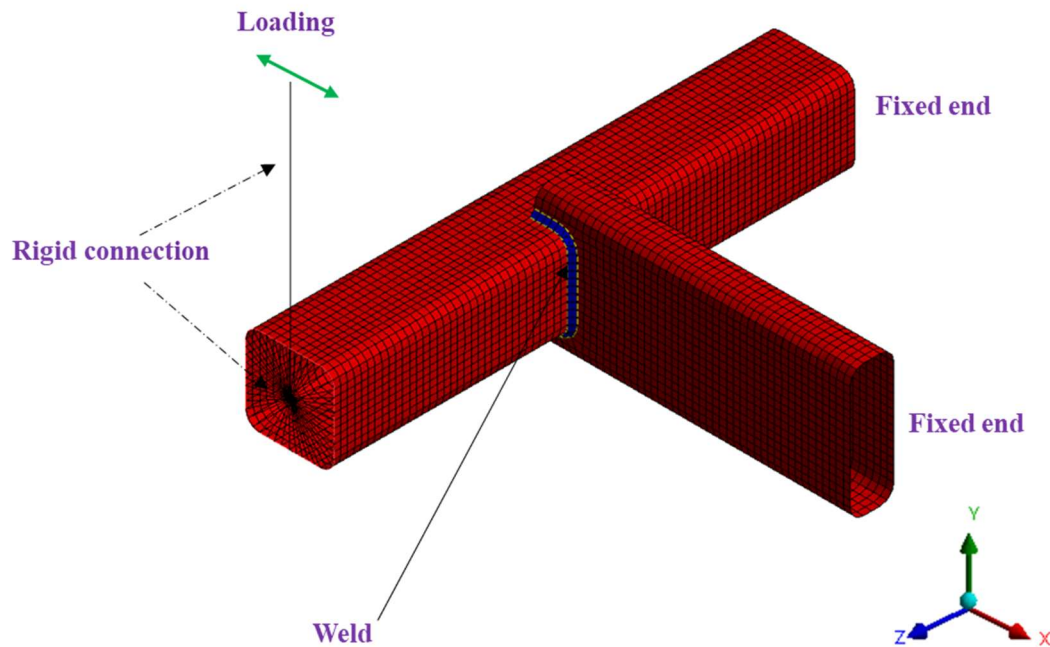


Figure 4-4: Finite element model with 1T mesh size, loading and boundary conditions

The global node forces and moments extracted from the FEA simulation solution are utilized in the MATLAB program. This MATLAB algorithm incorporates Equations (2.24), (2.25) and (2.28) to calculate the required EESS results variables.

The computed fatigue stress and life results are compared with the fatigue results in [19] to validate the appropriateness of the selected size and numerical model characteristics for subsequent analysis performed in this section. The fatigue results in the referenced literature are based on a

numerically and experimentally validated RHS structure subjected to a constant amplitude cyclic fatigue loading to determine the structure's damage crack initiation location and fatigue life using the EESS method for constant amplitude fatigue conditions.

By comparing the computed results with the fatigue results from [19], the appropriateness of the selected mesh size and numerical model characteristics for subsequent analyses in this section is validated. This comparison ensures that the FE model accurately captures the fatigue behaviour of the RHS T-joint welded structure and produces reliable and consistent results.

4.2 EESS-Based Frequency Domain Fatigue Analysis

After completing the preliminary analysis described in Section 4.1.3, the EESS-based frequency domain fatigue analysis is conducted. This analysis aims to estimate the fatigue damage and fatigue life of the RHS T-joint welded structure corresponding to the stress histories under random loading conditions using the computational procedure developed in Chapter 3.

Using the previously validated FE model of the structure from Section 4.1.3, the analysis progresses through a series of intermediate computational steps that culminate in the calculation of fatigue damage and life, as outlined in Section 3.2 and Section 3.3. The initial steps involve calculating the modal and FRF EESS responses, which are essential for obtaining the stress parameters required in the PSD stress evaluation equation defined by Equation (3.36).

By sequentially performing these computational steps and incorporating the EESS methodology, the frequency domain fatigue analysis comprehensively assesses the structural response to random loading. This analysis allows for estimating critical fatigue-related parameters, enabling insights

into the expected fatigue performance and potential life expectancy of the RHS T-joint welded structure.

4.2.1 Calculating the Modal EESS of the Structure

The modal EESS $\phi_i^{\Delta S_s}$ on the weld joints for each mode of the structure is calculated using a developed MATLAB algorithm that considers the established equations and procedures outlined in Section 3.2.1. To compute the modal EESS, the element modal line forces $\phi_i^{f'}$ and modal moments $\phi_i^{m'}$, together with the weld throat thickness and loading mode parameters, are required as input in the stress evaluation equation, Equation (3.21). The modal element line forces are derived from the corresponding modal global components based on the relationship defined by Equation (3.17). The required global modal node forces $\phi_i^{F_e}$ and moments $\phi_i^{M_e}$ are extracted from the FE frequency response analysis solution of the structure for all considered modal responses.

The modal analysis, the first step in the frequency domain fatigue analysis, is conducted in ANSYS FEA using the FE model developed in Section 4.1.3. The structure is structurally undamped, with no consideration of excitation loading. The modal analysis provides information about the structure's mode shapes and natural frequencies. These mode shapes and natural frequencies are obtained using the Lanczos mode extraction method, known for its reliability, efficiency, and support for sparse matrix methods that significantly increase computational speed and reduce storage space [60]. The extracted mode shapes and natural frequencies are crucial in defining and categorizing the structure's main dominant and critical modes and frequency ranges for the subsequent detailed frequency domain analysis. The selection of an adequate number of dominant mode shapes and natural frequency ranges is determined by considering the mass participation factors, which account for more than 85-90% of the structure's mass in the direction of the applied

loading [49], as discussed in Section 3.2.1. This mode selection criterion ensures that the selected modes accurately represent the dynamic response of the structure in subsequent detailed dynamic analysis and contribute significantly to the accumulated fatigue damage.

Using the global modal node forces and moments obtained from the FE frequency response analysis, the modal EESS stresses are computed along the weld paths of the structure for each mesh element node. This computation uses a MATLAB program incorporating the developed modal EESS equations, Equations (3.18) - (3.21). The modal EESS stresses provide crucial information about the stress distribution along the weld paths and contribute to the overall assessment of fatigue damage in the subsequent frequency domain analysis.

4.2.2 Calculating the EESS FRF of the Structure

After computing the modal EESS $\phi_i^{\Delta S_s}$, it is combined with the modal coordinates $\eta_i(\omega)$ using the established Equation (3.30) and procedures in Section 3.2.2. This calculation is performed in a MATLAB program to calculate the EESS FRF $H^{\Delta S_s}(\omega)$ of the structure. To obtain the modal coordinates responses $\eta_i(\omega)$, frequency response analysis is conducted in ANSYS using the prestressed modal analysis FE model. The model is subjected to a unit magnitude harmonic acceleration loading of $1m^2/s$ with a frequency spectrum ranging from 0 Hz - 2000 Hz in the vertical direction (Y-axis), as required by the methodology described in Section 3.2.2. This frequency range covers all the considered modes and natural frequencies of the structure and is in the same direction and quantity as the excitation loading. A constant damping ratio ζ of 2% is considered to simulate the structure's response. The EESS FRF is calculated for each node of the structure across the considered frequency ranges. To accurately capture stress frequency responses

and resolve them between frequency intervals, as well as around the natural frequencies of the structure, cluster points with a frequency spacing of 4 Hz are considered.

By extracting and evaluating the response modal coordinates from the FE frequency response analysis solution and substituting them into Equation (3.30), the EESS FRF of the structure is calculated for all modal responses and frequency ranges due to the unit loading excitation. This computation is performed for every mesh element node along the weld paths using a MATLAB program based on the developed FRF computational procedures.

4.2.3 Calculating the EESS PSD Response of the Structure

Once the EESS FRF $H^{\Delta S_s}(\omega)$ is calculated, it is combined with the input loading PSD loading $G(f)$ in Equation (3.36) to compute the EESS PSD $G^{\Delta S_s}(f)$ at the weld joints. This calculation is part of a frequency domain fatigue analysis procedure executed in the MATLAB program. To determine the EESS PSD, the structure is subjected to a 1-hour exposure duration of uniaxial stationary random base acceleration, representing an irregular road surface profile [34]. This loading is shown in Figure 4-5 in the time history domain and PSD frequency domain. The PSD loading is applied to the structure, and the resulting response is used to compute the EESS PSD at the weld joints.

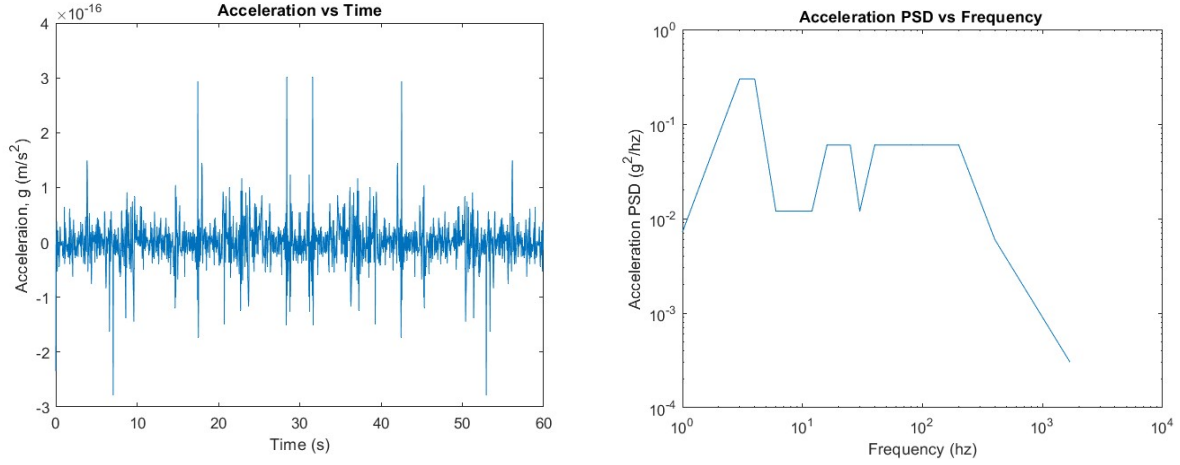


Figure 4-5: Input base acceleration PSD Load in the time domain and frequency domain form

The load, with a zero mean and a wide range of frequencies from 1Hz - 1700Hz , covering and exciting all the dominant main modes and natural frequencies of the structure, is applied in the vertical direction of the structure.

Next, the dynamic stress response PSD is computed for all the nodes along the weld paths of the structure. The PSD analysis provides valuable information about the distribution of stresses on the structure under the applied load. By importing the calculated FRF and the specified PSD loading into ANSYS ncode designlife glyphworks software [57], a specialized post-processing system, the structure's stress response distribution within the welds is analyzed and visualized. The software's computation enables further insights into the welded joints' stress patterns and fatigue behaviour, thus allowing for a comprehensive assessment of the structural integrity and fatigue life of the T-joint welded structure.

4.2.4 Estimating the Fatigue Damage and Life

Having computed the EESS PSD $G^{\Delta S_s}(f)$, the additional EESS amplitudes $S^{\Delta S_s}$ and related PDF $p(\Delta S_s)$ parameters are evaluated using Equations (3.39) and (3.40). Once these parameters are

calculated, the fatigue damage and life of the structure prior to damage crack initiation are subsequently assessed using Equation (3.41) and the procedural considerations outlined in Section 3.3. This analysis is performed in the MATLAB program.

To determine the fatigue design of the structure, the master S-N fatigue curve [18], described in Section 2.3.2 and depicted in Figure 4-6, is utilized. This curve considers the specific weld joint geometry details and material properties of the structure. The structure's fatigue performance and lifetime are comprehensively assessed by incorporating the calculated parameters into the analytical equations. This information is crucial for ensuring the integrity and durability of the welded joints in the T-joint structure.

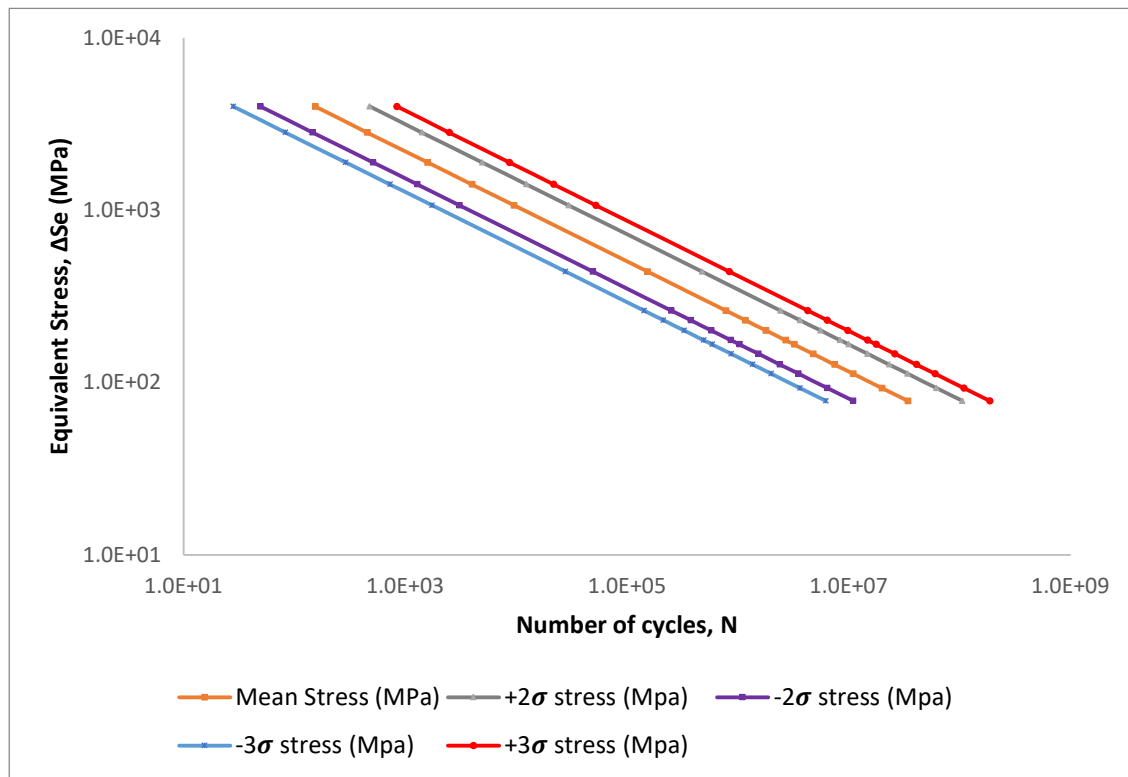


Figure 4-6: Mean and Standard Deviations Master S-N curves

The fatigue design analysis conducted in this research utilizes the properties of the mean S-N curve, specifically the slope C and intercept h parameters, as outlined in Equation (3.41) and presented in Table 2-1. These parameters play a significant role in quantifying the fatigue behaviour of the structure and are essential for accurately predicting its fatigue life. By incorporating these properties into the analysis, a comprehensive evaluation of the structure's fatigue performance can be achieved, enabling the identification of critical areas and ensuring adequate design measures are implemented to mitigate fatigue-related failures.

The overall procedure has also been implemented in ANSYS ncode designlife glyphworks to visualize damage and stress distribution, allowing for extracting stress cycle and fatigue damage distribution plots by importing the properties of the master S-N fatigue material curve, the calculated FRF and loading PSD. This approach makes it possible to analyze and visualize the distribution of stress and damage throughout the structure, providing valuable insights into the areas prone to fatigue failure. These visual representations aid in identifying critical locations and facilitate informed decision-making regarding design modifications or fatigue life improvements.

4.3 Results and Discussions

The results of the numerical preliminary quasi-static analysis and the dynamic frequency domain fatigue analysis, including the main intermediate computational steps leading to the fatigue damage and life calculations, are presented and discussed in this section. The discussion highlights the significance of each computational step and its impact on the overall fatigue analysis. The presented results serve as a basis for evaluating the structural integrity and identifying areas of concern for further design optimization and fatigue life improvement.

4.3.1 Preliminary Analysis Results and Discussions

The results of the mesh size insensitivity analysis for mesh element sizes of $1T$, $2T$ and $3T$ in the structure are depicted in Figure 4-7. The EESS values for each considered mesh size are plotted along the weld toe paths in the superimposed graph plot. The graph shows that the computed stresses based on EESS remain relatively constant for all the element nodes along the weld path as the mesh size changes. The constant nature of the stress indicates that the calculated stresses are insensitive to variations in mesh size. However, around the open ends of the weld and areas where there are abrupt changes in the weld path direction, reductions in stress peaks can be observed for mesh sizes larger than the minimum thickness of the structure. This phenomenon occurs because the nodal positions may miss capturing the peak stresses accurately, as evidenced by the $2T$ mesh size curve.

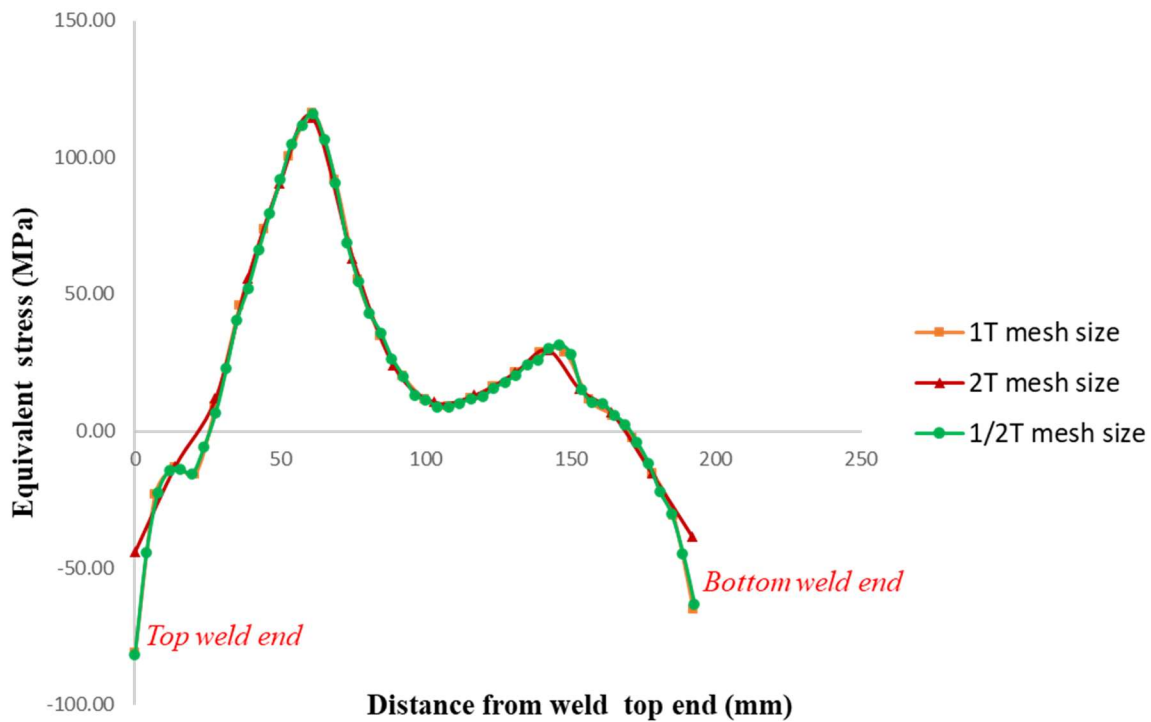


Figure 4-7: EESS along weld toe path for $1T$, $2T$ and $3T$ mesh sizes

Considering these observations, the absolute mesh insensitivity assumption is limited without considering the geometric thickness and complexities of the structural components around the weld joints, as Dong et al. proposed [16].

Based on the results, a constant mesh size distribution of $1T$ (equivalent to $7.9mm$) is selected for the subsequent analysis performed in this report. This mesh size comprises 5862 nodes and 5708 elements, providing an appropriate balance between accuracy and computational efficiency.

Based on the constant cyclic loading, the structure's estimated fatigue life prior to damage crack initiation is 73,933 cycles, as shown in Figure 4-8.

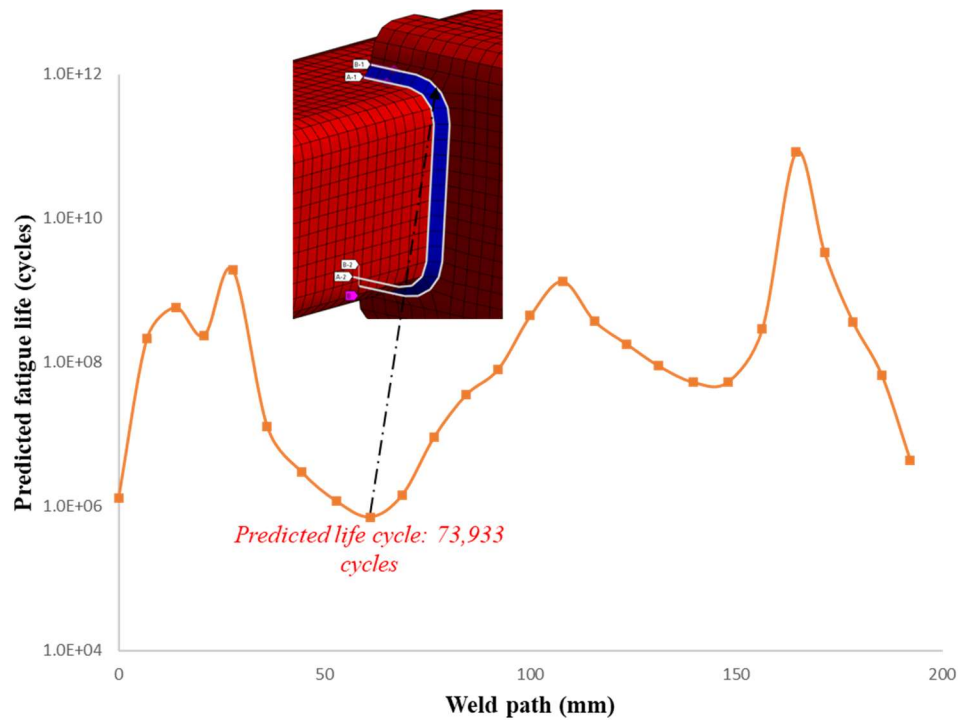


Figure 4-8: Calculated fatigue life along the weld path due to constant amplitude cyclic loading

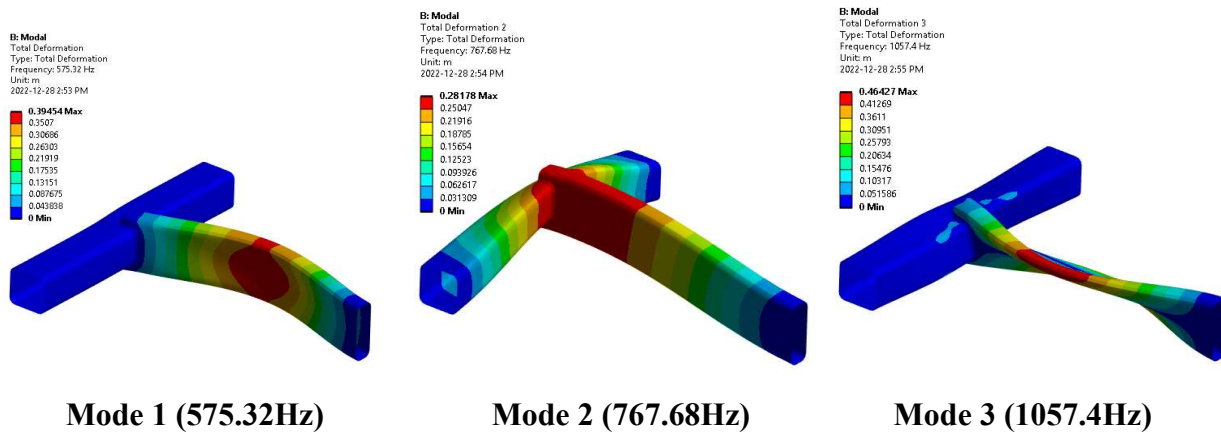
A relative percentage variation of approximately 1.4% between the fatigue life obtained from the numerical method and the referenced test fatigue life of 75,000 cycles [19] has been achieved, which is considered acceptable, thus validating the geometric and other modelling considerations of the FE model for further detailed frequency domain fatigue analysis.

4.3.2 Frequency Domain Fatigue Analysis Results and Discussion

The numerical simulation and analytical calculation results, including the main intermediate EESS modal, frequency, and PSD responses computational steps results leading to the structure's predicted fatigue damage and life results, are presented in this section.

4.3.2.1 Modal Response of the Structure

The modal analysis results for the displacement mode shapes $\phi(x)_i$ of the first ten selected modes are presented in Figure 4-9. These mode shapes provide insights into the structural response at different vibration frequencies.



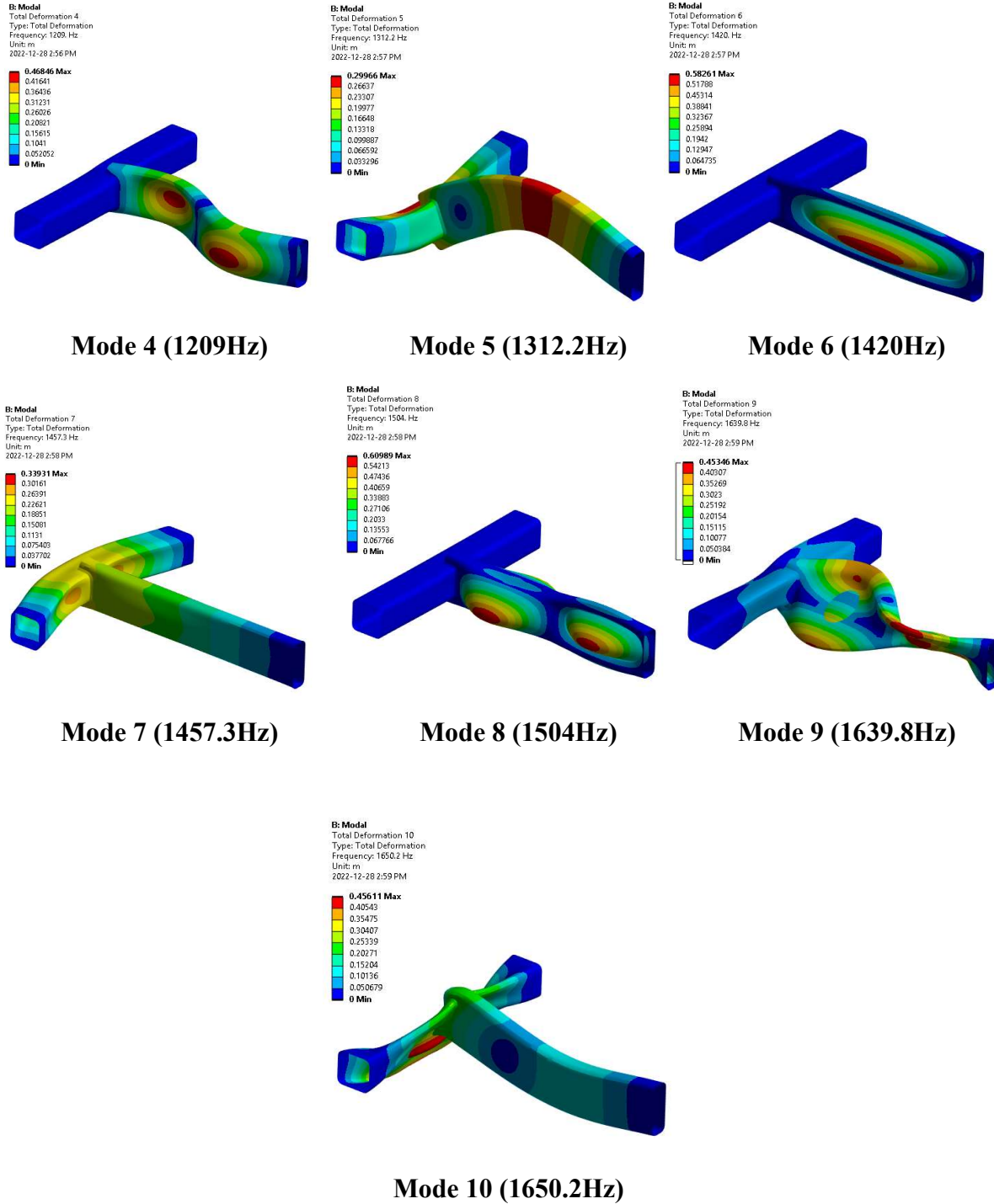


Figure 4-9: Mode shapes contour and corresponding natural frequencies of the first ten modes of the structure

By analyzing the participation factors of the contributing modes, it is determined that modes 2, 5, and 10, which exhibit in-plane displacement mode shapes aligned with the applied base acceleration excitation, are the dominant modes. These modes significantly influence the structural response and contribute substantially to the accumulated fatigue damage.

The natural frequencies ω corresponding to each mode shape within the frequency range of $575.32\text{Hz} - 1639.8\text{Hz}$ are listed in Table 4-3. The subsequent stress response and damage life evaluations consider all the first ten modes.

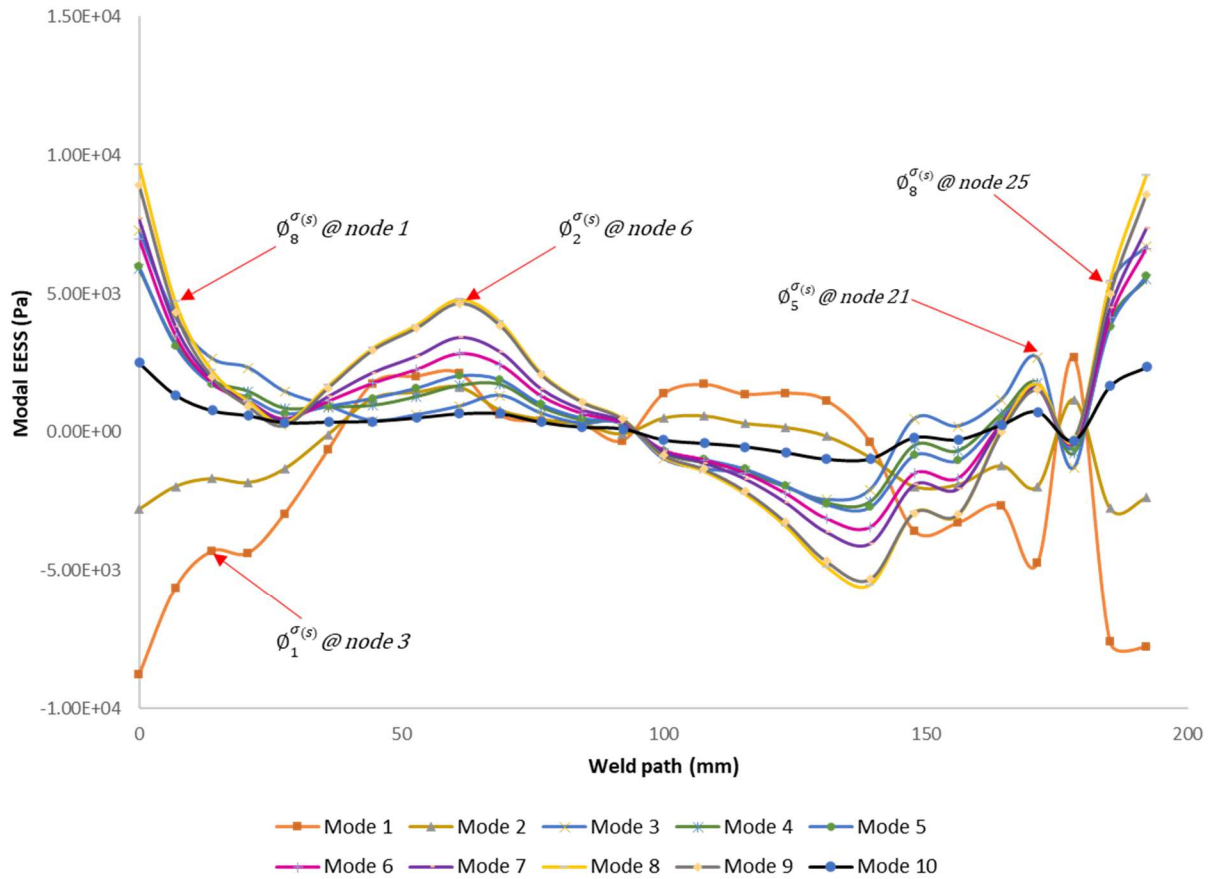
Table 4-3: First ten natural frequencies of the structure with the corresponding modes, participation factors and effective mass proportion

Mode	Frequency	Participation factor			Effective mass to total mass proportion		
		X-direction	Y-direction	Z-direction	X-direction	Y-direction	Z-direction
1	575.32	-8.77E-04	-4.67E-05	-3.52E+00	2.37E-08	6.72E-11	3.83E-01
2	767.68	1.21E-04	4.79E+00	-1.99E-05	4.55E-10	7.88E-01	1.22E-11
3	1057.4	3.09E-05	-3.60E-03	4.37E-04	2.95E-11	4.00E-07	5.90E-09
4	1209	-4.04E-03	-3.28E-05	6.72E-04	5.04E-07	3.32E-11	1.39E-08
5	1312.2	-7.82E-05	-1.02E-01	2.82E-05	1.89E-10	7.22E-02	2.46E-11
6	1420	-4.04E-01	-5.15E-05	-4.67E-06	5.04E-02	8.18E-11	6.72E-13
7	1457.3	-4.95E+00	2.67E-04	-2.10E-04	7.56E-01	2.19E-09	1.36E-09
8	1504	4.12E-01	1.90E-04	-5.64E-05	5.24E-02	1.11E-09	9.82E-11
9	1639.8	-1.99E-04	3.27E-03	-9.88E-04	1.22E-09	3.30E-07	3.01E-08
10	1650.2	-3.27E-04	-1.34E+00	-1.28E-04	3.31E-09	9.53E-02	5.05E-10
Total					8.59E-01	9.56E-01	3.83E-01

As indicated in Table Table 4-3, The natural frequency of the first mode is 575.32Hz , revealing the fundamental vibration characteristic of the structure. Modes 1-10 have natural frequencies within the loading frequency range. The selected modes, which account for more than 90% of the

structure's mass, are sufficient to accurately capture the dynamic response in the loading direction and evaluate the accumulated fatigue damage, as discussed in Section 3.2.1. Modes 3 and 6 exhibit torsional displacement shapes, while modes 1, 4 and 8 correspond to the out-of-plane displacement of the structure.

Figure 4-10 illustrates the plot of the modal EESS $\phi_i^{\Delta S_s}$ for the first ten modes for all 26 nodes along weld path 1A of the structure. The modal EESS values vary along the weld path, reflecting the different stress contributions from each mode.



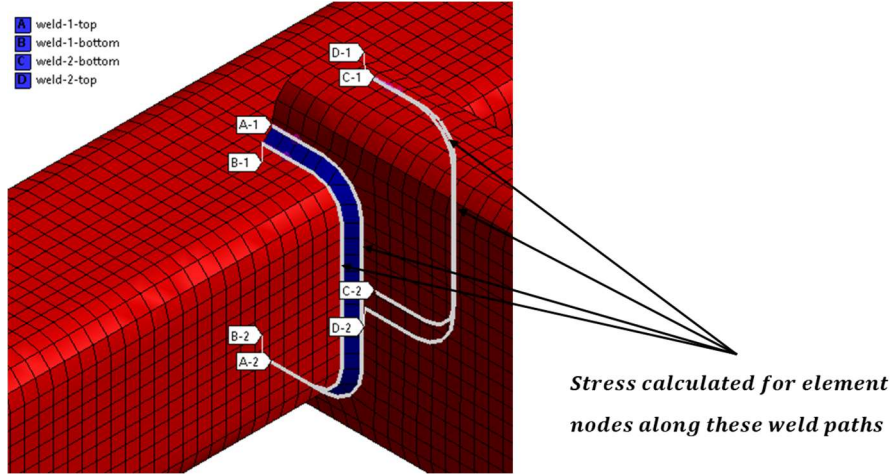


Figure 4-10: Evaluated modal EESS for the first ten modal responses of the structure along the weld toe paths

Mesh element nodes 6 and 25 on the modelled weld joint exhibit the highest modal EESS with stress values of $4645.97Pa$ and $9279.13Pa$, respectively, corresponding to modes 2 and 8, as seen in Figure 4-10. These nodes play a significant role in the stress response and damage accumulation due to their higher mass fraction and proximity to critical locations. These modal EESS results, based on the structure's modal responses, are considered in calculating the EESS FRF.

4.3.2.2 Frequency Response of the Structure

The frequency response coordinates $\eta_i(\omega)$ as a function of frequency plot results at the weld joints is presented in Figure 4-11. The frequency response coordinate plots showcase the structural response to the applied harmonic load across various frequencies for the first ten modal responses.

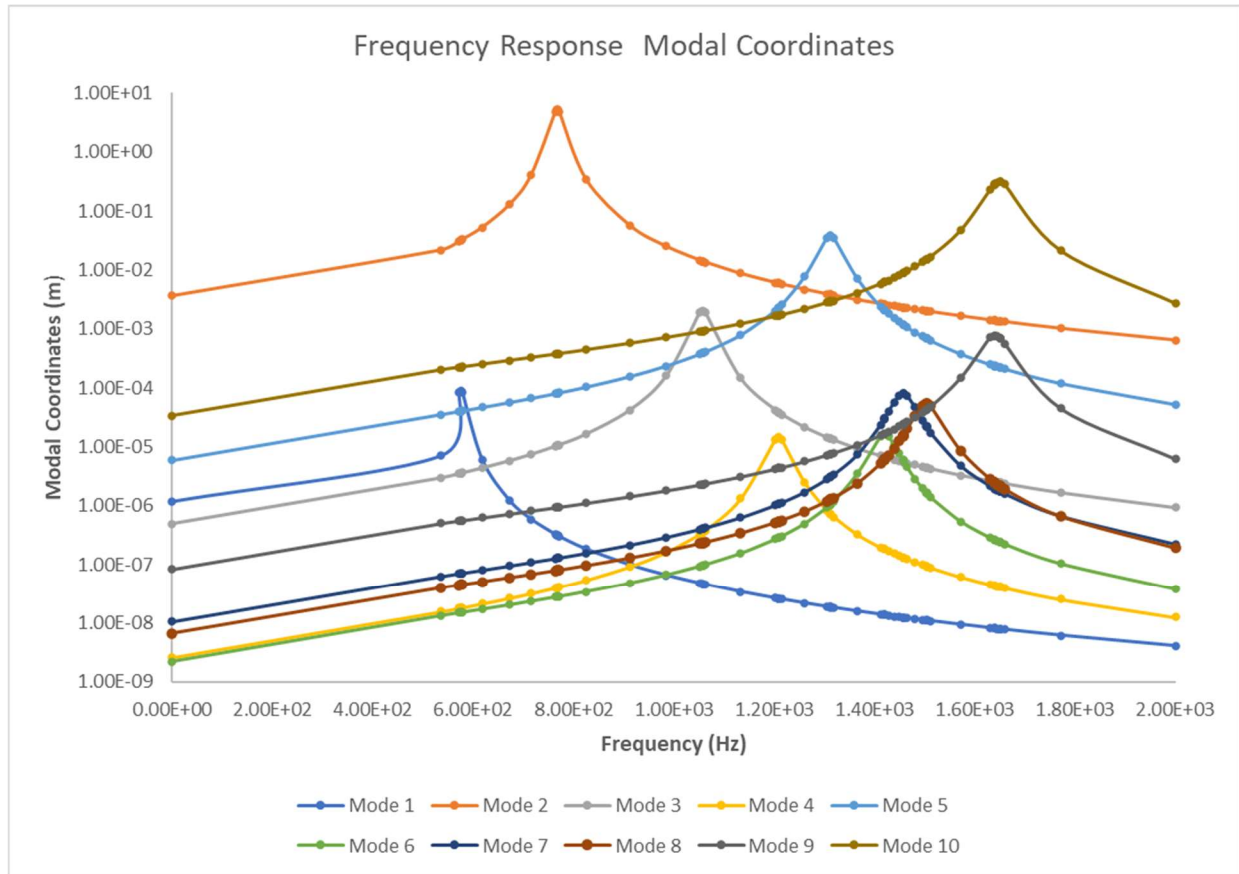


Figure 4-11: Evaluated frequency response coordinates for the first ten modal responses of the structure

Figure 4-11 shows that the frequency response modal coordinates corresponding to modes 2 and 10 are the highest, stipulating the most sensitivity to the applied harmonic loads. Utilizing these FRF coordinates and the calculated modal stress results presented in Section 4.3.2.1, the frequency response stresses are computed for all the nodes along four weld paths of the weld joints. Figure 4-12 displays the frequency response stress results obtained for these nodes, exhibiting multiple stress peaks around the structure's natural frequencies.

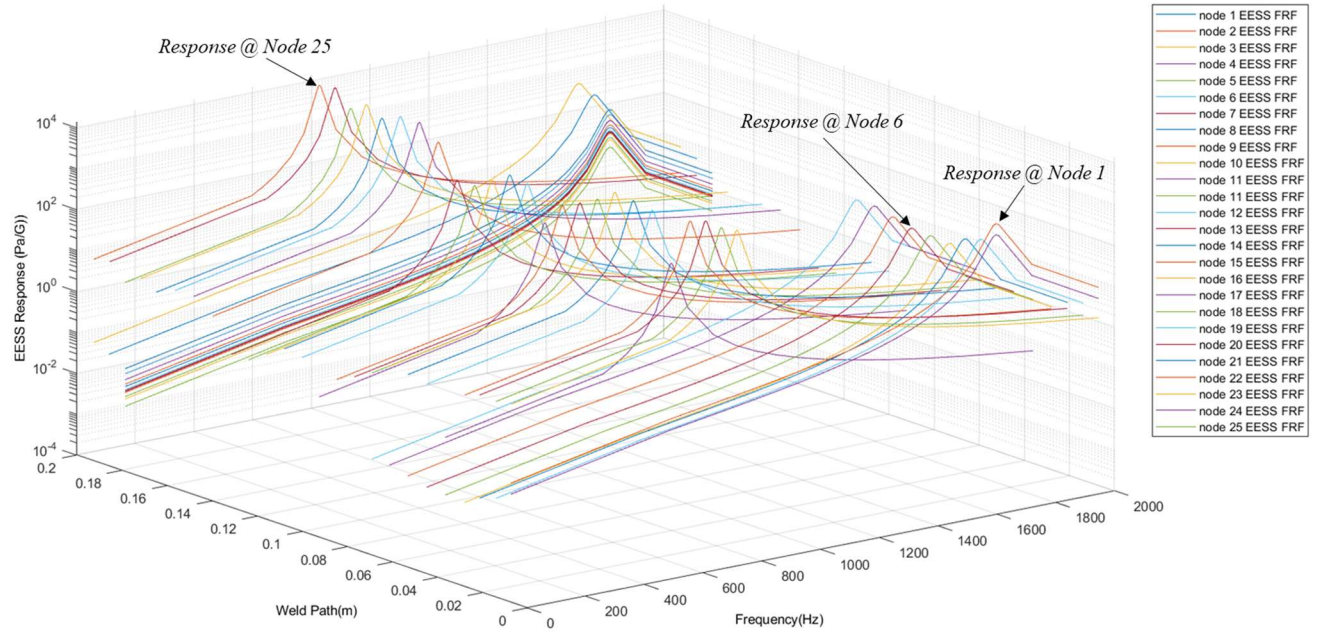


Figure 4-12: Calculated EESS FRF for the twenty-six nodes on the structure's weld toe paths

It is observed that modes with higher frequency magnitudes than the applied load do not contribute significantly to the structural response, as the load magnitude remains constant. However, modes 2 and 10, representing in-plane displacement modes, significantly impact the stress and damage experienced by the structure. To identify the mesh node with the maximum EESS FRF response, further post-processing is conducted on the calculated EESS FRF results. Figure 4-13 illustrates the stress frequency responses along weld path one for the twenty-six mesh nodes on the top weld path.

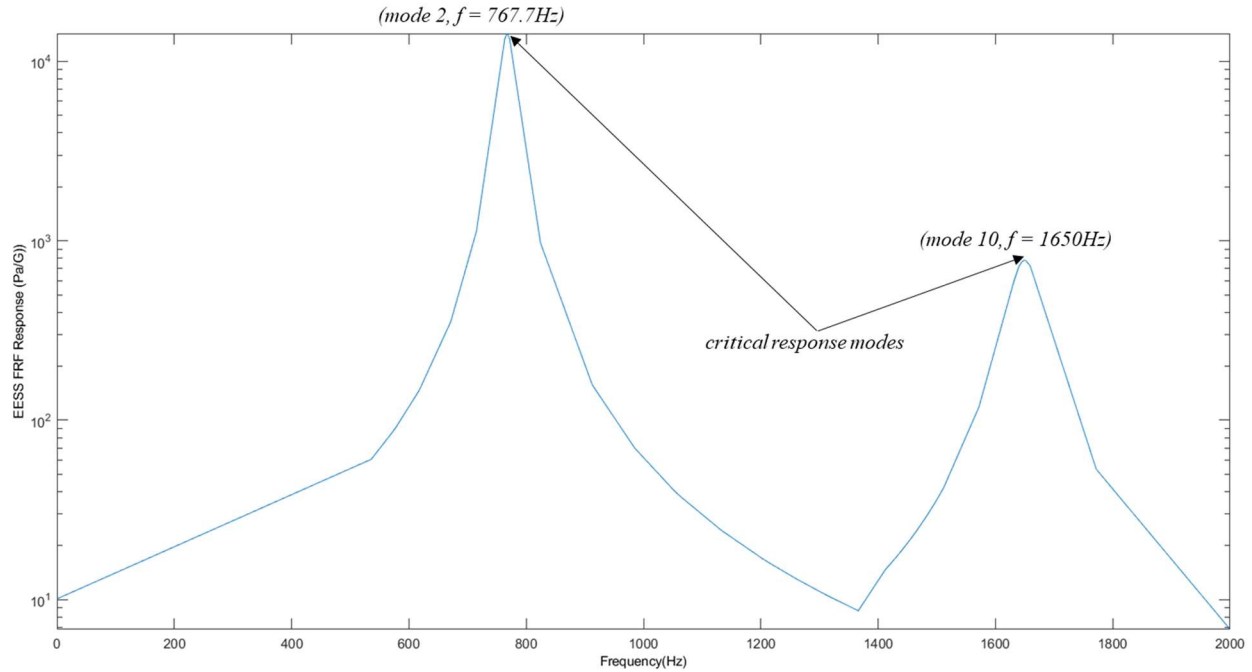


Figure 4-13: Maximum EESS FRF at node six on the weld toe paths

The maximum EESS response is observed at node six and is plotted separately below the stress frequency response plot. Notably, the peak stress frequency responses of $112,395 \text{ Pa/G}$ and $32,672 \text{ Pa/G}$ correspond to the natural frequencies of modes 2 and 10, respectively. These frequencies are extracted and incorporated into the maximum stress PSD and fatigue damage calculations.

These findings emphasize the significance of considering the EESS FRF responses, including stress frequency responses and their association with the structural modes, in accurately predicting the fatigue damage and life of the structure.

4.3.2.3 EESS PSD Response and PDF of the Structure

The maximum stress PSD responses $G^{\Delta S_s}(f)$ acting on node six along the top weld path of the structure, from which the damage and life evaluation is performed, are depicted in Figure 4-14.

This stress response location corresponds to the same location as the maximum EESS frequency response. The maximum EESS PSD responses of $6.91E+8Pa^2/Hz$ and $1.47E+7Pa^2/Hz$ occur at two input excitation loading frequencies of $767.7Hz$ and $1650Hz$, respectively, coinciding with the natural frequencies of the 2^{nd} and 10^{th} modes of the structure.

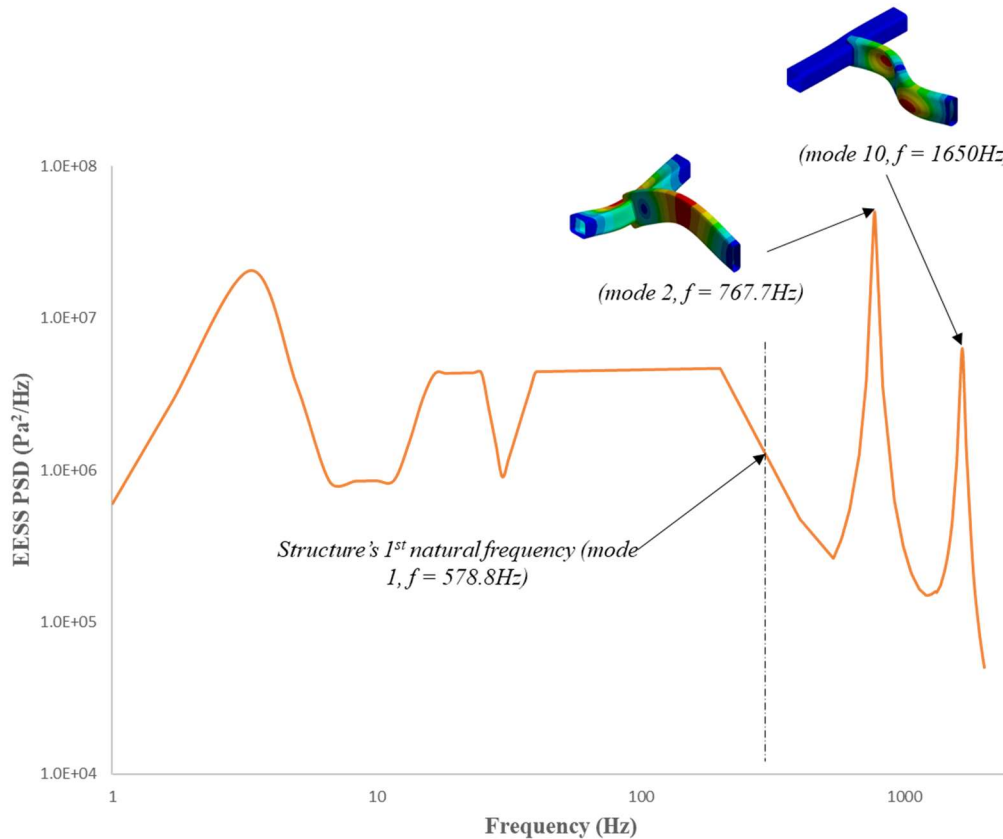


Figure 4-14: Maximum EESS response at node six: critical response at modes 2 and 10

The spectrum results reveal that these two critical frequencies exhibit the strongest response to the load due to maximum dynamic amplification around the structure's second and tenth vibration modes, with natural frequencies of $767.7Hz$ and $1650Hz$, respectively. These stresses, at the higher frequencies of the load excitation, contribute *over 50%* to the overall fatigue damage experienced by the structure. The structure's response before the first natural frequency is primarily governed by its structural stiffness, resulting in a spectrum response following the load PSD. Multiple peak

stresses within the natural frequencies are observed due to the applied loading. However, dynamic amplification effects do not influence stress responses below the first natural frequency of the structure. The peak stresses occur at node six, coinciding with the locations where the loading frequencies align with the structure's natural frequencies.

The stress PDF of the structure, which defines the likelihood of occurrence for each calculated EESS amplitude, is presented in Figure 4-15.

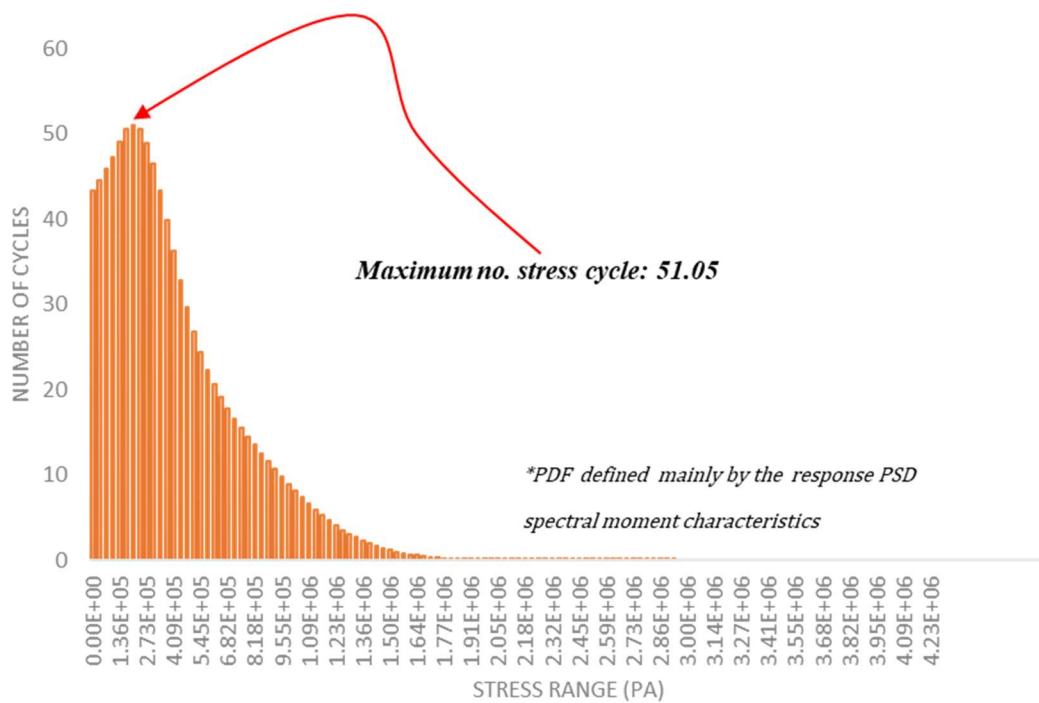


Figure 4-15: PDF of EESS amplitudes for the maximum EESS PSD

The stress amplitude PDF, with a maximum number of stress cycles of 51.5, is derived from the one-sided EESS PSD results across the excitation frequency range shown in Figure 4-15. From the figure, it can be observed that the $\pm 1\sigma$ stress range values of 0 Pa - 6.82E+5 Pa, with a 68.3% likelihood of occurrence during the period of exposure to the load excitation, have the highest

occurrence of repeated cycles, corresponding to a 32% chance of exceeding 50 cycles. These calculated stress range values, although considerably smaller compared to the maximum $\pm 3\sigma$ stress range values of $6.83E+6Pa - 2.86E+6Pa$, significantly contribute to the accumulated fatigue damage of the structure.

4.3.2.4 Estimated Accumulated Fatigue Damage and Life of the structure

The fatigue damage distribution, based on the contribution of each cyclic stress range, is plotted in Figure 4-16.

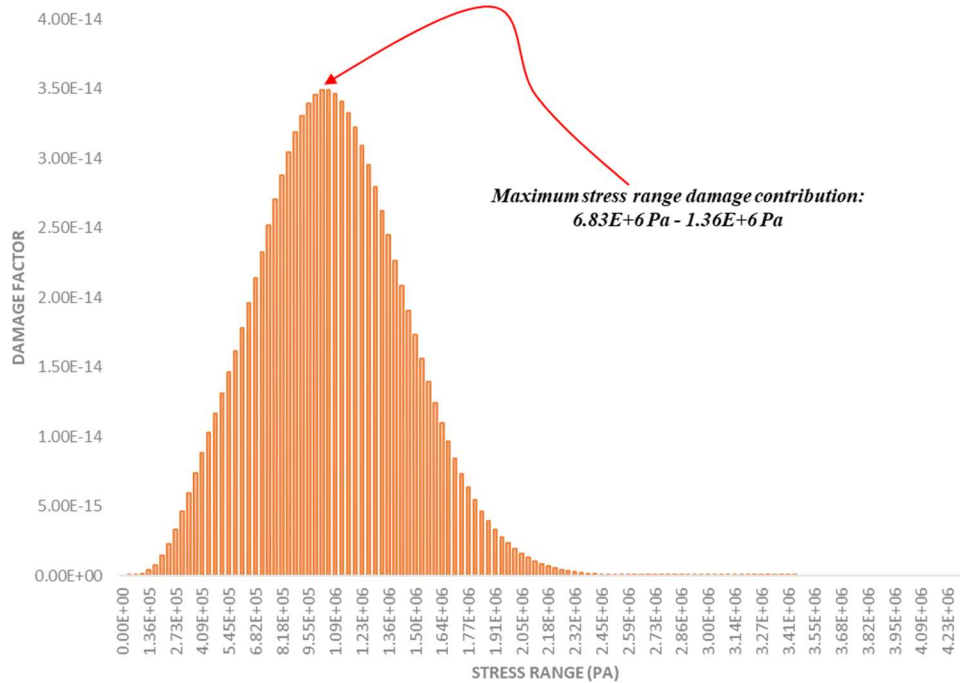


Figure 4-16: PDF of fatigue damage intensity

From the figure, it can be observed that 68.3% of the predicted accumulated fatigue damage induced in the structure is predominantly caused by the $\pm 3\sigma$ stress range of $6.83E+5Pa - 1.36E+6Pa$ which is expected to occur only approximately 4.3% of the time with a maximum number of cycles of eighteen, as shown in the stress distribution figure, Figure 4-15. The damage

contribution of the $\pm 1\sigma$ stress ranges is more than three times greater than that of the $\pm 2\sigma$ stress ranges, which are predicted to occur for about 27.1% of the load exposure time.

The variation in fatigue damage intensity along the weld paths is depicted in Figure 4-17. The region with the maximum cumulated estimated fatigue damage intensity, $D = 2.804E-6$ per year, is observed at node six.

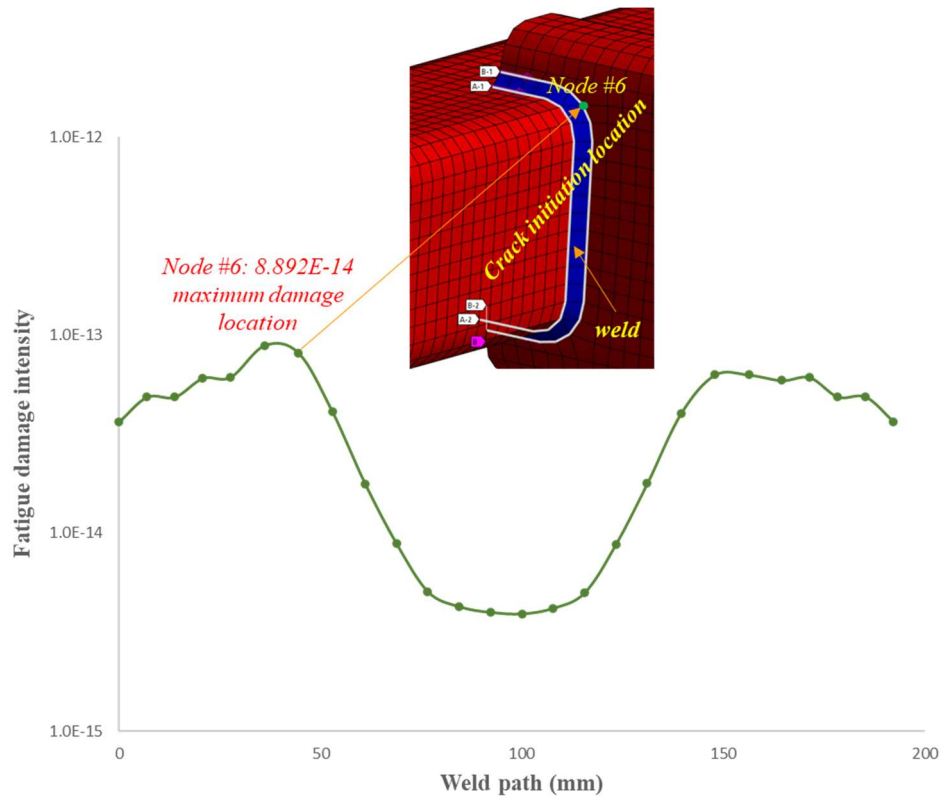


Figure 4-17: Predicted fatigue damage intensity along the weld toe path

This region, as expected, corresponds to the most stressed area within the welds and is found to be critical, experiencing the highest level of damage.

The corresponding fatigue life variation of the structure, calculated from each damage intensity value, is shown in Figure 4-18.

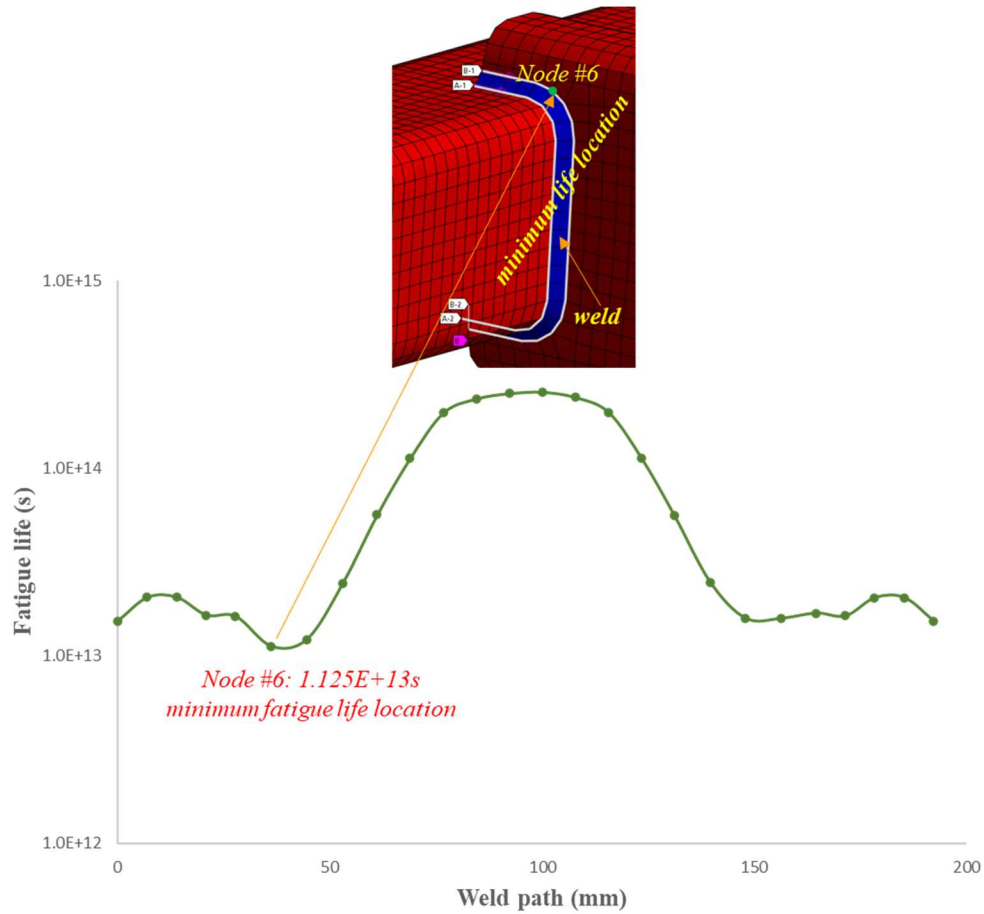


Figure 4-18: Predicted fatigue life along the weld toe path

The minimum estimated fatigue life at node six, where the maximum damage occurs, is 99 years. This minimum calculated fatigue life is also considered as the estimated fatigue life of the structure under the considered load magnitude and exposure duration. Thus, it implies that the structure can sustain repeated random loading for a fatigue lifetime period of 99 years, based on a 90-95% confidence interval and a 98% probability of survival before the initiation of a damage crack.

4.4 Validation of the Fatigue Damage and Life Results

In this section, the accumulated fatigue damage and life results of the welded structure obtained using the proposed frequency domain fatigue analysis method, as presented in 3.2, are validated.

The validation process involves a comparative analysis with fatigue test results reported in the literature [19] for the same structure and numerical analysis results obtained using the hotspot stress extrapolation-based frequency domain fatigue analysis method.

As depicted in Figure 4-19, the predicted fatigue damage crack initiation location on the structure's weld joint using the proposed method is consistent with the area reported in the literature [19] under the same conditions, where uniaxial tensile stresses are applied perpendicular to the weld throat. These similarities in damage results validate the proposed method's accuracy in predicting the fatigue damage location and estimating its intensity for the considered random loading condition. However, the fatigue damage results of the hotspot stress extrapolation-based frequency domain fatigue analysis do not match the test-predicted damage location.

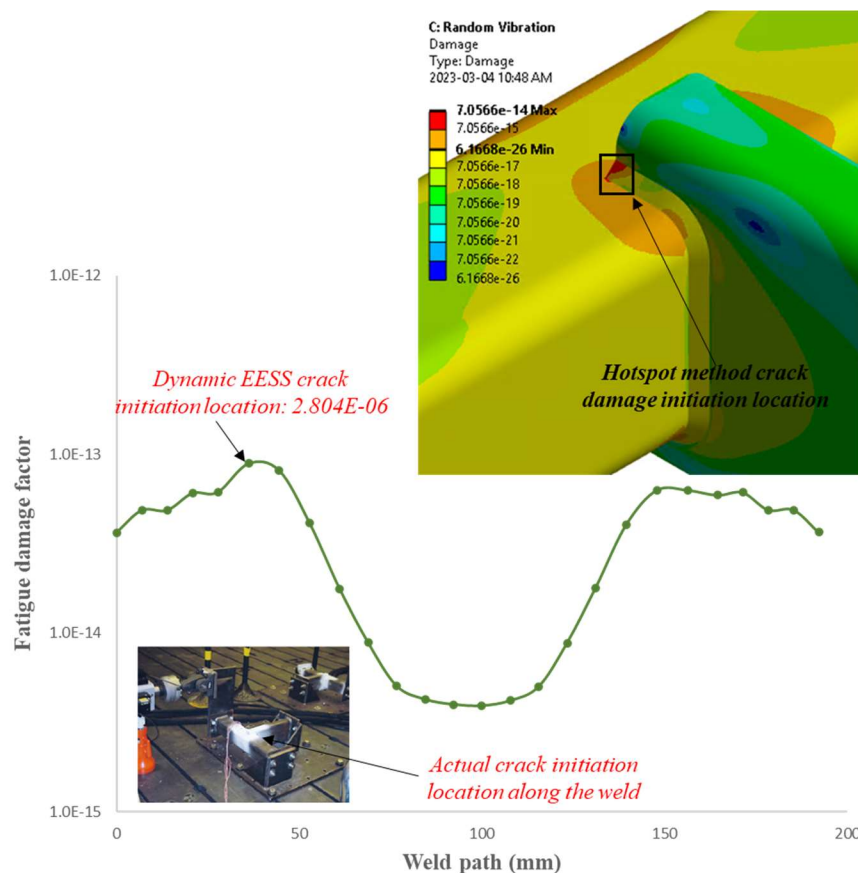


Figure 4-19: Predicted crack initiation comparison with experiment and hotspot results

The fatigue life comparison uses the S-N curve for the material and welds joint detail described in Hobbacher [59]. The fatigue properties of the S-N curve are based on uniaxial tensile and bending tests conducted under uniaxial fatigue load-controlled fully reversed conditions (tensile-compression testing with an $R=-1$ stress ratio) at a loading frequency range of 20Hz . The hotspot stress method analysis is performed using the procedures described in Section 2.2 of the literature review for the same FEA model and boundary conditions described in Section 4.1.2 and the PSD loading condition described in Section 4.2.3. To ensure the model produces a mathematically accurate solution as required in the hotspot stress extrapolation-based frequency domain fatigue analysis method, a mesh convergence analysis is conducted using mesh sizes of $T/4$, $T/3$, $T/2$, T , and $2T$. The results of the mesh analysis are depicted in Figure 4-20, considering the stress convergence extracted from non-singularity locations of the structure. Based on the convergence results, a mesh size of $T/4$ is selected.

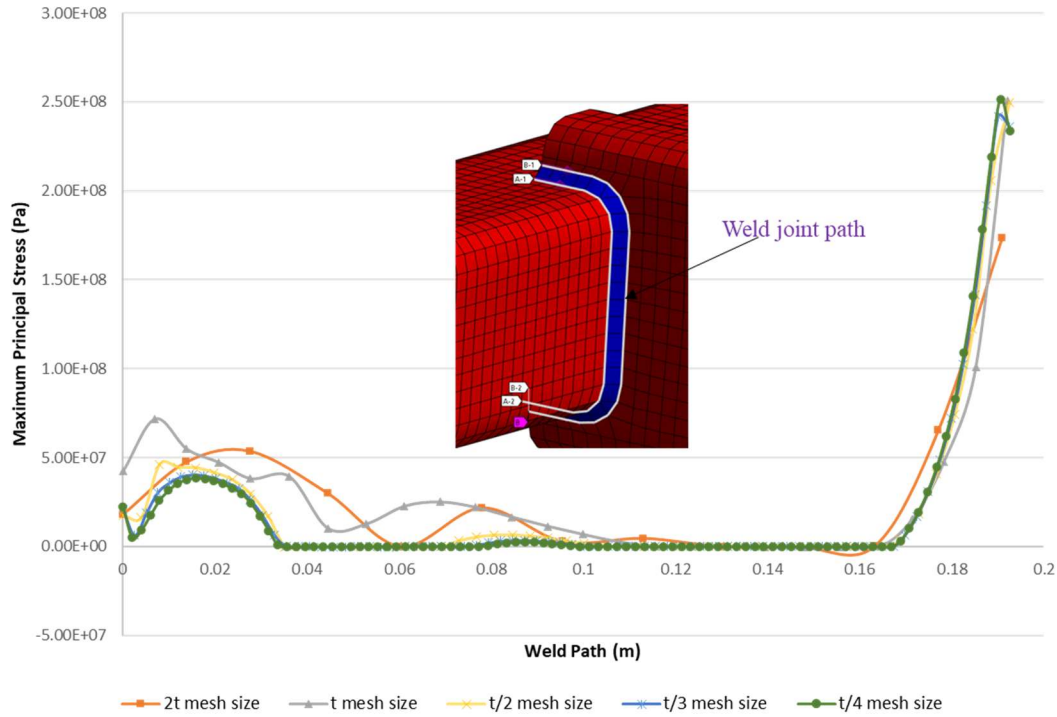


Figure 4-20: Extrapolated maximum principal hotspot stress convergence with mesh size variation

The fatigue life results obtained based on maximum principal hotspot extrapolated stresses are presented in Table 4-4. A 26% variation in fatigue life is observed, which considers the potential variability from existing methods and the proposed method. The variation in results between the structural hotspot stress-based evaluation of fatigue life using the recommended design curve and the EESS-based method using the master S-N curve aligns with the outcomes of additional extensive verification analysis performed in this research to study the fatigue life variations between the EESS and hotspot methods.

Table 4-4: EESS and hotspot frequency domain methods predicted fatigue life comparison

Frequency domain fatigue analysis method	Damage intensity/year	Fatigue life (years)	Variation (%)
EESS-based	2.804E-06	99.09	25.96
Hotspot stress-based	2.2254E-06	124.82	

Furthermore, the computational processing time and memory storage requirements for both methods are explored to investigate the computational efficiency of the proposed method compared to existing frequency domain fatigue analysis methods, as outlined in Table 4-5.

Table 4-5: Simulation memory, runtime, and output database requirements for EESS and hotspot frequency domain methods

Frequency domain fatigue analysis method	Storage memory requirement (GB)	processing memory requirement (GB)	Processing time (s)
EESS-based	8.3	3.5	134
Hotspot stress-based	50.5	14.3	321

The proposed EESS-based frequency domain analysis method exhibits a reduced processing time of approximately 58% compared to the existing method. Similarly, the computational processing and storage memory requirements are reduced by 76% and 84% when using the proposed method for fatigue design analysis of randomly loaded welded structures. The improved computational efficiency of the proposed method can be attributed to the use of coarse mesh sizes, leading to less computational processing required for each mesh node and element in a discretized structure. Additionally, since the EESS FRF of the structure is externally calculated in the MATLAB program before importing it into the FEA program, the computational requirements for this analysis step are conserved.

4.5 Summary

This chapter demonstrates the numerical viability and validity of the equations and procedures developed in Chapter 3 using an RHS T-joint welded structure subjected to irregular road surface profile-induced stationary random loading.

Initial analysis based on constant cyclic fatigue loading was performed to verify the reliability and performance of the FEA model in producing accurate and reliable results. A maximum peak stress value of 116.7MPa at the same weld toe region of the structure was obtained for the mesh element sizes of $1T$, $2T$ and $3T$. A relative percentage variation of approximately 1.4% between the numerical method predicted $73,933$ cycles fatigue life and the test $75,000$ cycles fatigue life in the referenced literature was also obtained. The obtained preliminary results validated the insensitivity of the calculated stresses to variations in mesh sizes, geometric and other modelling considerations of the FE model for the frequency domain fatigue analysis.

The validated FE model is then utilized to demonstrate and verify the numerical viability of the proposed EESS-based frequency domain fatigue analysis method in predicting the fatigue damage and life of the RHS T-joint welded structures. Intermediate modal analysis, frequency response analysis, and stress power spectral density (PSD) computational analysis were conducted to calculate the EESS modal stresses, EESS frequency response function (FRF), and EESS PSD for all the nodes at the weld joints of the structure respectively. These analyses allowed for calculating the fatigue damage and life of the structure.

Modal EESS for the first ten modes for all twenty-six nodes along weld path $1A$ of the structure was calculated. Mesh element nodes eight and twenty on the modelled weld joint exhibit the highest modal EESS with stress values of 645.97Pa and 9279.13Pa , respectively, corresponding

to modes two and eight. The obtained modal stresses were used with the extracted modal coordinates to calculate the corresponding EESS FRF at the same weld joint locations. Peak stress frequency responses of $112,395\text{Pa}/G$ and $32,672\text{Pa}/G$, corresponding to the natural frequencies of modes two and ten, respectively, were obtained. These frequencies are extracted and considered in the calculation of the maximum stress PSD EESS PSD responses of $6.91E+8\text{Pa}^2/\text{Hz}$ and $1.47E+7\text{Pa}^2/\text{Hz}$ occur at two input excitation loading frequencies of 767.7Hz and 1650Hz , respectively, coinciding with the natural frequencies of the second and tenth modes of the structure.

Utilizing the master S-N fatigue curve parameters and the calculated EESS PSD results, the accumulated fatigue damage D due to the maximum EESS PSD at node six was estimated to be $2.804E-6$ per year, and the corresponding predicted fatigue life of the structure prior to damage crack initiation, L , was 99 years. The predicted life is based on a 90-95% confidence interval and a 98% probability of survival before damage crack initiation.

The estimated fatigue damage and life results of the structure using the proposed method were validated by comparing them against test results from the literature and outcomes obtained from the hotspot stress extrapolation method. The predicted fatigue damage crack initiation location on the structure's weld joint is consistent with the location reported in the literature. A 26% variation in fatigue life between the existing hotspot and proposed EESS methods is observed. The predicted life using the proposed method exhibits a significant improvement of 26% compared to the hotspot method. The proposed EESS-based frequency domain analysis method indicates a reduced processing time of approximately 58% compared to the existing method.

5 Conclusions and Recommendations

The research methodology, derived results and inferences from the results are conclusively summarized in this chapter. The recommendations section discusses the limitations of the proposed research method, result outcomes, and future works.

5.1 Conclusions

This research has developed analytical equations and computational procedures integrating the well-established quasi-static Equilibrium Equivalent Structural Stress (EESS) fatigue methods and structural dynamics analysis principles for a new EESS-based frequency domain fatigue analysis approach for welded structures' fatigue damage and life evaluation prior to damage crack initiation under random loading conditions.

The proposed fatigue damage and life assessment method is based on integrating the developed analytical equations for evaluating the modal EESS, EESS FRF, EESS PSD, and EESS amplitudes PDF, including the master S-N curve parameters and derivatives, C and h into a frequency domain fatigue evaluation framework. These equations and computational procedures have been derived considering the well-established quasi-static EESS formulations adapted to account for the dynamic response characteristics of welded structures using the Mode Superposition technique.

The viability and validity of the proposed method in accurately evaluating the stresses at weld joints and improving the predicted fatigue damage and life of welded structures have been demonstrated through numerical analysis and comparative analysis process using an RHS T-joint

welded structure that is subjected to irregular road surface profile-induced stationary random loading.

A preliminary analysis based on constant cyclic fatigue loading was first performed to verify the reliability and performance of the FEA model in producing accurate and reliable results. The calculated maximum stress and fatigue life results of 116.7MPa and $73,933$ cycles are compared and validated by the corresponding results in the referenced literature. The validated preliminary analysis results confirmed that the subsequent frequency domain fatigue analysis stress, damage and life results computed using the FE model accurately represent the actual physical scenario with negligible or significantly reduced modelling and simulation effects induced errors.

The validated FE model is then utilized to demonstrate and verify the numerical viability of the proposed EESS-based frequency domain fatigue analysis method in predicting the fatigue damage and life of the RHS T-joint welded structures. Intermediate fundamental analysis, such as modal analysis, frequency response analysis, and stress power spectral density (PSD) computational analysis, was performed to calculate the EESS modal stresses, EESS frequency response function (FRF), and EESS PSD, respectively acting on all the welded joints nodes of the structure. The fatigue damage and life of the structure are subsequently estimated from the results of these analyses.

Utilizing the master S-N fatigue curve parameters and derivatives and the calculated EESS PSD and amplitude results, the accumulated fatigue damage D due to the maximum EESS PSD was estimated to be $2.804E-6$ per year, and the corresponding predicted fatigue life of the structure prior to damage crack initiation was 99 years. The predicted life is based on a 90-95% confidence interval and a 98% probability of survival before damage crack initiation.

The results of the proposed method are validated by comparison with fatigue test data from the literature and outcomes obtained from the hotspot stress extrapolation-based methods. The predicted fatigue damage initiation locations on the structure align with the reported literature locations, affirming the accuracy of the proposed method. Additionally, the fatigue life prediction indicates a significant improvement of 26% compared to the hotspot method, validating the effectiveness of the proposed approach. Notably, the proposed method achieves a maximum computational efficiency gain of 58% compared to the alternative hotspot stress-based fatigue analysis method.

This research contributes to the numerical fatigue design of welded structures subjected to random loading by introducing a significantly improved and effective frequency domain fatigue assessment method. Identifying potential fatigue damage crack initiation locations and estimating life with improved accuracy using the proposed method advances fatigue assessment in the design of welded structures by reducing the risk of premature failure, thereby mitigating economic and safety implications. The proposed method's demonstrated computational efficiency also justifies its use and application for the fatigue assessments of large and complex welded structures whose numerical fatigue analysis processes are usually computationally intensive.

5.2 Recommendations

While this research has introduced a significantly computationally efficient frequency domain fatigue analysis method with improved accuracy in predicting the fatigue damage and life of randomly loaded welded structures, it is essential to acknowledge some limitations and areas of improvement associated with its broad utilization and application.

The main limitations associated with the proposed method and results of the research include:

- (i) Neglecting the influence of welding-induced residual stresses, imperfections, defects, metallurgical and microstructural conditions, and dissimilar weld-base metal material properties
- (ii) Fatigue damage and life evaluation based on uniaxial stress state at the weld joints
- (iii) Consideration of uniaxial, ergodic, stationary random loading conditions
- (iv) No inclusion of environmental conditions effects on the predicted fatigue damage and life of the structure
- (v) Experimental validation of the predicted fatigue life results of the structure

Several areas of future research can be explored to address and improve these limitations and further enhance the accuracy and applicability of the proposed method. Firstly, the base metal-weld material properties similarities assumption is often made when the weld and base metals have similar material chemical compositions and mechanical and physical properties. It is important to note that this assumption should be carefully evaluated and validated based on the specific welding procedure and material composition being utilized. In cases where significant differences exist between the weld and base metal properties, a more detailed analysis considering the dissimilarities would be required to capture the structural response accurately. Considering the influence of the weld's residual stresses, imperfections, and material properties variations, metallurgical and manufacturing process conditions can provide more realistic predictions of fatigue damage and life. However, it will also require additional analysis techniques, such as thermal analysis and experimental data, to capture the complexities inherent in the weld joints of the structures.

Secondly, as much as uniaxial stress assumptions can be considered in completely characterizing the weld stress state and accurately estimating the damages at the weld joints under proportional

fatigue loading conditions where the effects of shear stresses are negligible, for non-proportional loading conditions, multiaxial stress states including shear stress effects must be included.

Thirdly, extending the analysis to include non-stationary and multi-axial loading random loading conditions will improve the method's ability to account for real-world fatigue loading and response behaviour of other welded structures exposed to these types of loading conditions. Multiaxial random loading conditions are typically experienced by welded structures such as marine, aircraft, and vehicle structures.

Fourthly, real-world structures generally operate under different environmental conditions in addition to their functional design loads. Considering these conditions' effects, such as temperature and corrosion, in the proposed method will further enhance its applicability to predict the welded structure's fatigue behaviour response and performance under varying environmental conditions.

Lastly, conducting experimental validation studies using the full-scale specimen of the structure considered in this research will validate the predicted fatigue life that has been estimated using the proposed method, ensuring its further reliability verifications and extended applications.

References

- [1] U. K. Ghosh, “Defects in welded joints,” in *Design of Welded Steel Structures: Principles and Practice*. Boca Raton, Florida, USA: CRC Press, 2010, ch. 3, pp. 23 – 33.
- [2] Z. Barsoum, “Guidelines for fatigue and static analysis of welded and un-welded steel structures,” KTH Royal Institute of Technology, Stockholm, Sweden, 2020
- [3] C. Bathias and A. Pineau, “Fatigue under variable welded amplitude loadings,” in *Fatigue of Materials and Structures: Fundamentals*. London, UK: ISTE, 2010, ch. 12, pp. 457 – 498.
- [4] A. Chattopadhyay, G. Glinka, M. El-Zein, J. Qian and R. Formas, “Stress analysis and fatigue of welded structures,” *Welding in the World*, vol. 55, Jul. 2011, Art. no. IIW-2201.
- [5] N. Bishop and F. Sheratt, *Finite Element Based Calculations*. Farnham, UK: RLD, 2000.
- [6] C. Braccesi, F. Cianetti, G. Lori, and D. Pioli, “Random multiaxial fatigue: A comparative analysis among selected frequency and time domain fatigue evaluation methods,” *Internal Journal of Fatigue*, vol. 74, pp. 107–118, Jan. 2015.
- [7] F. Guo, S. Wu, J. Liu, X. Wu, and W. Zhang, “An innovative stepwise time-domain fatigue methodology to integrate damage tolerance into system dynamics,” *Vehicle System Dynamics*, vol. 61, no. 2, pp. 550–572, Mar. 2023.
- [8] K. Rother and J. Rudolph, “Fatigue assessment of welded structures: Practical aspects for stress analysis and fatigue assessment,” *Fatigue and Fracture of Engineering Materials and Structure*, vol. 34, no. 3, pp. 177–204, Mar. 2011.

- [9] O. Doerk, W. Fricke, and C. Weissenborn, "Comparison of different calculation methods for structural stresses at welded joints," *International Journal of Fatigue*, vol. 25, no. 5, pp. 359–369, May 2003.
- [10] D. A. Osage, P. Dong, and D. Spring, "Fatigue assessment of welded joints in API 579-1/ASME FFS-1 2016-existing methods and new developments," in 7th International Conference on Fatigue Design, Senlis, France, Nov. 2018.
- [11] C. Ronchei *et al.*, "A frequency-domain approach for damage detection in welded structures," *Fatigue and Fracture of Engineering Materials and Structure*, vol. 44, no. 4, pp. 1134–1148, Apr. 2021.
- [12] D. Benasciutti and R. Tovo, "Frequency-based analysis of random fatigue loads: Models, hypotheses, reality," *Materials Science and Engineering Technology*, vol. 49, no. 3, pp. 345–367, Mar. 2018.
- [13] H. Bartsch, S. Citarelli, and M. Feldmann, "Generalization of the effective notch stress concept for the fatigue assessment of arbitrary steel structures," *Journal of Construction Steel Research*, vol. 201, Feb. 2023.
- [14] P. Dong, J. K. Hong, and M. Prager, "Fatigue of piping and vessel welds: ASME'S FSRF rules revisited," in 2002 ASME Pressure Vessels and Piping Conference, Aug. 5-9, 2002. [Online]. Available: http://asmedigitalcollection.asme.org/PVP/proceedings-pdf/17_1.pdf.
- [15] P. Dong and J. K. Hong, "The master S-N curve approach to fatigue evaluation of offshore and marine structures," in 23rd International Conference on Offshore Mechanics and Arctic

- Engineering, June 20-25, 2004. [Online]. Available: http://asmedigitalcollection.asme.org/OMAE/proceedings-pdf/847_1.pdf.
- [16] P. Dong, “A structural stress definition and numerical implementation for fatigue analysis of welded joints,” *International Journal of Fatigue*, vol. 23, pp. 865–876, Jun. 2001.
 - [17] P. Dong, J. K. Hong, and A. M. P. De Jesus, “Analysis of recent fatigue data using the structural stress procedure in ASME Div. 2 Rewrite,” *Journal of Pressure Vessel Technology, Transactions of the ASME*, vol. 129, no. 3, pp. 355–362, Aug. 2007.
 - [18] P. Dong, J. K. Hong, D. Osage, and M. Prager, “Master S-N curve method for fatigue evaluation of welded components,” *Welding Research Council*, vol. 474, Aug. 2002.
 - [19] H. Kyuba and P. Dong, “Equilibrium-equivalent structural stress approach to fatigue analysis of a rectangular hollow section joint,” *International Journal of Fatigue*, vol. 27, no. 1, pp. 85–94, Jan. 2005.
 - [20] Y. H. Su, X. W. Ye, and Y. Ding, “ESS-based probabilistic fatigue life assessment of steel bridges: Methodology, numerical simulation and application,” *Engineering Structures*, vol. 253, Feb. 2022.
 - [21] Z. Chen, B. Yu, P. Wang, and H. Qian, “Fatigue properties evaluation of fillet weld joints in full-scale steel marine structures,” *Ocean Engineering*, vol. 270, p. 113651, Feb. 2023.
 - [22] G. Alencar, J. K. Hong, A. de Jesus, J. G. S. da Silva, and R. Calçada, “The Master S-N curve approach for fatigue assessment of welded bridge structural details,” *International Journal of Fatigue*, vol. 152, Nov. 2021.

- [23] J. Li, Q. Zhang, Y. Bao, J. Zhu, L. Chen, and Y. Bu, “An equivalent structural stress-based fatigue evaluation framework for rib-to-deck welded joints in orthotropic steel deck,” *Engineering Structures*, vol. 196, Oct. 2019.
- [24] J. K. Hong and A. Cox, “Application of weld fatigue evaluation procedure for considering multiaxial stress states using the Battelle structural stress method,” *SAE Technical Paper 2017-01-0338*, Mar. 2017.
- [25] Y. Zhu *et al.*, “Fatigue failure modes of rib-to-deck joints under the multiaxial stress states caused by various wheel loading characteristics,” *Fatigue and Fracture of Engineering Materials and Structure*, vol. 46, no. 1, pp. 111–124, Jan. 2023.
- [26] H. T. Kang, P. Dong, and J. K. Hong, “Fatigue analysis of spot welds using a mesh-insensitive structural stress approach,” *International Journal of Fatigue*, vol. 29, no. 8, pp. 1546–1553, Aug. 2007.
- [27] L. Zhang, P. Dong, Y. Wang, and J. Mei, “A coarse-mesh hybrid structural stress method for fatigue evaluation of Spot-Welded structures,” *International Journal of Fatigue*, vol. 164, Nov. 2022.
- [28] J. K. Hong and T. Forte, “Development of fatigue evaluation procedure for weld-bonded joints using the Battelle structural stress method,” *SAE Technical Paper 2012-01-0477*, Apr. 2012.
- [29] K. Bao, Q. Zhang, Y. Liu, and J. Dai, “Fatigue life of the welding seam of a tracked vehicle body structure evaluated using the structural stress method,” *Engineering Failure Analysis*, vol. 120, Feb. 2021.

- [30] P. Dong, Z. Wei, and J. K. Hong, “A path-dependent cycle counting method for variable-amplitude multiaxial loading,” *International Journal of Fatigue*, vol. 32, no. 4, pp. 720–734, Apr. 2010.
- [31] A. Preumont, “Random Vibration and Spectral Analysis,” in *Solid Mechanics and Its Applications*. Dordrecht: Springer Netherlands, vol. 33.
- [32] T. Dirlik and D. Benasciutti, “Dirlik and Tovo-Benasciutti spectral methods in vibration fatigue: A review with a historical perspective,” *Metals (Basel)*, vol. 11, no. 9, Sep. 2021.
- [33] Christian. Lalanne, *Mechanical vibration and shock analysis*, 3rd edition. London, UK: ISTE, 2014
- [34] *Standard Practice for Performance Testing of Shipping Containers and Systems – ASTM D4169 Truck Profile Update Rationale*, ASTM Standard D4169 – 16, Sep. 2016.
- [35] Q. Wang, B. Ji, X. Chen, and Z. Ye, “Dynamic response analysis-based fatigue evaluation of rib-to-deck welds considering welding residual stress,” *International Journal of Fatigue*, vol. 129, Dec. 2019.
- [36] Y. Zhou and J. Tao, “Theoretical and numerical investigation of stress mode shapes in multiaxial random fatigue,” *Mechanical System & Signal Process*, vol. 127, pp. 499–512, Jul. 2019.
- [37] A. Hobbacher, “Recommendations for fatigue design of welded joints and components,” *International Institute of Welding Collection*, XIII-1539-96 / XV-845-96, Dec. 2008.

- [38] E. Niemi, W. Fricke, and S. J. Maddox, “Structural hot-spot stress approach to fatigue analysis of welded components designer’s guide second edition,” *International Institute of Welding Collection*, IIW – 978-981-10-5568-3_11, 2018.
- [39] A. Niesłony and M. Böhm, “Frequency-domain fatigue life estimation with mean stress correction,” *International Journal of Fatigue*, vol. 91, pp. 373–381, Oct. 2016.
- [40] T. Dirlik, “Application of computers in fatigue analysis,” Ph.D. dissertation, Dept.Eng., Warwick Univ., Coventry, England, 1985.
- [41] A. Fatemi and L. Vangt, “Cumulative fatigue damage and life prediction theories: a survey of state of the art for homogeneous materials,” *International Journal of Fatigue*, vol. 20, pp. 9–34, Jun. 1997.
- [42] S. Kwofie and N. Rahbar, “A fatigue driving stress approach to damage and life prediction under variable amplitude loading,” *International Journal of Damage Mechanics*, vol. 22, no. 3, pp. 393–404, Apr. 2013.
- [43] Z. Wei, H. Jin, X. Pei, and L. Wang, “A simplified approach to estimate the fatigue life of full-scale welded cast steel thin-walled tubular structures,” *Thin-Walled Structures*, vol. 160, Mar. 2021.
- [44] J. K. Hong and T. P. Forte, “Development of Friction Stir Weld Fatigue Evaluation Procedure Using Battelle Structural Stress Method,” *SAE International Journal of Materials and Manufacturing*, vol. 7, no. 2, pp. 432–438, Apr. 2014.

- [45] Z. Fang, A. Li, W. Li, and S. Shen, “Wind-induced fatigue analysis of high-rise steel structures using equivalent structural stress method,” *Applied Sciences (Switzerland)*, vol. 7, no. 1, 2017.
- [46] K. Zhang, L. Wu, and T. Chen, “Weld Fatigue Life Analysis of Truck Mixer Sub-frame Based on Equivalent Structural Stress Method,” in *Journal of Physics: Conference Series*, IOP Publishing Ltd, Feb. 2022..
- [47] X. Tan, C. Wang, K. Xie, L. Xie, and P. Wang, “Research on fatigue reliability prediction model and structural improvement of welded drive axle housing based on master S-N Curve method,” *Quality Reliability and Engineering International*, vol. 39, no. 1, pp. 302–319, Feb. 2023.
- [48] Z. Luo, S. Vantadori, C. Ronchei, A. Carpinteri, and H. Chen, “Vibration fatigue analysis of circumferentially notched specimens under coupled multiaxial random vibration environments,” *Fatigue Fract Eng Mater Struct*, vol. 44, no. 9, pp. 2412–2428, Sep. 2021.
- [49] L. H. Yam, T. P. Leung, D. B. Li, and K. Z. Xue, “Theoretical and experimental study of modal strain analysis,” *Journal of Sound and Vibration*, vol. 191, no. 2, pp. 251–260, Apr. 1996.
- [50] Z. C. Wang, D. Geng, W. X. Ren, and H. T. Liu, “Strain modes based dynamic displacement estimation of beam structures with strain sensors,” *Smart Materials and Structures*, vol. 23, no. 12, Dec. 2014.

- [51] Y. Zhou, Q. Fei, and S. Wu, “Utilization of modal stress approach in random-vibration fatigue evaluation,” *Journal of Aerospace Engineering*, vol. 231, no. 14, pp. 2603–2615, Dec. 2017.
- [52] G. Alencar, A. de Jesus, J. G. S. da Silva, and R. Calçada, “A finite element post-processor for fatigue assessment of welded structures based on the Master S-N curve method,” *International Journal of Fatigue*, vol. 153, Dec. 2021.
- [53] J. K. Hong Battelle Columbus and U. P. Thomas Forte, “Fatigue evaluation procedures for multiaxial loading in welded structures using Battelle structural stress approach.” [Online]. Available: <http://asmedigitalcollection.asme.org/OMAE/proceedings-pdf/omae-23459.pdf>
- [54] M. Mršnik, J. Slavič, and M. Boltežar, “Vibration fatigue using modal decomposition,” *Mechanical System & Signal Process*, vol. 98, pp. 548–556, Jan. 2018.
- [55] M. Decker, “Vibration fatigue analysis using response spectra,” *International Journal of Fatigue*, vol. 148, Jul. 2021.
- [56] M. Kepka, “Consideration of random loading processes and scatter of fatigue properties for assessing the service life of welded bus bodyworks,” *International Journal of Fatigue*, vol. 151, Oct. 2021.
- [57] ANSYS. (2022R2). Ansys, Inc.
- [58] MATLAB. (R2023a). MathWorks.

- [59] X. L. Zhao, and J. A. Packer, “Fatigue design procedure for welded hollow section joints,” International Institute of Welding: IIW Document XIII-1804-99 and IIW Document XV-1035-99 : recommendations of IIW Subcommittee XV-E, 2018.
- [60] Ansys, Inc. *ANSYS HELP*, 2022R2. Accessed: Jun. 2023